

Parametric Instability of Woven Fiber Composite Plates

Itishree Mishra



Department of Civil Engineering
National Institute of Technology, Rourkela
Rourkela-769008, Orissa, India
July, 2012

Parametric Instability of Woven Fiber Composite Plates

Thesis submitted in partial fulfillment of the requirements for the degree of

Master of Technology

in

Civil Engineering

(Specialization: Structural Engineering)

By

Itishree Mishra

(Roll No: 609CE606)

Under the supervision of

Prof. Shishir Kumar Sahu



**Department of Civil Engineering
National Institute of Technology, Rourkela
Rourkela-769 008, Orissa, India
July 2012**



DEPARTMENT OF CIVIL ENGINEERING
NATIONAL INSTITUTE OF TECHNOLOGY
ROURKELA – 769008, ODISHA, INDIA
www.nitrkl.ac.in

Dr. Shishir Kumar Sahu
Professor

July, 2012

CERTIFICATE

*This is to certify that the work in this thesis entitled “**Parametric Instability of Woven Fiber Composite plates**” submitted by **Itishree Mishra** is a record of an original research work carried out by her under my supervision and guidance in partial fulfillment of the requirements for the award of the degree of Master of Technology in **Civil Engineering** with the specialization of **Structural Engineering** from the department of Civil Engineering, National Institute of Technology, Rourkela in academic year 2010-2012.*

This thesis fulfils the requirements relating to the nature and standard of work for the award of Master of Technology in Civil Engineering. The results embodied in this thesis have not been submitted for award for any other degree or diploma from any other institution earlier.

Date:

Dr. Shishir Kumar Sahu

(Professor in Civil Engineering Department)
National Institute of Technology
Rourkela-769008

ACKNOWLEDGEMENTS

I sincerely express my deep sense of gratitude to honorable thesis supervisor **Professor Shishir Kumar Sahu**, Professor, civil engineering Department, National Institute of Technology, Rourkela, for providing me an opportunity to work with him. His profound insights, constant encouragement and invaluable suggestion in all phases have been true inspirations to my research.

I would also like to express my deep appreciation and sincere thanks to **Professor N. Roy**, Head of the department, who extended all the academic, experimental and other related facilities of the department to make my progress of work smooth. My sincere regards to **Professor P. K. Datta** and **Professor A. Ghosh** of IIT, Kharagpur for providing all kinds of possible help and valuable suggestion for instability test.

The help and support received from **Mr. Himanshu shekhar Panda**, Ph.D. Scholar, Civil Engineering was vital for the success of the project. I am indebted to all the professors, co-researchers, and friends at National Institute of Technology Rourkela for their active or hidden cooperation. Their contributions have always been unfeigned. I am also thankful to staff members of Structural Engineering Laboratory for their assistance & cooperation during the course of experimentation. The facilities and co-operation received from the staff of INSTRON Laboratory of Metallurgical & Material Engg. Deptt. and mechanical Engg. Deptt. are thankfully acknowledged.

The author gratefully acknowledges the financial support provided by the Department of Science and Technology (DST), New Delhi, India. (Project No.SR/S3/MERC/009/2008)

I would conclude with my deepest gratitude to my parents and all my loved ones. My full dedication to the work would have not been possible without their blessings and moral support. Last but not the least; I am thankful to ALMIGHTY, who kept me fit both mentally and physically throughout the year for the project work.

Date:

Itishree Mishra

CONTENTS

Chapter	Title	Page No.
	Contents	i
	Abstract	iv
	List of symbols	vii
	List of tables	ix
	List of figures	x
	List of Publications	xiii
1	INTRODUCTION	1
	1.1 Introduction	1
	1.2 Importance of the present structural stability study	1
2	REVIEW OF LITERATURE	3
	2.1 Introduction	3
	2.2 Review on laminated composite plates	3
	2.2.1 Free vibration analysis of plates	3
	2.2.2 Buckling analysis of plates	7
	2.2.3 Dynamic stability analysis of plates	10
	2.3 Critical discussion	13
	2.4 Objectives and scope of the present study	14
3	MATHEMATICAL FORMULATION	15
	3.1 The basic problem	15
	3.2 Proposed analysis	16
	3.2.1 Assumptions of the analysis	16
	3.3 Governing equations	17
	3.3.1 Governing differential equations	17
	3.4 Dynamic stability studies	18
	3.5 Finite element formulation	20
	3.5.1 Discretisation of structure	20
	3.5.2 The plate element	20

	3.5.3	Strain displacement relations	22
	3.5.4	Constitutive relations	24
	3.5.5	Elastic stiffness matrix	28
	3.5.6	Geometric stiffness matrix	28
	3.5.7	Element mass matrix	30
	3.6	Computer program	31
4		EXPERIMENTAL PROGRAMME	32
	4.1	Introduction	32
	4.2	Materials	32
	4.3	Fabrication procedure	32
	4.4	Determination of material constants	34
	4.5	Description of test specimen	36
	4.6	Vibrations of woven fiber composite plates	38
	4.6.1	Equipments required for free vibration test	38
	4.6.2	Setup and test procedure for free vibration Test	40
	4.6.3	Setting up the template in Pulse lab shop	42
	4.6.4	Pulse report	44
	4.7	Buckling of woven fiber composite plates	45
	4.7.1	Buckling experiment (Static stability)	45
	4.7.2	Buckling experiment (By dynamic approach)	47
	4.8	Parametric instability of woven fiber composite plates	48
	4.8.1	Parametric instability test setup	48
	4.8.2	Parametric instability experimental procedure	50
5		RESULTS AND DISCUSSIONS	51
	5.1	Introduction	51
	5.2	Free vibration of woven fiber laminated composite plates	51
	5.2.1	Convergence study	51
	5.2.2	Comparison with previous studies	52
	5.2.3	Experimental and numerical results of vibration	53
	5.3	Buckling effects of woven fiber laminated composite plates	58
	5.3.1	Convergence study	58

	5.3.2	Comparison with previous studies	58
	5.3.3	Experimental and numerical results of buckling	60
	5.3.4	Experimental buckling study by dynamic approach	66
5.4		Parametric instability of woven fiber laminated composite plates subjected to in-plane periodic loading	67
	5.4.1	Convergence study	68
	5.4.2	Comparison with previous studies	68
	5.4.3	Experimental results for parametric instability	70
	5.4.4	Numerical results for parametric instability	71
6		CONCLUSIONS	81
	6.1	Introduction	81
	6.2	Vibration of laminated composite plates	81
	6.3	Buckling effects of laminated composite plates	82
	6.4	Parametric instability of composite plates	83
	6.5	Further scope of research	84
		BIBLIOGRAPHY	85
		APPENDIX	94

ABSTRACT

Composites have increasing applications in aerospace, civil, automobile and marine engineering. Structural components are often subjected to in-plane periodic loads which may lead to parametric instability, due to certain combinations of the applied in-plane forcing parameters and natural frequency of transverse vibrations. This phenomenon is called parametric instability or parametric resonance and is often studied in the spectrum of natural frequency and buckling load of structures.

The present study deals with free vibration, buckling and parametric instability behavior of industry driven laminated woven fiber composite plates under harmonic in-plane periodic loads. In this analysis, the effects of various parameters such as increase in number of layers, aspect ratios, side-to thickness ratios, ply-orientations, and increase in static load factors, lamination angle and the degree of orthotropic are studied.

The study is experimental but also includes numerical analysis using finite element method (FEM). A simple laminated plate model based on first order shear deformation theory (FSDT) is developed for the free vibration, buckling and parametric instability effects of composite plates subjected to in-plane loading. The principal instability regions are obtained using Bolotin's approach employing finite element method (FEM). An eight-node isoparametric quadratic element is employed in the present analysis with five degree of freedom per node considering the effects of transverse shear deformation and rotary inertia. The elastic stiffness matrix, geometric stiffness matrix and mass matrix of the element are derived using the principle of minimum potential energy. They are evaluated using the Gauss quadrature numerical integration technique. A computer program based on FEM in MATLAB environment is developed to perform all necessary computations.

The composite plates of different layers with different dimension are manufactured using woven glass fiber and epoxy matrices. The experiments are performed for vibration and buckling (both static and dynamic approach) on the industry driven woven fiber Glass/Epoxy plates after tensile testing, used for characterization. Free vibration characteristics are studied using FFT analyzer, accelerometer using impact hammer excitation.

The FRFs are studied to obtain a clear understanding of the vibration characteristics of the specimens. The buckling loads of specimen are found by both static and dynamic approach. Finally, parametric instability experiment is conducted and the effects of increase in static load factor on excitation frequency are studied. Dynamic instability regions (DIR) are plotted for different plate specimens, applying both static and dynamic loading numerically.

The numerical and experimental result shows that the natural frequency is the least for cantilever and highest for fully clamped boundary conditions. Comparisons between experimental and FEM results are much better for the free-free and cantilever boundary conditions than other boundary conditions. The different fiber orientation angle affects the buckling load. When ply orientation is increased from 0^0 to 45^0 fiber orientation angles, then the buckling load values are observed to decrease in both experimental method and FEM. So the composite plate with $[0]_8$ layup shows highest buckling load and with $[45/-45]_{2s}$ layup had lowest buckling load. The critical/buckling loads reduce significantly depending upon the side-to-thickness ratios and aspect ratios. It is observed that with the increase of static load factor from 0 to 0.8, the excitation frequencies decrease both numerically and experimentally. The excitation frequencies decrease with increase in lamination angle due to reduction of stiffness and strength of laminated plates. The onset of instability, the width of instability region and its strength are highly dependent on lamination angle. The greater the lamination angle the smaller is the width of instability region for this geometry and material properties.

From the above studies, it can be concluded that the parametric instability behavior of woven fiber composite plates is greatly influenced by different parameters such as number of layers, aspect ratios, side-to thickness ratios, ply-orientations, increase in static load factors and dynamic load factors. So, designer has to be cautious while dealing with structures subjected to dynamic loading. This can be used to the advantage of tailoring during design of composite structures.

The thesis is presented in six chapters. **Chapter 1** deals with the general introduction and importance of the present structural stability studies. **In chapter 2**, a detailed review of the literature pertinent to the previous works done in this field is listed. A critical discussion of the earlier studies is done. The aim and scope of the present study is also outlined in this chapter.

ABSTRACT

In chapter 3, a description of the theory and formulation of the problem and the finite element procedure used to analyze the vibration, buckling and parametric instability characteristics of laminated composite panels and it is explained in detail. The computer program based on MATLAB environment used to implement the formulation is also briefly described. **In chapter 4**, all the experimental work related to fabrication of laminated industry driven woven fiber composite plates, their material constants determination and free vibration test, buckling test and parametric instability test set up and test procedure are well documented. **In chapter 5**, the results of experimental investigation obtained in the study are presented in detail. The effects of various parameters like lamination sequence, ply orientation, degree of orthotropy, aspect ratio, width to thickness ratio and in-plane load parameters on the vibration, buckling and dynamic instability regions is investigated. The studies have been done separately. **Finally, in chapter 6**, the conclusions drawn from the above studies are described. There is also a brief note on the scope for further study in this field. At the end, some important publications and books referred during the present investigation have been listed in **Bibliography** section.

The programme features along with flow chart are presented in Appendix.

Keywords: Finite Element Method, Woven fiber composite, Vibration, Stability, Parametric instability, Natural frequency, Critical Buckling load, Excitation Frequency, Periodic load.

LIST OF SYMBOLS

The principal symbols in this thesis are presented for easy reference. A single symbol is used different meanings depending on the contest and defined in the text as they occur.

English

a, b	Dimensions of Plate
h	Thickness of the plate
$[B]$	Strain matrix for the element
$[D]$	Flexural rigidity of plate
dx, dy	Element length in x and y direction
E_{11}, E_{22}	Modulus of elasticity
G_{12}, G_{13}, G_{23}	Shear modulus of rigidity
$ J $	Jacobian
N_x, N_y, N_{xy}	In plane stress resultants of the plate
M_x, M_y, M_{xy}	Bending moments of the plate
Q_x, Q_y	Transverse shear resultants.
u, v	In plane displacement
w	Out of plane displacement
x, y, z	Global axis system
$A_{ij}, B_{ij}, D_{ij}, S_{ij}$	extensional, bending-stretching coupling, bending stiffness and transverse shear stiffness
$[K]$	Global elastic stiffness matrix
$[M]$	Global consistent mass matrix
$[K_g]$	Geometric stiffness matrix
ξ, η	Natural co-ordinates of an element
N_s	the static portion of load N (t)
N_t	the amplitude of the dynamic portion of N (t)

Greek

$\sigma_{xx}, \sigma_{yy}, \sigma_{xy}$	Stresses at a point
$\varepsilon_{xx}, \varepsilon_{yy}, \gamma_{xy}$	Strains at a point
ν_{12}, ν_{21}	Poisson's ratio
θ_x, θ_y	Slopes normal and transverse to the boundary
α, β	Static and dynamic load factors
ω	Natural frequency
N_{cr}	Critical loads
Ω	Excitation frequency
θ	Fiber orientation in a lamina
ρ	Mass density

Mathematical Operators

$[\]^{-1}$	Inverse of a matrix
$[\]^T$	Transpose of a matrix

LIST OF TABLES

Table No	Title	Page No.
4.1	Dimensions of the test specimens for tensile test.	34
4.2	Material properties of the composite plate from tensile tests	35
4.3	Geometrical Dimensions of composite plates	37
5.1	Convergence study on free vibration of 4-layer simply supported laminated composite plates	52
5.2	Comparison of natural frequency (Hz) for composite plates with previous study at different boundary conditions	53
5.3	Convergence study on buckling of 8- layer symmetric cross ply composite plate for C-F-F-F and C-F-C-F boundary conditions.	58
5.4	Comparison of Buckling Load in Newton for composite plates with C-F-C-F boundary conditions.	59
5.5	Comparison of non dimensional buckling load for simply supported angle-ply ($\theta^0/\theta^0/\theta^0$) plates.	59
5.6	Convergence study on excitation frequency of 8-layer symmetric cross ply C-F-C-F composite plate.	68
5.7	Comparison of natural frequency and buckling load of the composite plate for C-F-F-F and C-F-C-F boundary conditions for cross ply symmetric (0/90/0/90) panels.	69
5.8	Comparison of excitation frequency in rad/sec for 4- layer symmetric cross-ply simply supported composite plates.	70

LIST OF FIGURES

Figure	Title	Page No.
3.1	Laminated composite plate under in-plane harmonic loading	15
3.2	Lamination sequence of the composite plate	16
3.3	Plan-form of the composite plate subjected to in-plane load $N(t)$	16
3.4	[a] In-plane forces on a laminate	17
3.4	[b] Moments on a laminate	17
3.5	N-layered laminate configurations	21
4.1	[a] Application of gel coat on mould releasing sheet	33
	[b] Placing of woven roving glass fiber on gel coat	
	[c] Removal of air entrapment using steel roller	
	[d] Composite plate after casting.	
4.2	[a] Specimens in “x” direction	34
	[b] Specimens in “y” direction	
	[c] Specimens in “45⁰” direction	
4.3	Tensile test of woven fiber glass/epoxy composite specimen in INSTRON 1195 UTM	36
4.4	Failure pattern of woven fiber glass/epoxy composite specimen	36
4.5	Modal impact hammer (B&K type 2302-5)	38
4.6	Accelerometer (B&K 4507)	39
4.7	FFT analyzer (Model B&K3560-B)	39
4.8	[a] Display unit used in free vibration test.	40
	[b] Various Pulse output windows	
4.9	Vibration test set-up	41
4.10	[a] Iron Frame for making different boundary conditions (b.c) setup	41-42
	[b] Set up for free-free b.c	
	[c] Set up for cantilever b.c	
	[d] Set up for clamped b.c	
	[e] Set up for simply supported b.c	

4.11	Configuration window	42
4.12	Measurement window	43
4.13	Function window	43
4.14	Typical FRF of test specimen.	44
4.15	Typical coherence of test specimen	44
4.16	[a] INSTRON universal testing machine (SATEC) of 600 KN	46
	[b] Buckling test set up and test frame	
	[c] Specimen before buckling	
	[d] Specimen after buckling	
4.17	[a] Experimental test set up for buckling test by dynamic approach	47
	[b] Vibration test set up	
4.18	[a] Parametric instability test set up with loading system	48-49
	[b] Measurement system	
	[c] Oscilloscope indicating x-y plot	
	[d] Schematic diagram for parametric instability experiments	
5.1	Variation of natural frequency with different no. of layers of woven fiber composite plates.	54
5.2	Variation of natural frequency with different fiber orientations of woven fiber composite plates.	55
5.3	Variation of natural frequency with different aspect ratio of woven fiber composite plates.	56
5.4	Variation of natural frequency with different boundary condition of woven fiber composite plates.	57
5.5	Variation of critical buckling load with number of layers of C-F-C-F woven fiber laminated composite plates.	61
5.6	Variation of critical buckling load with fiber orientation of C-F-C-F woven fiber laminated composite plates.	62
5.7	Variation of critical buckling load with aspect ratio of C-F-C-F woven fiber laminated composite.	63
5.8	Variation of critical buckling load with L/t ratio of C-F-C-F woven fiber laminated composite plates.	64

5.9	Variation of critical buckling load with no. of layers of woven fiber composite plates under different boundary conditions using FEM.	65
5.10	Typical variation of compressive load with end shortening displacement of 12-layer woven fiber laminated composite plates	66
5.11	Variation of natural frequency of the plate with in-plane load	66
5.12	Variation of excitation frequencies with static load factor for 12-layer C-F-C-F woven fiber composite plates.	71
5.13	Variation of instability regions with no. of layers for C-F-C-F woven fiber laminated composite plates.	73
5.14	Variation of instability regions with static load factor for 16-layer C-F-C-F woven fiber composite plates.	74
5.15	Variation of instability regions with aspect ratio for 8-layer C-F-C-F woven fiber laminated composite plates.	75
5.16	Variation of instability regions with boundary condition for 8 layer woven fiber laminated composite plates.	76
5.17	Variation of instability regions with fiber orientation for 8-layer C-F-C-F woven fiber laminated composite.	77
5.18	Variation of instability regions with thickness for C-F-C-F woven fiber laminated composite plates.	78
5.19	Variation of instability regions with side to thickness ratio for C-F-C-F woven fiber laminated composite plates.	79
5.20	Variation of instability regions with degree of orthotropy for 8-layer C-F-C-F woven fiber laminated composite plates.	80

List of Publications Out of This Research Work

International Journals

1. **I. Mishra** and **S. K. Sahu**, “An Experimental Approach to Free Vibration Response of Woven Fiber Composite Plates under Free-Free Boundary Condition”, *International Journal of Advanced Technology in Civil Engineering (IJATCE)*, Vol-1,(2), pp.67-72, 2012
2. **I. Mishra** and **S. K. Sahu**, “Modal Analysis of Woven Fiber Composite Panels in Different Boundary Conditions” *International Journal of Structural Stability and Dynamics*, (Communicated for publication).
3. **I. Mishra** and **S. K. Sahu**, “Buckling Analysis of Woven Fiber Laminated Composite Plates- An Experimental Study” *Experimental Techniques*, (Communicated for publication).

International Conferences

1. **I. Mishra** and **S. K. Sahu**, “Modal Analysis Of Woven Fiber Composite Plates In Different Boundary Conditions”, *Fourth International Conference on Structural Stability and Dynamics (ICSSD2012)*, Jan 4-6, 2012 at MNIT, Jaipur
2. **I. Mishra** and **S. K. Sahu**, “An Experimental Approach to Free Vibration of Woven Fiber Composite Plates In Free-Free Boundary Conditions”, 1st *International Conference in Advance in Civil Engineering (ICACE2011)*, December 17-18 at Bhubaneswar.

Chapter-1

INTRODUCTION

1.1 Introduction

Composite materials are ingenious invention that provided immense benefits in the application of different engineering design of structures such as aerospace, civil, marine, automobiles, biomedical and sports equipments because of their ability to offer outstanding strength, high specific stiffness and strength, excellent fatigue resistance, high hygroscopic sensitivity, high resistance to impact damage and longer durability.

1.2 Importance of the Present Structural Parametric Instability Studies

Plate structures are an important class of structural system, since they are major load-carrying components. Structural elements subjected to in-plane periodic loads may undergo unstable transverse vibration, leading to parametric instability due to certain combinations of in-plane load parameters and natural frequency of transverse vibrations. This type of resonance is known as dynamic instability or parametric instability or parametric resonance. A number of catastrophic incidents can be traced to parametric resonance. Several means of combating parametric instability such as damping and vibration isolation may be inadequate and sometimes dangerous with reverse results.

In structural mechanics, dynamic stability has received considerable attention over the years and encompasses many classes of problems. The parametric instability may arise not merely at a single excitation frequency but even for small excitation amplitudes and combination of frequencies. The primary instability region is the most dangerous and has greatest practical importance. The distinction between stable and unstable vibration regimes of a structure, subjected to in-plane periodic loading can be distinguished through an analysis of dynamic instability region (DIR) spectra. The calculation of these spectra is often provided in terms of natural frequencies and the static buckling loads. So, the calculation of these parameters with high precision is an integral part of parametric instability analysis of laminated composite plates. Thus the vibration, buckling and parametric instability characteristics are of great technical importance for understanding the dynamic system under in-plane periodic loading.

A comprehensive analysis of the vibration and buckling effects of plates is studied exhaustively. Most of the studies on dynamic stability of composite plates are done either analytically or by different numerical methods. Woven fabric composites is a class of textile composite materials with a fully integrated, continuous spatial fiber network oriented on at least two axes, in order to provide excellent integrity and conformability for advanced structural composite applications. For a two-dimensional woven-fabric composite, the reinforcing element is a fabric preform typically consisting of two orthogonal families of fiber bundles. Woven glass fibers is used to achieve higher reinforcement loading and consequently, higher strength. Woven roving are plainly woven from roving, with higher dimensional properties and regular distribution of glass fiber with excellent bonding strength among laminates possesses higher fiber content, tensile strength, impact resistance. It is being used as the new industrial composites in many structural applications. Most of them focused on the impact response, damage initiation or failure mode of woven composite plates. So far, no previous experimental work has been reported on instability of woven composite plates subjected to in-plane harmonic loading. The study of dynamic stability itself requires investigation on vibration and buckling load of structures. A thorough review of earlier works done in this area becomes essential to arrive at the objective and scope of the present investigation. The detailed review of literature along with critical discussions is presented in the next chapter.

Chapter-2

REVIEW OF LITERATURE

2.1 Introduction

As laminated composite materials are increasingly used in structural applications, there arises a need for more information on the behavior of structural components, such as plates. The vast uses of composite materials in plates are subjected of research for many years. Though the investigations is mainly focused on parametric instability analysis of structures especially composite plates, some relevant researches on vibration, static stability or buckling of plate are also studied for the sake of its relevance and completeness. Some of the pertinent studies done recently are reviewed elaborately and critically discussed to identify the lacunae in the existing literature. The study of parametric instability itself requires investigation on vibration and buckling load of structures.

2.2 Reviews on Laminated composite Plates

The related literature was critically reviewed so as to provide the background information on the problems to be considered in the research work and to emphasize the relevance of the present study. The behavior of structures subjected to in-plane loads is less understood in comparison with structures under transverse loads. The following areas of analysis pertaining to the plate are covered in the review of literature.

- Free vibration of composite plates.
- Buckling of composite plates.
- Parametric instability of composite plates.

2.2.1 Free Vibration Analysis of Plates

With the continually increasing use of composites, especially in aerospace and automobile sectors, the study of vibration problems arising in laminated plates has become important. The prediction of dynamic behavior of laminated composite plates plays a significant role in the applications of structural composites. Plenty of analytical and numerical studies on vibration of composite plates are available in literature.

A considerable amount of analytical models and numerical analyses is reported for the free vibration analysis and is reviewed extensively by Leissa [1987], Kapania [1989], Liew, Xiang & Kitipornchai [1995] and Bhat *et.al* [1999] and Zhang and Yang [2009].

Bert and Mayberry [1969] presented a linear analysis for determining the natural frequency of vibration of laminated anisotropic plates using an approximate solution obtained by the Rayleigh-ritz energy method. Numerical results are presented for fully clamped boundary conditions and compared with experimental results of symmetrically and unsymmetrically laminated plates determined by the peak amplitude response of a small metallic-foil strain gauge at the plate center. Ashton and Anderson [1969] investigated experimentally and theoretically the natural frequencies and mode shapes of laminated boron-epoxy plates with clamped edges. Wu and Vinson [1969] studied the effect of shear deformations on the fundamental natural frequency of composite plates with different boundary conditions: clamped, simply supported, and combined clamped and simply supported edges. This solution was based on Galerkin's method. Clary [1972] investigated the natural frequencies and mode shapes of unidirectional composite material panels. He investigated the change in frequencies and mode shapes as the angle between the fibers and boundaries was changed. The maximum response amplitude was used to determine the natural frequencies. Clary and Cooper [1973] studied the vibration characteristics of aluminum plates reinforced with Boron-epoxy composites experimentally and compared with analytical results. To overcome the poor correlation, they indicated towards a sophisticated finite element analysis. Bert and Chen [1978] presented the effects of shear deformation on vibrations of antisymmetric angle-ply laminated rectangular plates. The displacement formulation of heterogeneous shear deformation plate theory oriented by Yang, Norris, and Stavsky [1966] was used. Numerical results were presented showing the parametric effect of aspect ratio, length-to-thickness ratio, number of layers and lamination angle.

Crawley [1979] experimentally and theoretically investigated the natural frequencies and mode shapes of composite cantilever plates and shells. He used the 90° phase difference between the periodic excitation and the response as a criterion to determine the natural frequencies. The natural frequency and mode shapes of a number of Graphite/ Epoxy and Graphite/Epoxy-Aluminum plates and shells were experimentally determined by Cawley and

Adams [1978]. The samples tested include eight ply graphite/epoxy plates with different fiber orientations and aspect ratios. The natural frequency and mode shape results obtained from experiment are compared with finite element method. Bhimaraddi and Stevens [1984] used higher order theory for free vibration of orthotropic, homogeneous, and laminated rectangular plates. The theory accounts for in-plane inertia, rotary inertia, and shear deformation effects. The proposed method used Hamilton's principle and assumed parabolic variations for transverse shear strains across the thickness of plate. In recent years, the Higher order Shear Deformation Theory (HSDT) as well as the Layer-wise Shear Angle Theory (LSAT) was developed by Owen and Li [1987] and Kant and Mallikarjuna [1989] to improve the predictions of laminate static and dynamic behavior. The First order Shear Deformation Theory [FSDT] was considered more efficient for the prediction of the global responses, i.e., the transverse displacements, the free vibration Frequencies, and the buckling loads as reported by Reddy [1979]. Reddy [1990] presented a layer wise theory for the analysis of free vibration of laminated plates. The elasticity equations were solved by utilizing the state-space variables and the transfer matrix. Results were also obtained for symmetric and antisymmetric laminates. Narita and Leissa [1992] presented an analytical approach for the free vibration of cantilevered, symmetrically laminated rectangular plates. The natural frequencies were calculated for a wide range of parameters: e.g., composite material constants, fiber angles and stacking sequences.

An experimental and numerical investigation into the structural behavior of symmetrically laminated carbon fiber-epoxy composite rectangular plates subjected to vibration was studied by Chai *et al.* [1993]. The experimental vibrational response was studied using TV-holography technique and comparison with finite element results was reasonably good. Chai [1994] employed Raleigh-Ritz method to study the free vibration behavior of laminated plates with various edge support conditions. In addition experiments were performed using TV-holography technique to verify the predicted results for a rectangular C-S-C-S laminated carbon-fibre reinforced plastic plate of symmetric stacking sequence. Linear vibration analysis of laminated rectangular plates was reported by Han and Petyt [1996], who describe the free and forced vibration analysis of symmetrically laminated rectangular plates with clamped boundary condition using hierarchical finite element techniques. A study on the free vibration analysis of orthogonal-woven fabric composites was analyzed by Chen and Chou

[1999] analytically. Based upon the one-dimensional (1D) elasto-dynamic analysis developed by the authors for such a woven fabric composite, the free vibration problem was formulated and solved for four basic boundary conditions. Stanbridge and Ewins [1999] described a number of vibration mode-shape measurement techniques, in which the measurement point of a laser Doppler vibrometer (LDV) was continuously scanned over the surface of a sinusoidally excited structure.

An experimental procedure to estimate the dynamic damped behavior of woven fiber Glass/Epoxy composite cantilever beams in flexural vibrations was given by Tita, Carvalho and Lirani [2001]. Berthelot and Sefrani [2006] investigated the damping of unidirectional glass fiber composites with a single or two interleaved viscoelastic layers experimentally. Laila [2008] presented aeroelastic characteristics of a cantilevered composite wing, idealized as a composite flat plate laminate. The composite laminate was made from woven glass fibers with epoxy matrix. The elastic and dynamic properties of the laminate were determined experimentally for aeroelastic calculations. An experimental amplitude-fluctuation electronic speckle pattern interferometry method for out-of-plane displacement measurement was employed to investigate the vibration behavior of square and rectangular composite plates with different stacking sequences by Ma and Lin [2001]. Both resonant frequencies and corresponding mode shapes can be obtained experimentally. Lei *et al.* [2010] reported the effects of woven structures on the vibration properties of the composites. The composites plates with adequate thickness were prepared by epoxy resin curing, and their fiber volume fractions were examined. Five typical weaving sets including the ordinary plain weaved and the warp interlocked were adopted in fabric processing. The result showed that the woven structure have a strong effect on the fiber volume fraction, resin-rich area, and the warp architectures of the composites, which determined the performances of the composites in vibration For laminated plates. Natural frequency with different fiber orientations was studied. Due to the advancement in weaving processes, a woven composite evolved as an attractive structural material for structural applications and the modeling strategies are reviewed recently by Mahmood *et al.* [2011].

To better understand any structural vibration problem, the resonant frequencies of a structure need to be identified and quantified. Today, due to the advancement in computer aided data

acquisition systems and instrumentation, experimental modal analysis has become an extremely important tool in the hands of an experimentalist. Ewin [1984] has discussed in details the technology of modal testing. A combined experimental and numerical study of the free vibration of composite GFRP plates was carried out by Chakraborty *et.al.* [2000]. Modal testing was conducted using impact excitation to determine the respective frequency response functions. FEM results, NISA package results were compared with experimental results. Dutt and Shivanand [2011] studied the free vibration response of C-F-F-F and C-F-C-F woven carbon composite laminates using a FFT analyzer and compared with FEM tool ANSYS. This work presents an experimental study of modal testing of woven fiber Glass/Epoxy laminated composite plates using FFT analyser. Avila *et.al* [2005] presented vibration analysis of fiber glass/epoxy/nanoclay nanocomposites using modal analysis. By performing a modal analysis it was be possible to identify crossing modes or changes in the vibration frequency sequence of the modes, variations on frequencies and on modal properties for each mode for each set of nanocomposites.

2.2.2 Buckling Analysis of Plates

The static stability or buckling of mechanical, civil engineering structures under compressive loading has always been an important field of research with the introduction of steel a century ago. Buckling phenomenon is critically dangerous to structural components because the buckling of composite plates usually occurs at a lower applied stress and generates large deformation. Buckling can cause severe damage in the structure before the stresses reach the ultimate strengths. This led to a focus on the study of buckling behavior in composite materials. The use of finite-elements analysis for investigation of buckling problem of composite panels is becoming popular due to the improvement in computational hardware and emergence of highly specialized software. Several workers have attempted to model and analyze the buckling problem. The relevant theoretical studies have been focused on the formulation of analytical solutions to predict the buckling load behavior using perturbation techniques such as the Bernoulli–Euler beam theory, the von Karman kinetic approach, elliptic integration, Rayleigh–Ritz method, thin film model, and differential quadrature method.

Most of these methods contain a collection of non-linear equations, or need the support of numerical tools. Loading or geometric parameters are not explicitly expressed. In view of the difficulty of theoretical analysis for composite laminated structure behaviors, numerical and experimental methods have become important in solving the buckling problem of a laminated composite plate.

The initial theoretical research into elastic flexural-torsional buckling was preceded by Euler's treatise on column flexural buckling, which gave the first analytical method of predicting the reduced strengths of slender columns. An experimental study of the uniaxial compressive stability of rectangular boron/epoxy laminated plates, clamped on the loaded edges and the unloaded edges simply supported was presented by Ashton and Love [1969]. Leissa [1987] provided a thorough overview of the countless number of papers available which are relevant to the stability of composite plates and shells. The buckling loads were determined by means of Southwell plots. Chai and Khong [1993] investigated the laminated plates under unidirectional loading using LVDT and strain gage to measure the out-of-plane deflection and in-plane strain respectively. The buckling loads from experiment well correlate with finite element solutions. Fleck *et al.* [1995] studied the effect of fiber architecture upon the compressive failure mechanism for fiber composite made up woven fabric. An experimental investigation was conducted by Gu and Chattopadhyay [1999] to study the behavior of delamination buckling, post buckling and delamination growth in composites. The variation in structural configurations, such as ply stacking sequence and the location and the length of the delamination, were considered. The delamination buckling mode was found to be closely related to the location and the length of the delamination. Excellent agreement was observed between the experimental values of critical load and those predicted by the previously developed new higher-order theory. Good comparisons are also presented for the initial post buckling behavior. Shrivastava and Singh [1999] studied experimentally the effect of aspect ratio on buckling of composite plates. Buckling loads were determined for different aspect ratios. It is observed that the effect of boundary conditions on the buckling load increases with increasing aspect ratio. Tuttle *et al.* [1999] determined buckling loads from plots of applied load vs. out-of-plane displacement. Shadow moiré technique method was used to monitor the whole-field out-of-plane deflections of the buckled plates. The maximum out-of-plane displacement was measured by placing a dial indicator on the specimen.

Roberts *et al.* [1999] found an experimental, numerical and analytical result for bending and buckling of rectangular orthotropic plates. There was a reasonably agreement between FEA, analytical and experimental buckling stresses for unstiffened solid plates. Shukla *et al.* [2005] proposed a formulation based on the first-order shear deformation theory and von-Karman-type nonlinearity to estimates the critical/buckling loads of laminated composite rectangular plates under in-plane uniaxial and biaxial loadings. Pannok and Singhatanadgid [2006] studied the buckling behavior of rectangular and skew thin composite plates with various boundary conditions using the Ritz method along with the proposed out-of-plane displacement functions. The boundary conditions considered in this study were combinations of simple support, clamped support and free edge. The out-of-plane displacement functions in form of trigonometric and hyperbolic functions were determined from the Kantorovich method. An experimental measurements and Numerical solutions on the buckling of single-delaminated glass –fiber composite laminates were carried out on rectangular Plates were presented by Pekbey and Sayman [2006]. ANSYS was used to analyze the critical buckling load of various laminated plates. Baba [2007] studied the influence of boundary conditions on the buckling load for rectangular plates. Numerical and experimental studies were conducted to investigate the effect of boundary conditions, length/thickness ratio, and ply orientation on the buckling behavior of E-glass/epoxy composite plates under in-plane compression load. Pein and Zahari [2007] investigated the structural behaviour of woven fabric composites subject to compressive load. The ultimate load and the structural and material behaviour of the composite laminated plates under compression were studied. Besides analytical study, there are several experimental studies on buckling of rectangular plates. A procedure for determining the buckling load of the aluminum rectangular plate was discussed by Supasak and Singhatanadgid [2012]. Buckling load of aluminum rectangular plates were determined using four different techniques, i.e. plot of applied load vs. out-of-plane displacement, plot of applied load vs. end shortening, plot of applied load vs. average in-plane strain, and the South well plot. In this study, the experimental results suggest that a plot of average strain gives the most reliable buckling load. The plots of out-of-plane displacement and end shortening produce a good tendency of buckling load from specimen to specimen. Analysis of critical buckling load of laminated composites plate with different boundary conditions using FEM and analytical methods was presented by Ozben [2009]. In this study, the critical buckling

load of fiber reinforced composite plate was calculated by analytical and finite element methods. The critical buckling loads and composite deformations were obtained on the basis of plate dimensions ratio (L_x/L_y). The critical buckling loads were obtained for different support conditions for the composite plates with symmetric and antisymmetric layup. However little attention has been given on experimental static stability analysis of woven fiber laminated composite plates. Recently, Zhange and Fu [2000, 2001] have proposed a new micromechanical model for predicting the buckling of woven fabrics using a combination of the traditional orthotropic model and their developed micromechanical model.

2.2.3 Dynamic Stability Analysis of Plates

Structural elements subjected to in-plane load may lead to dynamic instability, due to certain combinations of the values of load parameters. The instability may occur below the critical load of the structure under compressive loads over a range or ranges of excitation frequencies. Several means of combating parametric resonance such as damping and vibration isolation may be inadequate and sometimes dangerous with reverse results [1965]. Dynamic instability was first observed by Faraday [1831]. He observed that the liquid (wine) in a cylinder (wineglass) oscillated with half of the frequency of the exciting force movement of moist fingers around the glass edge. The first mathematical explanation of the phenomenon is given by Rayleigh [1883]. The general theory of dynamic stability of elastic systems of deriving the coupled second order differential equations of the Mathiew-Hill type and the determination of the regions of instability by seeking a periodic solution using Fourier series expansion was explained by Bolotin [1964]. Since Bolotin introduced the subject of dynamic stability under periodic loads, the topic has attracted much interest. A comprehensive review of early developments in the parametric instability of structural elements including plates was presented in the review articles by Simites [1987] and Sahu and Datta [2007].

To bypass difficulties obtained due to analytical results, the finite element is proposed for the by Hutt and Salam [1971] using four noded thin plate finite element models under few boundary conditions, neglecting shear deformation using a four noded thin plate finite

element method. Srinivasan and Chellapandi [1986] analyzed laminated composite plates under uniaxial loading. The edges were clamped and the finite strip method was used to discretize the problem. With damping neglected, a set of coupled Mathieu equations was obtained, and Hill's method of infinite determinants was applied to obtain instability regions. Prabhakara and Datta [1993] explained the parametric instability characteristics of rectangular plates subjected to in-plane periodic load using finite element method, considering shear deformation. Deolasi and Datta [1995] studied the parametric instability characteristics of rectangular plates subjected to localized tension and compression edge loading using Bolotin's approach. They presented results of dynamic stability of thin, square, isotropic plates for classical simply supported boundary conditions having three degrees of freedom per node.

There is a renewed interest on the subject after Birman [1987] investigated the effect of shear deformation on dynamic stability of simply supported antisymmetric angle-ply rectangular plate's neglecting in-plane displacement and rotary inertia. The effect of unsymmetrical lamination on the distribution of the instability regions was investigated in this study. Chen and Yang [1990] investigated on the dynamic stability of thick anti-symmetric angle-ply laminated composite plates subjected to uniform compressive stress and/or bending stress using Galerkin's finite element. The thick plate model included the effects of transverse shear deformation and rotary inertia. The instability of composite laminated plates under uniaxial in-plane loads was investigated by Moorthy *et al.* [1990] without static load component using finite element method. The dynamic instability of antisymmetric angle-ply and cross-ply laminated plates subjected to periodic in-plane loads was investigated using a higher order shear deformation lamination theory and the method of multiple-scale analysis by Cederbaum [1991]. Kwon [1991] studied the dynamic instability of layered composite plates subjected to biaxial loading using a high order bending theory. Chattopadhyay and Radu [2000] used the higher order shear deformation theory to investigate the dynamic instability of composite plates by using the finite element approach. The first two instability regions were determined for various loading conditions using both first and second order approximations. Sahu and Datta [2000] studied the parametric instability of laminated composite plates subjected to non-uniform in-plane periodic loads using finite element, considering static component of

load. Extensive results were presented on the effects of different parameters on dynamic stability of angle-ply plates. Wang and Dawe [2002] presented B-spline finite strip method for the dynamic instability analysis of composite laminated rectangular plates and prismatic plate structures, based on the use of first-order shear deformation plate theory. Chakrabarti and Sheikh [2006] studied the dynamic instability of laminated sandwich plates subjected to inplane partial edge loading by using finite element method. Dey and Singh [2006] examined the dynamic stability characteristics of simply supported laminated composite skew plates subjected to a periodic in-plane load by using finite element approach.

Recently an extensive bibliography of earlier works on dynamic stability of plates was given by Sahu and Datta [2006]. A review of composite structures subjected to dynamic loading is studied by Hampson and Moatamedi [2007]. Particular attention was given to experimental apparatus and techniques used for the different impact velocity regimes, and the implementation of failure criteria in finite element (FE) methods which predict material behavior. However, most of the investigations were limited to the theoretical studies for the determination of parametric resonance zones. Chen *et al.* [2009] studied the dynamic stability of laminated hybrid composite plates subjected to periodic uniaxial and bending stress and the instability region was marked by Bolotin's method.

Experimental investigations of parametrically excited rectangular plates, however, have not been too numerous. Apparently, the first experimental studies on plates were conducted by Somerset and Evan-Iwanowski [1967] and they pertained mainly nonlinear parametric response of simply supported square plates. Dixon and Wright [1972] studied experimentally the parametric instability behavior of plates subjected to in-plane periodic forces. In this paper, the theoretical and experimental results of an investigation into the parametric instability of flat rectangular plates were presented and discussed. Carlson [1974] conducted experiments on the parametric response characteristics of a tensioned sheet with a crack like opening. Cutouts, cracks and other kinds of discontinuities were inevitable in structures due to practical considerations. Nguyen, Ostiguy and Samson [1989] were performed experimentally to investigate the dynamic stability and responses of four rectangular plates subjected to periodic in-plane loads and under four different sets of boundary conditions. Special attention is paid to satisfy the boundary conditions assumed in the analytical models

so as to draw conclusion with sufficient degree of confidence. The results also show that a parametric combination resonance is not important as compared with a principal parametric resonance for the problem under investigation. Deolasi and Datta [1997] experimentally investigated on parametric vibration response characteristics of aluminum plates subjected to tensile edge loading. Two distinct types of parametric instability behavior were observed: i.e. principal resonance and secondary resonance. The principal resonance was found to be more dominant. The location of loading on the edge is found to have a considerable influence on natural frequencies and parametric instability behavior of plates. Yang and Huang [2009] presents a dynamic stability analysis of a simply supported 3D braided composite laminated plate with surface-bonded piezoelectric layers, subjected to electrical and periodic in-plane mechanical loads. Theoretical formulations were based on Reddy's higher order shear deformation plate theory and include piezoelectric effects.

2.3. Critical Discussion

On the whole, the focus of the research is changing from vibration to buckling effects and then to parametric instability. Recently more studies were conducted on woven fiber laminated composites than unidirectional composite materials. As regards to the methodology, the focus is shifted from analytical methods to numerical method using finite element methods and experimental method.

The study reveals that investigators were now concentrating on analysis of complicated aspects of different parameters and different boundary conditions of plates. From the above review of literature, the inherent lacunae of earlier investigations which need further attention of future researchers are summarized below.

However, in most of the studies mentioned on dynamic instability of unidirectional composite plates were reported. The study of the parametric instability of woven fiber laminated composite plates subjected to harmonic in-plane loading is relatively new subject. To author's knowledge no experiment has been done on parametric instability of woven fiber composite plates subjected to harmonic in-plane loading. The effect of different parameters on the parametric instability has been studied in details. The laboratory apparatus, plate

specimens, boundary conditions of the plate specimen, test procedure and recorded data are described in some details. Experimental data compared with FEM results in order to form a qualitative and quantitative verification of the solutions. It is found that theoretical results are generally in good agreement with experimental results.

2.4. Objective and Scope of the Present Investigation

No work is reported in literature on parametric instability of industry driven woven fiber laminated composite plates subjected to harmonic in-plane loading. The present study is mainly aimed at filling some of the lacunae that exist in the proper understanding of the parametric instability of woven fiber composite plates subjected to in plane periodic loads. The present research aimed at mostly experimental but also includes numerical study using finite element method on parametric instability characteristics of industry driven woven fiber composite panels subjected to in plane harmonic loading. The influence of various parameters like side to thickness ratios, number of layers, lamination sequence, and ply orientation, degree of orthotropy, static and dynamic load factors on the vibration and instability behavior of laminated plates is examined.

Based on the review of literature, the different modules identified for the present investigation are presented as follows

- Experimental and Numerical Study on Free vibration of woven fiber composite plates.
- Experimental and Numerical Study on Buckling of woven fiber composite plates.
- Experimental and Numerical Study on Parametric instability of woven fiber composite plates.

Due to its practical importance and uniqueness in the above fields, this influence the various parameters such as aspect ratio, side to thickness ratio, static and dynamic load factors, ply-orientations, lamination angle, orthotropic on the parametric resonance characteristics of laminated composite plates are examined in detail.

Chapter-3

MATHEMATICAL FORMULATION

3.1 The Basic Problems

This chapter presents the mathematical formulation for vibration, static and dynamic stability analysis of the laminated composite plate structures. So, numerical method like finite element method (FEM) is more preferred than analytical method for solving problems involving composite laminate. In this method the structure is divided into a finite number of elements reducing the structure having infinite degrees of freedom to finite degrees of freedom and each element is normally of simple geometry and therefore easier to analyze than the actual structure.

The basic configuration of the problem considered here is a composite laminated plate of sides 'a' and 'b' subjected to harmonic in-plane edge loading $N(t)$ as shown in the Figure 3.1. The lamination sequence and Plan-form subjected to in-plane load $N(t)$ is also shown in Figure 3.2 and Figure 3.3.

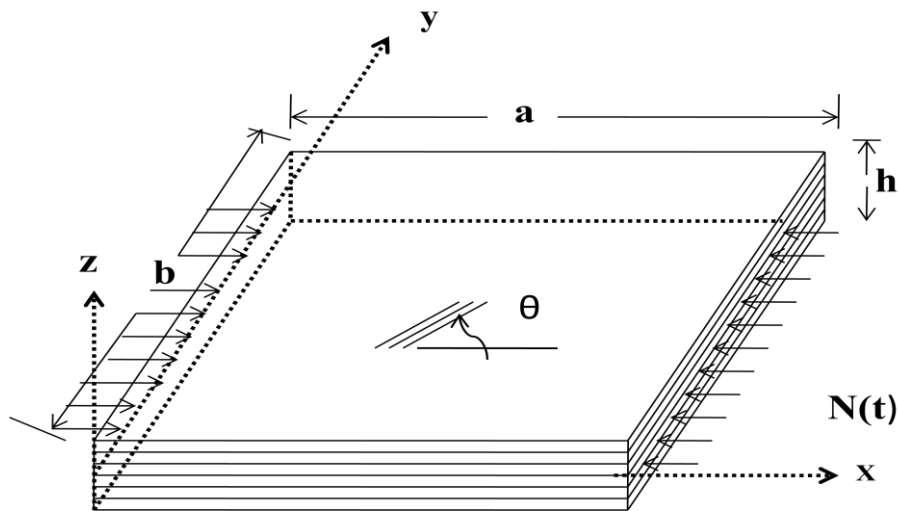


Figure 3.1: Laminated Composite Plate under in-plane harmonic Loading

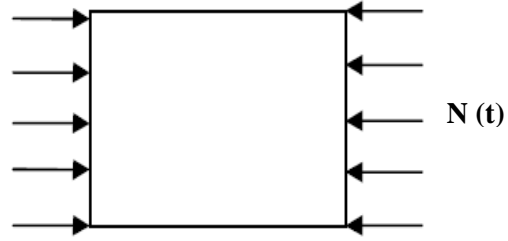
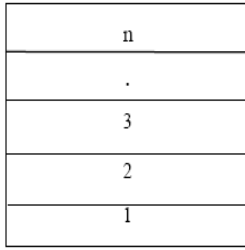


Figure 3.2: **Lamination sequence** Figure 3.3: **Plan-form subjected to in-plane load $N(t)$**

3.2 Proposed Analysis

The governing equations for the structural behavior of the laminated plates are derived on the basis of first order shear deformation theory. The element elastic stiffness, geometric stiffness and mass matrices are derived on the basis of principle of minimum potential energy and Lagrange's equation. The governing equations for the dynamic stability of laminated woven fiber composite plate subjected to in-plane loading are developed using first order shear deformation theory (FSDT). The equation of motion represents a system of second order differential equation with periodic coefficients of the Mathieu-Hill type. The development of the regions of instability arises from Floquet's theory and the solution is obtaining using Bolotin's approach using finite element method (FEM). The assumptions made in this analysis are summarized as follows:

3.2.1 Assumptions of the Analysis

- The material behavior is linear and elastic.
- The thickness of the laminate is small compared to the other dimensions. The deflections of the laminated plate are small compared to laminate thickness.
- The loading considered is axial with simple harmonic fluctuation with respect to time.
- All damping effects are neglected.

3.3 Governing Equations

The governing differential equations, the strain energy due to loads, kinetic energy and formulation of general buckling problems are derived on the basis of minimum potential energy and Lagrange's equation.

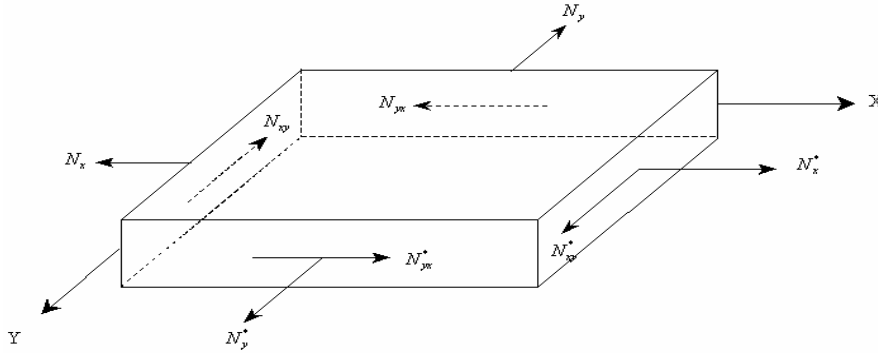


Figure 3.4 [a]: Inplane Forces on a Laminate

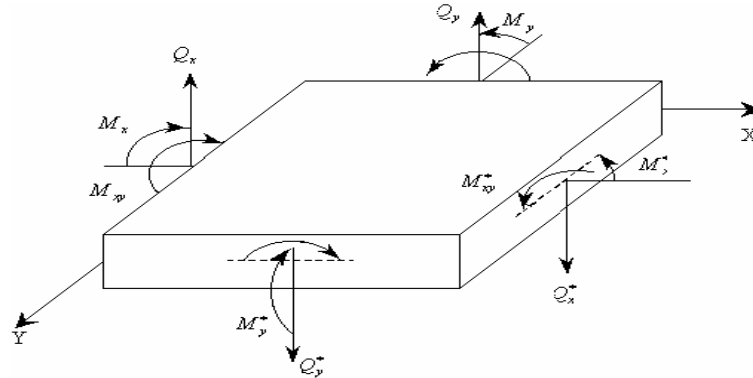


Figure 3.4 [b]: Moments on a Laminate

3.3.1 Governing Differential Equation

The equation of motion is obtained by taking a differential element of plate as shown in figure 3.4[a] and 3.4[b]. The figure shows an element with internal forces (N_x , N_y , N_{xy}), shearing forces (Q_x and Q_y) and the moment resultants (M_x , M_y and M_{xy}) on laminate. The governing differential equations for vibration of general laminated composite plates derived on the basis of first order shear deformation theory (FSDT) subjected to in-plane loading can be written as:

$$\left. \begin{aligned} \frac{\partial N_x}{\partial x} + \frac{\partial N_{xy}}{\partial y} &= P_1 \frac{\partial^2 u}{\partial t^2} + P_2 \frac{\partial^2 \theta_x}{\partial t^2} \\ \frac{\partial N_{xy}}{\partial x} + \frac{\partial N_y}{\partial y} &= P_1 \frac{\partial^2 v}{\partial t^2} + P_2 \frac{\partial^2 \theta_y}{\partial t^2} \\ \frac{\partial Q_x}{\partial x} + \frac{\partial Q_y}{\partial y} + N_x^0 \frac{\partial^2 w}{\partial x^2} + N_y^0 \frac{\partial^2 w}{\partial y^2} &= P_1 \frac{\partial^2 w}{\partial t^2} \\ \frac{\partial M_x}{\partial x} + \frac{\partial M_{xy}}{\partial y} - Q_x &= P_3 \frac{\partial^2 \theta_x}{\partial t^2} + P_2 \frac{\partial^2 u}{\partial t^2} \\ \frac{\partial M_{xy}}{\partial x} + \frac{\partial M_y}{\partial y} - Q_y &= P_3 \frac{\partial^2 \theta_y}{\partial t^2} + P_2 \frac{\partial^2 v}{\partial t^2} \end{aligned} \right\} \quad (3.3.1)$$

Where N_x , N_y and N_{xy} are the in-plane stress resultants, N_x^0 and N_y^0 are the external loading in X and Y directions respectively.

M_x , M_y and M_{xy} are moment resultants and Q_x , Q_y = transverse shear stress resultants.

$$(P_1, P_2, P_3) = \sum_{k=1}^n \int_{z_{k-1}}^{z_k} (\rho)_k (1, z, z^2) dz \quad (3.3.2)$$

Where n= number of layers of laminated composite plates, $(\rho)_k$ = mass density.

3.4 Dynamic Stability Studies:

The equation of motion for vibration of a laminated composite panel, subjected to generalized in-plane load $N(t)$ May be expressed in the matrix form as:

$$[M]\{\ddot{q}\} + [[K] - N(t)[K_g]]\{q\} = 0 \quad (3.4.1)$$

Where ‘q’ is the vector of degrees of freedoms (u, v, w, θ_x , θ_y). The in-plane load ‘N (t)’ may be harmonic and can be expressed in the form:

$$N(t) = N_s + N_t \cos \Omega t \quad (3.4.2)$$

Where N_s the static portion of load N (t), N_t the amplitude of the dynamic portion of N (t) and Ω is the frequency of the excitation. The stress distribution in the panel may be periodic.

Considering the static and dynamic component of load as a function of the critical load,

$$N_s = \alpha N_{cr} , \quad N_t = \beta N_{cr} \quad (3.4.3)$$

Where α and β are the static and dynamic load factors respectively. Using Eq. (3.4.2), the equation of motion for panel in under periodic loads is reduced to:

$$[M]\{\ddot{q}\} + [[K] - \alpha N_{cr}[K_g] - \beta N_{cr}[K_g]\cos\Omega t]\{q\} = 0 \quad (3.4.4)$$

The above Eq. (3.4.4) represents a system of differential equations with periodic coefficients of the Mathieu-Hill type. The development of regions of instability arises from Floquet's theory which establishes the existence of periodic solutions of periods T and $2T$. The boundaries of the primary instability regions with period $2T$, where $T=2\pi/\Omega$ are of practical importance and the solution can be achieved in the form of the trigonometric series:

$$q(t) = \sum_{k=1,3,5,\dots}^{\infty} [\{a_k\}\sin(k\Omega t/2) + \{b_k\}\cos(k\Omega t/2)] \quad (3.4.5)$$

Putting this Eq. (3.4.5) in Eq. (3.4.4) and if only first term of the series is considered, equating coefficients of $\sin \Omega t/2$ and $\cos \Omega t/2$, the Eq. (3.4.4) reduces to

$$[[K] - \alpha N_{cr}[K_g] \pm \frac{1}{2}\beta N_{cr}[K_g] - \frac{\Omega^2}{4}[M]]\{q\} = 0 \quad (3.4.6)$$

Eq. (3.4.6) represents an eigen value problem for known values of α , β and N_{cr} , where α , β and N_{cr} are static load factor, dynamic load factor and reference load respectively. K , K_g and M are elastic stiffness, geometric stiffness and mass matrices respectively. The two conditions under the plus and minus sign correspond to two boundaries (upper and lower) of the dynamic instability region. The above eigenvalue solution gives of Ω , which give the boundary frequencies of the instability regions for the given values of α and β . In this analysis, the computed static buckling load of the panel is considered as the reference load. Before solving the above equations, the stiffness matrix $[K]$ is modified through incorporation of conditions and imposition of boundary conditions. In this analysis, the

computed static buckling load of the panel is considered as the reference load in line with many previous investigations (Ganapati *et al.* [1999], and Moorthy, Reddy and Plaut [1990]). This equation represents a solution to a number of related problems:

(1) Free vibration: $\alpha = 0$, $\beta = 0$ and $\omega = \Omega/2$

$$[[\mathbf{K}] - \omega^2 [\mathbf{M}]] \{q\} = 0 \quad (3.4.7)$$

(2) Vibration with static axial load: $\beta = 0$ and $\omega = \Omega/2$

$$[[\mathbf{K}] - \alpha N_{cr} [\mathbf{K}_g] - \omega^2 [\mathbf{M}]] \{q\} = 0 \quad (3.4.8)$$

(3) Static stability: $\alpha = 1$, $\beta = 0$, $\Omega = 0$

$$[[\mathbf{K}] - \alpha N_{cr} [\mathbf{K}_g]] \{q\} = 0 \quad (3.4.9)$$

3.5 Finite Element Formulation

For problems involving complex geometrical and boundary conditions, analytical methods are not easily adaptable and numerical methods like finite element methods (FEM) are preferred. The finite element formulation is developed hereby for the structural analysis of composite plates based on first order shear deformation theory.

3.5.1 Discretisation of Structure

The process of modeling a structure using suitable number, shape and size of the elements is called discretization. The modeling should be good enough to get the results as close to actual behavior of the structure as possible. The continuum is divided into ‘finite’ number of elements and connected only at the nodal points.

3.5.2 The Plate Element

An eight noded isoparametric element is employed in the present analysis with five degrees of freedom u , v , w , θ_x and θ_y per node. A Composite plate of length ‘a’ and width ‘b’ consisting of ‘n’ number of thin homogeneous arbitrarily oriented orthotropic layers having a total thickness ‘h’ is considered as shown in figure 3.5. The x-y axes refer to the reference axes and the principal material axes are indicated by the axes 1-2. The angle ‘ θ ’ measured in the anti-clockwise direction of x-axis represents the fiber orientation.

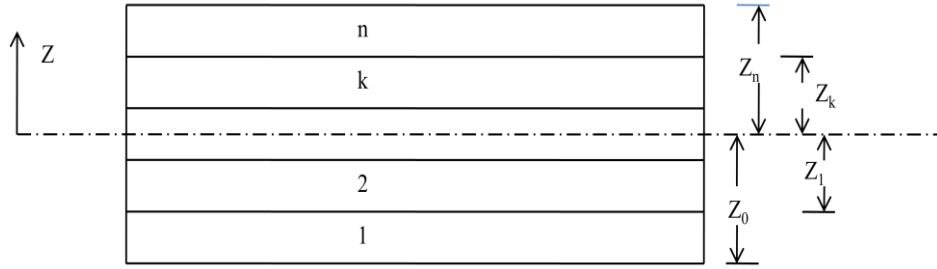


Fig 3.5: **N layered laminate configurations**

The displacement field assumes that mid-plane normal remains straight before and after deformation, but not normal even after deformation so that:

$$\left. \begin{aligned} u(x, y, z) &= u^0(x, y) + z\theta_x(x, y) \\ v(x, y, z) &= v^0(x, y) + z\theta_y(x, y) \\ w(x, y, z) &= w^0(x, y) \end{aligned} \right\} \quad (3.5.1)$$

Where u , v , w are displacements in the x , y , z directions respectively for any point, u^0, v^0, w^0 are those at the middle plane of the plate. θ_x, θ_y are the rotations of the cross section normal to the y and x axis respectively. Assuming small deformations, the generalized linear in-plane strains of the laminate at a distance z from the mid-surface is given by:

$$\{\epsilon_{xx} \epsilon_{yy} \gamma_{xy}\}^T = \{\epsilon_{xx} \epsilon_{yy} \gamma_{xy}\}^T + z \{k_{xx} k_{yy} k_{xy}\}^T \quad (3.5.2)$$

Where $\epsilon_{xx}, \epsilon_{yy}, \gamma_{xy}$ are mid-plane strains and k_{xx}, k_{yy}, k_{xy} are curvatures of the laminated plate.

The elastic stiffness matrix, geometric stiffness matrix due to applied in-plane loads and mass matrices of the elements are derived using the principle of minimum potential energy. The shape functions of the element are derived using the interpolation polynomial given below based on Pascal's triangle for convergence criteria.

$$u(\xi, \eta) = a_1 + a_2\xi + a_3\eta + a_4\xi^2 + a_5\xi\eta + a_6\eta^2 + a_7\xi^2\eta + a_8\xi\eta^2 \quad (3.5.3)$$

The displacements are expressed in terms of their nodal values by using the element shape functions and are given by.

$$\begin{aligned}
 u &= \sum_{i=1}^8 N_i u_i, v = \sum_{i=1}^8 N_i v_i, w = \sum_{i=1}^8 N_i w_i \\
 \theta_x &= \sum_{i=1}^8 N_i \theta_{xi}, \theta_y = \sum_{i=1}^8 N_i \theta_{yi}
 \end{aligned} \tag{3.5.4}$$

The shape function N_i are defined as

$$\begin{aligned}
 N_i &= \frac{1}{4} (1 + \xi \xi_i) (1 + \eta \eta_1) (\xi \xi_1 + \eta \eta_1 - 1) \quad \text{For } i = 1, 2, 3 \text{ \& } 4 \\
 N_i &= \frac{1}{2} (1 - \xi^2) (1 + \eta \eta_i) \quad \text{For } i = 5, 7 \\
 N_i &= \frac{1}{2} (1 - \xi \xi_i) (1 - \eta^2) \quad \text{For } i = 6, 8
 \end{aligned} \tag{3.5.5}$$

ξ, η = Local natural co-ordinates of an element

N_i = Shape function at a node i

3.5.3 Strain Displacement Relations

Green-Lagrange's strain displacement relations are presented in general throughout the analysis. The linear part of the strain is used to derive the elastic stiffness matrix and the non-linear part of the strain is used to derive the geometric stiffness matrix. The total strain is given by

$$\{\epsilon\} = \{\epsilon_l\} + \{\epsilon_{nl}\} \tag{3.5.6}$$

The linear generalized shear deformable strain displacement relations are

$$\epsilon_{xl} = \frac{\partial u}{\partial x} + z k_x$$

$$\varepsilon_{yl} = \frac{\partial v}{\partial y} + z k_y$$

$$\gamma_{xyl} = \frac{\partial u}{\partial y} + \frac{\partial v}{\partial x} + z k_{xy} \quad (3.5.7)$$

$$\gamma_{xzl} = \frac{\partial w}{\partial x} + \theta_x$$

$$\gamma_{yzl} = \frac{\partial w}{\partial y} + \theta_y$$

The bending strains k_j are expressed as,

$$k_x = \frac{\partial \theta_x}{\partial x}, \quad k_y = \frac{\partial \theta_y}{\partial y}$$

$$k_{xy} = \frac{\partial \theta_x}{\partial y} + \frac{\partial \theta_y}{\partial x} \quad (3.5.8)$$

The linear strain $\{\varepsilon\}$ can be expressed in terms of displacement as:

$$\{\varepsilon\} = [B] \{\delta_e\} \quad (3.5.9)$$

$$\text{Where } \{\delta_e\} = \{u_1, v_1, w, \theta_{x1}, \theta_{y1}, \dots, u_8, v_8, w_8, \theta_{x8}, \theta_{y8}\}^T, \quad (3.5.10)$$

$$\text{And } [B] = [[B1], [B2], \dots, [B8]] \quad (3.5.11)$$

$$[B] = \sum_{i=1}^8 \begin{bmatrix} N_{i,x} & 0 & 0 & 0 & 0 \\ 0 & N_{i,y} & 0 & 0 & 0 \\ N_{i,y} & N_{i,x} & 0 & 0 & 0 \\ 0 & 0 & 0 & 0 & N_{i,x} \\ 0 & 0 & 0 & N_{i,y} & 0 \\ 0 & 0 & 0 & N_{i,x} & N_{i,y} \\ 0 & 0 & N_{i,x} & 0 & N_i \\ 0 & 0 & N_{i,y} & N_i & 0 \end{bmatrix} \quad (3.5.12)$$

[B] is called the strain displacement matrix

3.5.4 Constitutive Relations

A macro-mechanical analysis was carried out to establish the relationship between the forces and general strains of a laminate. The elastic behavior of each lamina is essentially two dimensional and orthotropic in nature. So the elastic constants for the composite lamina are given below.

E_{11} = Modulus of Elasticity of Lamina along 1-direction

E_{22} = Modulus of Elasticity of Lamina along 2-direction

G_{12} = Shear Modulus

ν_{12} = Major Poisson's ratio

ν_{21} = Minor Poisson's ratio

The stress strain relation for the k^{th} lamina is,

$$\begin{Bmatrix} \sigma_x \\ \sigma_y \\ \tau_{xy} \\ \tau_{xz} \\ \tau_{yz} \end{Bmatrix} = \begin{bmatrix} Q_{11} & Q_{12} & 0 & 0 & 0 \\ Q_{12} & Q_{22} & 0 & 0 & 0 \\ 0 & 0 & Q_{66} & 0 & 0 \\ 0 & 0 & 0 & Q_{44} & 0 \\ 0 & 0 & 0 & 0 & Q_{55} \end{bmatrix} \begin{Bmatrix} \epsilon_x \\ \epsilon_y \\ \gamma_{xy} \\ \gamma_{xz} \\ \gamma_{yz} \end{Bmatrix} \quad (3.5.13)$$

Where

$$\begin{aligned} Q_{11} &= \frac{E_{11}}{(1-\nu_{12}\nu_{21})}, Q_{12} = \frac{E_{11}\nu_{21}}{(1-\nu_{12}\nu_{21})}, Q_{21} = \frac{E_{22}\nu_{12}}{(1-\nu_{12}\nu_{21})}, Q_{22} = \frac{E_{22}}{(1-\nu_{12}\nu_{21})} \\ Q_{66} &= G_{12} \\ Q_{44} &= kG_{13} \\ Q_{55} &= kG_{23} \end{aligned} \quad (3.5.14)$$

The on-axis elastic constant matrix $[Q_{ij}]_k$ corresponding to material axes 1-2 for k^{th} layer is given by

$$\left. \begin{aligned} [Q_{ij}]_k &= \begin{bmatrix} Q_{11} & Q_{12} & 0 \\ Q_{12} & Q_{22} & 0 \\ 0 & 0 & Q_{66} \end{bmatrix} \text{ For } i, j = 1, 2, 6 \\ [Q_{ij}]_k &= \begin{bmatrix} Q_{44} & 0 \\ 0 & Q_{55} \end{bmatrix} \text{ For } i, j = 4, 5 \end{aligned} \right\} \quad (3.5.15)$$

For obtaining the off-axis elastic constant matrix, $[Q_{ij}]_k$ corresponding to any arbitrarily oriented reference x-y axes for the k^{th} layer, appropriate transformation is required. Hence the off-axis elastic constant matrix is obtained from the on axis elastic constant matrix by the relation:

$$\left. \begin{aligned} [\bar{Q}_{ij}]_k &= \begin{bmatrix} \bar{Q}_{11} & \bar{Q}_{12} & \bar{Q}_{16} \\ \bar{Q}_{12} & \bar{Q}_{22} & \bar{Q}_{26} \\ \bar{Q}_{16} & \bar{Q}_{26} & \bar{Q}_{66} \end{bmatrix} \text{ for } i, j = 1, 2, 6 \\ [\bar{Q}_{ij}]_k &= \begin{bmatrix} \bar{Q}_{44} & \bar{Q}_{45} \\ \bar{Q}_{45} & \bar{Q}_{55} \end{bmatrix}_k \text{ for } i, j = 4, 5 \end{aligned} \right\} \quad (3.5.16)$$

$$[\bar{Q}_{ij}]_k = [T]^{-1} [Q_{ij}]_k [T] \quad (3.5.17)$$

Where $[T]$ = Transformation matrix = $\begin{bmatrix} m^2 & n^2 & 2mn \\ n^2 & m^2 & -2mn \\ -mn & mn & m^2 - n^2 \end{bmatrix}_k$

The off-axis stiffness values are:

$$\begin{aligned}
 \bar{Q}_{11} &= Q_{11}m^4 + 2(Q_{12} + 2Q_{66})m^2n^2 + Q_{22}n^4 \\
 \bar{Q}_{12} &= (Q_{11} + Q_{22} - 4Q_{66})m^2n^2 + Q_{12}(m^4 + n^4) \\
 \bar{Q}_{22} &= Q_{11}n^4 + 2(Q_{12} + 2Q_{66})m^2n^2 + Q_{22}m^4 \\
 \bar{Q}_{16} &= (Q_{11} - Q_{12} - 2Q_{66})m^3n + (Q_{12} - Q_{22} + 2Q_{66})n^3m \\
 \bar{Q}_{26} &= (Q_{11} - Q_{12} - 2Q_{66})mn^3 + (Q_{12} - Q_{22} + 2Q_{66})m^3n \\
 \bar{Q}_{66} &= (Q_{11} + Q_{22} - 2Q_{12} - 2Q_{66})m^2n^2 + Q_{66}(m^4 + n^4)
 \end{aligned} \tag{3.5.18}$$

The stiffness corresponding to transverse deformations are:

$$\begin{aligned}
 \bar{Q}_{44} &= G_{13}m^2 + G_{23}n^2 \\
 \bar{Q}_{45} &= (G_{13} - G_{23})mn \\
 \bar{Q}_{55} &= G_{13}n^2 + G_{23}m^2
 \end{aligned} \tag{3.5.19}$$

Where $m=\cos\theta$ and $n=\sin\theta$; and θ =angle between the arbitrary principal axis with the material axis in a layer.

The force and moment resultants are obtained by integrating the stresses and their moments through the laminate thickness as given by

$$\begin{Bmatrix} N_x \\ N_y \\ N_{xy} \\ M_x \\ M_y \\ M_{xy} \\ Q_x \\ Q_y \end{Bmatrix} = \int_{-h/2}^{h/2} \begin{Bmatrix} \sigma_x \\ \sigma_y \\ \tau_{xy} \\ \sigma_x z \\ \sigma_y z \\ \tau_{xy} z \\ \tau_{xz} \\ \tau_{yz} \end{Bmatrix} dz \tag{3.5.20}$$

$$\begin{Bmatrix} N_x \\ N_y \\ N_{xy} \\ M_x \\ M_y \\ M_{xy} \\ Q_x \\ Q_y \end{Bmatrix} = \begin{bmatrix} A_{11} & A_{12} & A_{16} & B_{11} & B_{12} & B_{16} & 0 & 0 \\ A_{12} & A_{22} & A_{26} & B_{12} & B_{22} & B_{26} & 0 & 0 \\ A_{16} & A_{26} & A_{66} & B_{16} & B_{26} & B_{66} & 0 & 0 \\ B_{11} & B_{12} & B_{16} & D_{11} & D_{12} & D_{16} & 0 & 0 \\ B_{12} & B_{22} & B_{26} & D_{12} & D_{22} & D_{26} & 0 & 0 \\ B_{16} & B_{26} & B_{66} & D_{16} & D_{26} & D_{66} & 0 & 0 \\ 0 & 0 & 0 & 0 & 0 & 0 & S_{44} & S_{45} \\ 0 & 0 & 0 & 0 & 0 & 0 & S_{45} & S_{55} \end{bmatrix} \begin{Bmatrix} \varepsilon_x \\ \varepsilon_y \\ \gamma_{xy} \\ k_x \\ k_y \\ k_{xy} \\ \gamma_{xz} \\ \gamma_{yz} \end{Bmatrix} \quad (3.5.21)$$

This can also be stated as

$$\begin{Bmatrix} N_i \\ M_i \\ Q_i \end{Bmatrix} = \begin{bmatrix} A_{ij} & B_{ij} & 0 \\ B_{ij} & D_{ij} & 0 \\ 0 & 0 & S_{ij} \end{bmatrix} \begin{Bmatrix} \varepsilon_j \\ k_j \\ \gamma_m \end{Bmatrix} \quad (3.5.22)$$

Or

$$\{F\} = [D]\{\varepsilon\} \quad (3.5.23)$$

Where A_{ij} , B_{ij} and S_{ij} are the extensional, bending- stretching coupling, bending and transverse shear stiffnesses. They may be defined as

$$\begin{aligned} A_{ij} &= \sum_{k=1}^n (\overline{Q_{ij}})_k (z_k - z_{k-1}) \\ B_{ij} &= \frac{1}{2} \sum_{k=1}^n (\overline{Q_{ij}})_k (z_k^2 - z_{k-1}^2) \\ D_{ij} &= \frac{1}{3} \sum_{k=1}^n (\overline{Q_{ij}})_k (z_k^3 - z_{k-1}^3) \quad \text{For } i, j = 1, 2, 6 \\ S_{ij} &= \kappa \sum_{k=1}^n (\overline{Q_{ij}})_k (z_k - z_{k-1}) \quad \text{For } i, j = 4, 5 \end{aligned} \quad (3.5.24)$$

κ = shear correction factor =5/6 in-line with previous studies [Whitney and Pagano [1970] and Reddy [1979]]

z_k, z_{k-1} = top and bottom distance of lamina from mid-plane.

3.5.5 Elastic stiffness matrix

The element matrices in natural coordinate system are derived as

$$[K]_e = \int_{-1}^{+1} \int_{-1}^{+1} [B]^T [D] [B] |J| d\xi d\eta \quad (3.5.25)$$

Where $[B]$ is called the strain displacement matrix

3.5.6 Geometric stiffness matrix $[K_g]_e$

The element geometric stiffness matrix is derived using the non-linear in-plane strains. The strain energy due to initial stresses is

$$[U]_2 = \int_v [\sigma^0]^T \{\varepsilon_{nl}\} dV \quad (3.5.26)$$

Using non-linear strains, the strain energy can be written in matrix form as

$$[U]_2 = \frac{1}{2} \int_v [f]^T [S] [f] dV \quad (3.5.27)$$

Where

$$[f] = \left[\frac{\partial u}{\partial x}, \frac{\partial u}{\partial y}, \frac{\partial v}{\partial x}, \frac{\partial v}{\partial y}, \frac{\partial w}{\partial x}, \frac{\partial w}{\partial y}, \frac{\partial \theta_x}{\partial x}, \frac{\partial \theta_x}{\partial y}, \frac{\partial \theta_y}{\partial x}, \frac{\partial \theta_y}{\partial y} \right]^T \quad (3.5.28)$$

And

$$[S] = \begin{bmatrix} s & 0 & 0 & 0 & 0 \\ 0 & s & 0 & 0 & 0 \\ 0 & 0 & s & 0 & 0 \\ 0 & 0 & 0 & s & 0 \\ 0 & 0 & 0 & 0 & s \end{bmatrix} \quad (3.5.29)$$

Where

$$[s] = \begin{bmatrix} \sigma_x & \tau_{xy} \\ \tau_{xy} & \sigma_y \end{bmatrix} = \frac{1}{h} \begin{bmatrix} N_x & N_{xy} \\ N_{xy} & N_y \end{bmatrix} \quad (3.5.30)$$

The in-plane stress resultants N_x, N_y, N_{xy} at each gauss point are obtained by applying uniaxial stress in x-direction and the geometric stiffness matrix is formed for these stress resultants.

$$\{F\} = [G] \{\delta_e\} \quad (3.5.31)$$

The strain energy becomes

$$[U]_2 = \frac{1}{2} \int_v \{\delta_e\}^T [G]^T [S] [G] \{\delta_e\} dV = \frac{1}{2} \{\delta_e\}^T [K_g] \{\delta_e\} \quad (3.5.32)$$

Where element geometric stiffness matrix

$$[K_g]_e = \int_{-1}^{+1} \int_{-1}^{+1} [G]^T [S] [G] |J| d\xi d\eta \quad (3.5.33)$$

where

$$[G] = \begin{bmatrix} N_{i,x} & 0 & 0 & 0 & 0 \\ N_{i,y} & 0 & 0 & 0 & 0 \\ 0 & N_{i,x} & 0 & 0 & 0 \\ 0 & N_{i,y} & 0 & 0 & 0 \\ 0 & 0 & N_{i,x} & 0 & 0 \\ 0 & 0 & N_{i,y} & 0 & 0 \\ 0 & 0 & 0 & N_{i,x} & 0 \\ 0 & 0 & 0 & N_{i,y} & 0 \\ 0 & 0 & 0 & 0 & N_{i,x} \\ 0 & 0 & 0 & 0 & N_{i,y} \end{bmatrix} \quad (3.5.34)$$

3.5.7 Element mass matrix

$$[M]_e = \int_{-1}^{+1} \int_{-1}^{+1} [N]^T [P] [N] |J| d\xi d\eta \quad (3.5.35)$$

Where the shape function matrix

$$[N] = \sum_{i=1}^8 \begin{bmatrix} N_i & 0 & 0 & 0 & 0 \\ 0 & N_i & 0 & 0 & 0 \\ 0 & 0 & N_i & 0 & 0 \\ 0 & 0 & 0 & N_i & 0 \\ 0 & 0 & 0 & 0 & N_i \end{bmatrix}$$

$$[P_1] = \begin{bmatrix} P_1 & 0 & 0 & 0 & 0 \\ 0 & P_1 & 0 & 0 & 0 \\ 0 & 0 & P_1 & 0 & 0 \\ 0 & 0 & 0 & I & 0 \\ 0 & 0 & 0 & 0 & I \end{bmatrix}$$

$$\text{In which, } P_1 = \sum_{k=1}^n \int_{e_{k-1}}^{e_k} \rho dz \quad \text{And} \quad I = \sum_{K=1}^n \int_{e_{k-1}}^{e_k} z^2 \rho dz$$

The element load vector due to external transverse static load ‘p’ per unit area is given by

$$[P]_e = \int_{-1}^{+1} \int_{-1}^{+1} [N_i] \begin{bmatrix} P \\ 0 \\ 0 \end{bmatrix} |J| d\xi d\eta \quad (3.5.36)$$

3.6 Computer Program

A computer program is developed by using MATLAB environment to perform all the necessary computations. The element stiffness, geometric stiffness and mass matrices are derived using the formulation. Numerical integration technique by Gaussian quadrature is adopted for the element matrices. Since the stress field is non-uniform, plane stress analysis is carried out using the finite element techniques to determine the stresses and these stresses are used to formulate the geometric stiffness matrix. The overall matrices $[K]$, $[K_g]$, and $[M]$ are obtained by assembling the corresponding element matrices. The boundary conditions are imposed restraining the generalized displacements in different nodes of the discretized structure. The program features and flow charts, used in this study are presented in the Appendix.

Chapter-4

EXPERIMENTAL PROGRAMME

4.1 Introduction

This chapter presents the details of experimental works carried out for vibration, buckling or static stability and parametric instability of plate separately. Therefore composite plates with different geometry are fabricated and their material properties are found out by tensile test. The further studies of this section are grouped into three parts as follows:

- Vibration of woven fiber composite plates
- Buckling of woven fiber composite plates
- Dynamic stability of woven fiber composite plates

4.2 Materials

The following constituent materials were used for fabricating the plate:

- Glass woven roving fibers as reinforcement.
- Epoxy as resin
- Hardener as catalyst(10% of the weight of epoxy)
- Polyvinyl Alcohol (PVA) as a releasing agent

4.3 Fabrication Procedure

The FRP composite specimens were casted using hand layup technique. In hand lay-up method, liquid resin was placed along with reinforcement (woven glass fiber) against finished surface of an open mould. Chemical reactions in the resin hardened the material to a strong, light weight product. The percentage of fiber and matrix was taken as 50:50 in weight for fabrication of the plates. A flat plywood rigid platform was selected. A plastic sheet i.e. a mould releasing sheet was kept on the plywood platform and a thin film of polyvinyl alcohol was applied as a releasing agent as shown in Figure 4.1[a]. Laminating started with the application of a gel coat (epoxy and hardener) deposited on the mould by brush as shown in Figure 4.1[b], whose main purpose was to provide a smooth external surface and to protect

the fibers from direct exposure to the environment. Glass fiber was cut from roll of woven roving. Layers of reinforcement were placed on the mould at top of the gel coat and gel coat was applied again by brush. Any air which may be entrapped was removed using steel rollers as shown in Figure 4.1[c]. The process of hand lay-up was the continuation of the above process before the gel coat had fully hardened. After completion of all layers, again a plastic sheet was covered on the top of last ply by applying polyvinyl alcohol inside the sheet as releasing agent. Again one flat ply board and a heavy flat metal rigid platform were kept top of the plate for compressing purpose. The plates were left for a minimum of 48 hours in room temperature before being transported and cut to exact shape for testing. The fabricated plate after drying is shown in Figure 4.1 [d].



Figure 4.1[a]



Figure 4.1[b]



Figure 4.1[c]



Figure 4.1[d]

Figure 4.1 [a]: **Application of gel coat on mould releasing sheet**, Figure 4.1 [b]: **Placing of woven roving glass fiber on gel coat**, Figure 4.1 [c]: **Removal of air entrapment using steel roller**, Figure 4.1 [d]: **Plate after casting**.

4.4 Determination of Material constants

The characteristics of woven fiber Glass/Epoxy composite plate which can be defined completely by four material constants: E_1 , E_2 , G_{12} , and ν_{12} where the suffixes 1 and 2 indicate principal material directions. For material characterization, 12 numbers of samples of 8 layer Glass/Epoxy plate was tested by INSTRON 1195 machine for determining tensile strength and Young's modulus in different direction. Out of which, 4 number samples are in X-direction, 4 number samples in Y-direction and 4 numbers of samples in 45° direction. From the test data, E_1 , E_2 and G_{12} were calculated for the Glass/Epoxy plate as described in ASTM standard: D 3039/D 3039M-2008. The dimensions of the specimen were taken as below as given Table 4.1.

Table 4.1: Dimensions of tensile specimens for tensile test

Angle(degree)	Length(mm)	Width(mm)	Thickness(mm)	Overall Length(mm)
0°	150	25	3	250
90°	150	25	3	250
45°	150	25	3	250

The specimens were cut from the plates themselves by diamond cutter. At least four replicate sample specimens were prepared. The tests specimens are shown in Figure 4.2[a], Figure 4.2[b] and Figure 4.2[c] for specimen in x, y and 45° directions respectively.

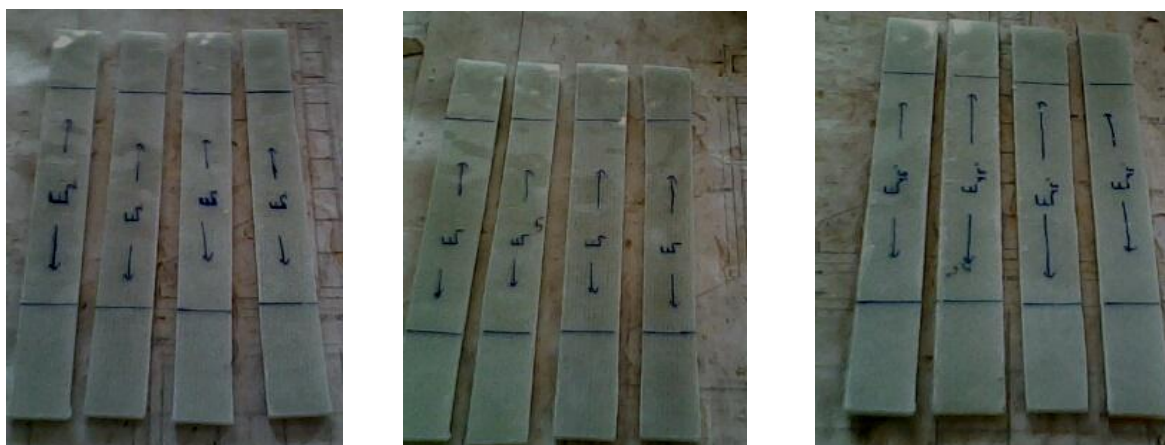


Figure 4.2 [a]: Specimens in “x” direction, [b] Specimens in “y” direction, [c] Specimens in “ 45° ” direction.

EXPERIMENTAL PROGRAMME

For measuring the Young's modulus, the specimen is loaded in INSTRON 1195 universal testing machine as shown in Figure 4.3, monotonically to failure with a recommended rate of extension (rate of loading) of 0.2in/minute. Specimens were fixed in the upper jaw first and then gripped in the movable jaw (lower jaw). Gripping of the specimen was as much as possible to prevent the slippage. Here, it was taken as 50mm in each side for gripping. Initially strain was kept at zero. The load, as well as the extension, was recorded digitally with the help of a load cell and an extensometer respectively. From these data, engineering stress vs. strain curve was plotted; the initial slope of which gives the Young's modulus. The ratio of transverse to longitudinal strain directly gives the Poisson's ratio by using two strain gauges in longitudinal and transverse direction.

The shear modulus was determined using the following formula from Jones [1975] as:

$$G_{12} = \frac{1}{\frac{4}{E_{45}} - \frac{1}{E_1} - \frac{1}{E_2} + \frac{2\nu_{12}}{E_1}}$$

Table 4.2: **Material properties of glass/epoxy lamina**

Lay-up	N	E ₁ (GPa)	E ₂ (GPa)	E ₄₅ (GPa)	G ₁₂ (GPa)	ν ₁₂	ρ(kg/m ³)
WR	8	7.4	7.4	5.81	2.15	0.17	1580

Where, WR: - Woven Roving

N: - Number of layers

E₁, E₂: Elastic modulus in longitudinal direction (1) and transverse direction (2) respectively.

E₄₅ :- Tensile modulus obtained in 45° tensile test,

G₁₂ :- In-plane shear modulus

ν₁₂ :- Poisson's ratio, ρ:-Density



Figure 4.3: **Tensile test of woven fiber Glass/Epoxy composite specimen in INSTRON 1195 UTM**

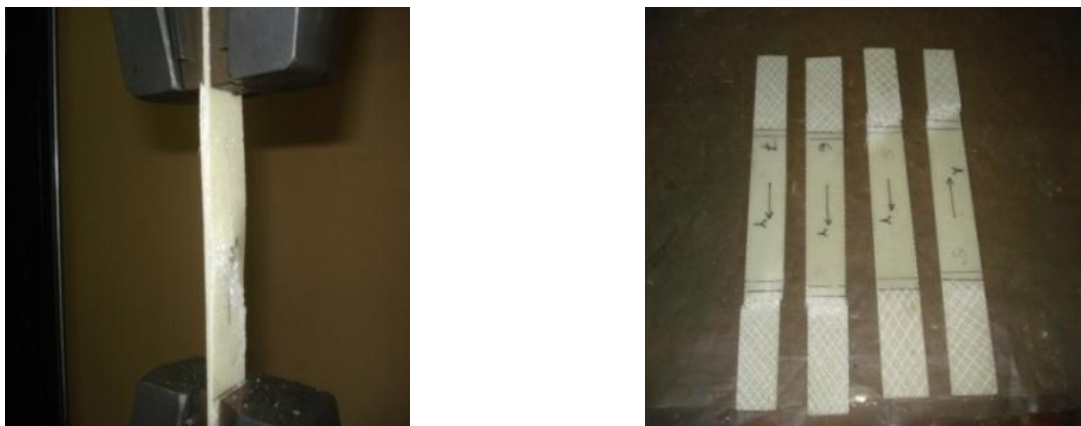


Fig 4.4: **Failure pattern of woven fiber Glass/Epoxy composite specimen**

4.5: Description of Test Specimen

The woven roving Glass/Epoxy composite plates were fabricated for the present experimental work. The geometrical dimensions (i.e. Length, breadth, and thickness), and ply orientations of the fabricated plates are shown below in Table 4.3.

For Free vibration and stability (Buckling) study, the plate of dimensions 240mmx240mm was considered with different thickness as the no. of layers varies. Only for simply supported boundary conditions in free vibration test the plate dimensions is taken as 237mmx237mm

EXPERIMENTAL PROGRAMME

due to frame conditions. For Experimental Study of parametric instability plate dimension of 600mmx350mmx4.7mm and for numerical study of parametric instability again 240mmx240mm which was same as vibration and buckling considered as plate dimensions.

Table 4.3: **Geometrical Dimensions of Composite Plate:**

All the specimens described in Table 4.3 were tested for free vibration, buckling and dynamic stability study.

Size of plate In ‘mm’	No. of layers	Thickness In ‘mm’	Stacking Sequence
240X240	16	5.6	[0] ₁₆
240X240	12	4.7	[0] ₁₂
240X240	8	3.1	[0] ₈
240X240	8	3.1	[(30/-30) ₂] _s
240X240	8	3.1	[(30/-30) ₂] _s
240X240	8	3.1	[(45/-45) ₂] _s
240X240	8	3.1	[(45/-45) ₂] _s
237X237	8	3.1	[0] ₈
600x350	12	4.7	[0] ₁₆

4.6 Vibrations of woven fiber composite plates

In order to achieve the right combination of material properties and service performance, the dynamic behavior is the main point to be considered. To avoid the typical problems caused by vibrations, it is important to determine natural frequency of the structure.

The fundamental frequency is a key parameter. The natural frequencies are sensitive to the orthotropic properties of composite plates and design-tailoring tools may help in controlling this fundamental frequency. Due to the advancement in computer aided data acquisition systems and instrumentation, experimental modal analysis or free vibration analysis has become an extremely important tool in the hands of an experimentalist.

4.6.1 Equipments Required for Vibration Test

The apparatus which are used in free vibration test are

- Modal hammer.
- Accelerometer.
- FFT Analyzer.
- PULSE software.

4.6.1.1 Modal hammer

The modal hammer excites and measure impact forces on to the specimens. Three interchange tips are provided which determine the width of the input pulse and thus the band width of the hammer structure is acceleration compensated to avoid glitches in the spectrum due to hammer structure resonance. For present experiment, modal hammer type 2302-5 was used, which is shown in Figure 4.5.



Figure 4.5: **Modal Impact Hammer (B&K type 2302-5)**

4.6.1.2 Accelerometer:

Miniature DeltaTron Accelerometers is specifically designed to withstand the robust environment of the industry. A combination of high sensitivity, low mass and small physical dimensions make the accelerometer ideal for modal measurements, such as on aircraft, automobiles and satellites. It can be easily fitted to different test objects using a selection of mounting clips. For the present experiment accelerometer type 4507 was used and which was fixed on plates by using bee wax. The accelerometer for free vibration test is shown in Figure 4.6.



Figure 4.6: Accelerometer (B&K 4507) used in Free Vibration Test.

4.6.1.3 Portable FFT Analyzer- type (3560B)

Four channels Bruel & kjaer pulse analyzer system type-3560 B as shown in fig.4.7, was used to measure the frequency for any structure. It can be used for both free vibration as well as forced vibration study. The system has some channels to connect the cables for analyzing both input and output signals. Bruel & Kjaer FFT analyzer 3560-B is shown in Figure 4.7.



Figure 4.7: FFT Analyzer (Model B&K3560-B)

4.6.1.4 Display unit

This is mainly in the form of PC (Laptop) as shown in Figure 4.8[a]. When the specimen was excited in a selected point by means of Impact hammer (Model 2302-5), the signal of resulting vibrations of the specimens were received to the FFT Analyzer by an accelerometer (B&K, Type 4507) mounted on the specimen by means of bees wax. The output from the analyzer was displayed on the display unit in the graphical form which includes graph of force amplitude spectrum, response amplitude spectrum, coherence and frequency response functions as shown in Figure 4.8[b].

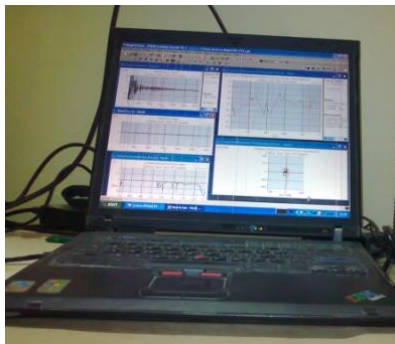


Figure 4.8 [a]: **Display unit**

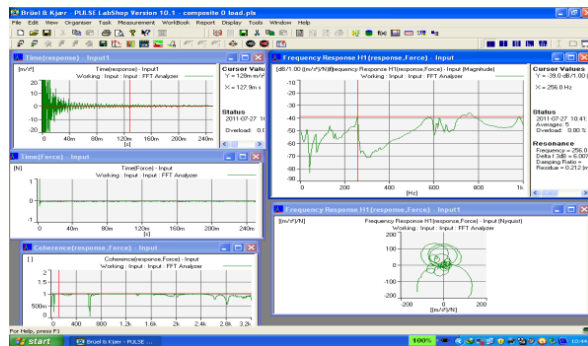


Figure 4.8 [b]: **Various Pulse output windows**

4.6.2: Setup and Test Procedure for Free Vibration Test

The vibration test setup is shown in Figure 4.9. The test frame which was fabricated for conducting different boundary conditions (B.C) i.e. free-free, four sides simply supported, cantilever and fully clamped were shown in Figure 4.10 [a] to Figure 4.10[e].

The test specimens were fitted properly to the iron frame. The connections of FFT analyzer, laptop, transducers, modal hammer, and cables to the system were done. The plate was excited in a selected point by means of Impact hammer (Model 2302-5). The resulting vibrations of the specimens on the selected point were measured by an accelerometer (B&K, Type 4507), mounted on the specimen by means of bees wax. For FRF, at each singular point the modal hammer was struck five times and the average value of the response was displayed on the screen of the display unit.



Figure 4.9: **Vibration Test Set-up**

At the time of striking with modal hammer to the points on the specimen, precaution were taken for making the stroke to be perpendicular to the surface of the plates. Then, by moving the cursor to the peaks of the FRF, the frequencies were measured. The output from the analyzer was displayed on the analyzer screen by using pulse software.



Figure 4.10 [a]

For different B.C one iron frame was used. Some of the test specimens with different boundary conditions are shown in Figure 4.10.



Figure 4.10 [b]



Figure 4.10 [c]



Figure 4.10[d]



Figure 4.10 [e]

Figure 4.10: [a] **Iron Frame for making different B.C. Setup**, [b] **free-free B.C**, [c] **Cantilever B.C**, [d] **Clamped B.C**, [e] **Simply Supported B.C**

4.6.3: Setting up the template in Pulse lab shop

In order to setup a template, there are four important windows. These are opened by selecting 'Organizer' from the menu and then clicking on each of the four window titles listed below.

4.6.3.1: Configuration

This window contains details of the inputs and outputs on the Pulse Front-end and to specify what components are connected to this Front-end.

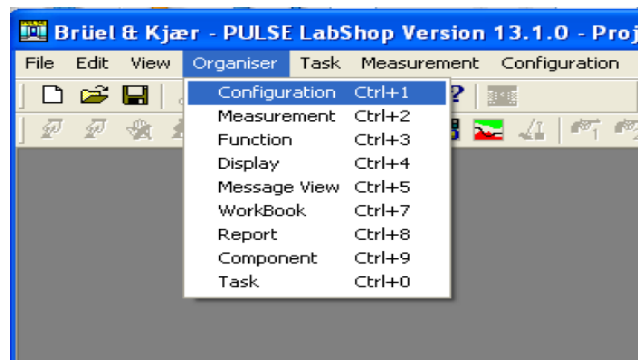


Figure 4.11

4.6.3.2: Measurement

This window is used to setup signal grouping and to specify which analyzers are to be used.

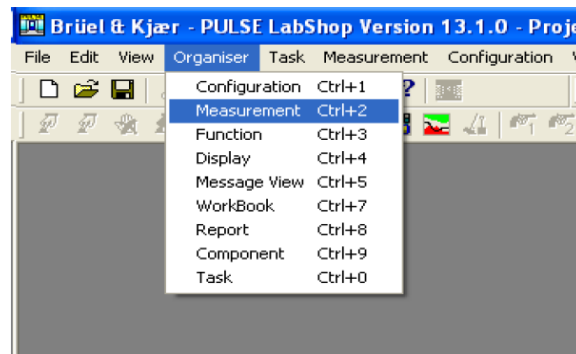


Figure 4.12

4.6.3.3: Function

This window is used to setup the outputs from the analyzers and how they are to be used. The function like FRF, response in time domain, coherence and excitation in time domain are chosen for the test.

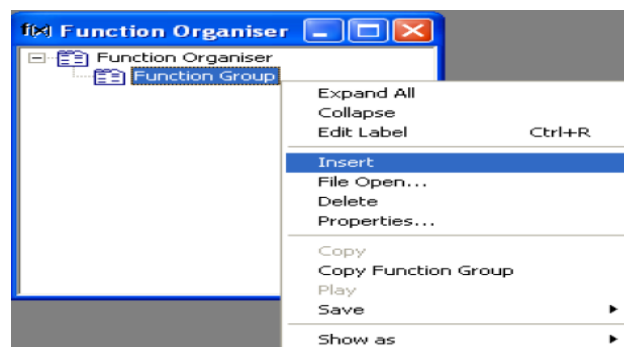


Figure 4.13

4.6.3.4: Display

This window shows which measurements are currently displayed and allows modifications to be made to the way the measurements are displayed. The four windows mentioned previously are very important for setting up the Pulse Labshop template. It is important that they are easily accessible. This configuration follows the flow that the setup process uses. i.e. Configuration → Measurement → Function → Display.

4.6.4: Pulse Report (Frequency Response function):

A typical FRF (pulse report) of the measurement from FFT analyzer along with coherence curve is shown in Figure.4.14. and Figure 4.15 respectively. As shown in Figure 4.14, the different peaks of FRF shows the different modes of vibrations and the coherence value of nearly 1 in Figure 4.15 shows the accuracy of the measurement.

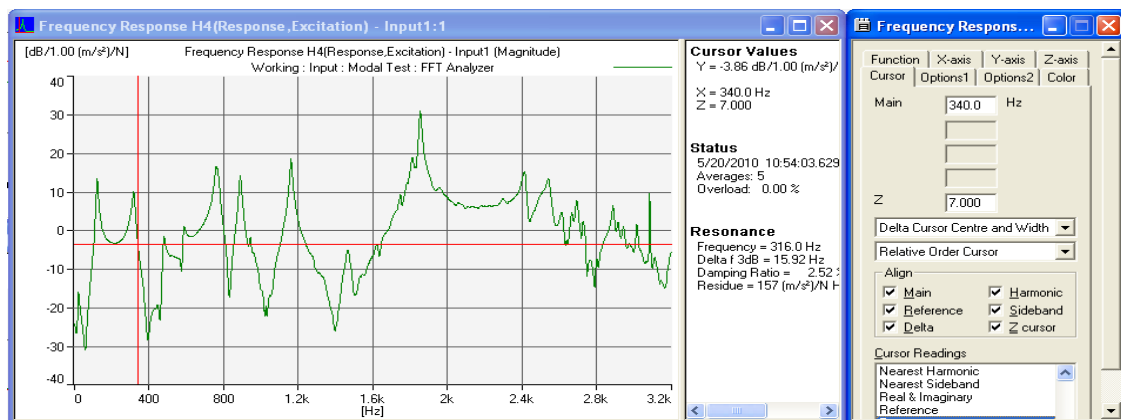


Figure 4.14: Typical FRF of test specimen. In X-axis: Frequency in Hz In Y-axis: Acceleration in $\text{m/s}^2/\text{Force}$

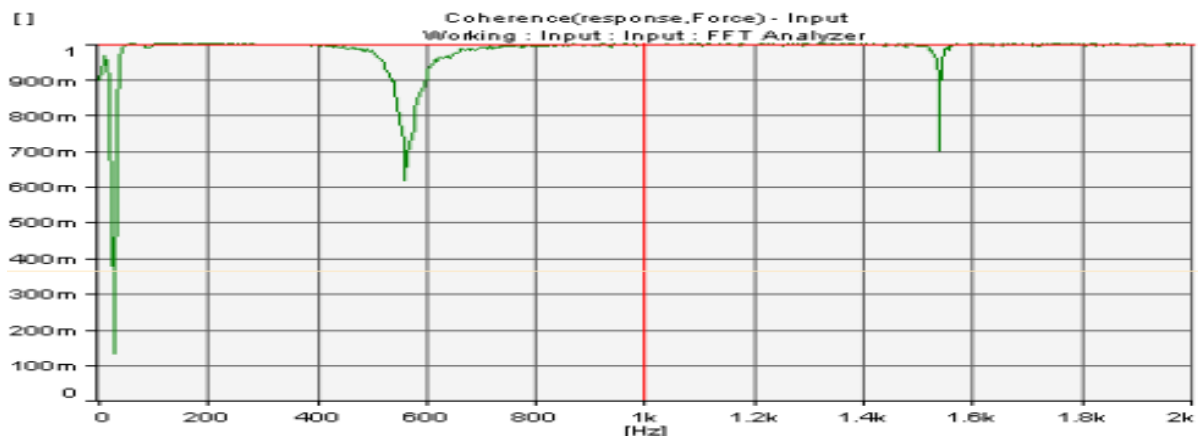


Figure 4.15: Typical coherence of test specimen.

4.7: Buckling of Woven Fiber Composite Plates

The complex behavior of woven fabric composite laminates under compressive loading conditions is still not well understood and requires further experimental investigations in order to better understand their behavior especially buckling load. Studies of buckling analysis of woven fabric or bi-directional composite laminates are limited. Therefore, woven fabric glass/epoxy composites were used in this study to demonstrate the capability of the static stability analysis of woven fiber composite panels.

There are several techniques of identifying the buckling load in the experiment used in the past studies. Four of the methods which are examined in the present study are: Plot of applied load vs. out-of-plane displacement, plot of load vs. end shortening, average strain method and South well plot. With the available experimental data, a plot of average strain method is the most reliable technique, while a plot of out-of-plane displacement and a plot of end shortening show a good tendency of determination of buckling loads. In the present study, buckling loads of woven fabric composite plates is determined from end shortening method and compared to the numerical solutions using present FEM based formulation.

4.7.1 Buckling Experiment (Static stability)

In view of difficulty of theoretical and numerical analysis for laminated structure behaviors, experimental methods have become important in solving the buckling problem of laminated composite plates. The specimens was clamped at two sides and kept free at other two sides. The specimens were loaded in axial compression by using an INSTRON universal testing machine (SATEC) of 600 kN capacity.

4.7.1.2 Test Procedure

The specimens were loaded in axial compression using INSTRON universal testing machine (SATEC) of 600 KN capacities as shown in Figure 4.16 [a]. The specimen was clamped at two ends and kept free at the other two ends as shown in Figure 4.16 [b]. All specimens were loaded slowly until buckling. Clamped boundary conditions were simulated along the top and bottom edges, restraining 2.5cm length. For axial loading, the test specimens were placed between the two extremely stiff machine heads, of which the lower one was fixed during the

EXPERIMENTAL PROGRAMME

test, whereas the upper head was moved downwards by servo hydraulic cylinder. All plates were loaded at constant cross-head speed of 0.5mm/min. The load-displacement diagrams for all composite configurations were plotted. The motion of the machine was stopped when the load dropped. The data acquisition system which was linked with the INSTRON machine was used to record all the necessary results and the buckling loads were determined from the recorded data. The plate before buckling and after buckling is shown in fig.4.16[c] and fig.4.16 [d]. The load v/s end shortening curve was plotted. The displacement is plotted on the x -axis and load was plotted on the y- axis. The load, which is the initial part of the curve deviated linearity, is taken as the critical buckling load.

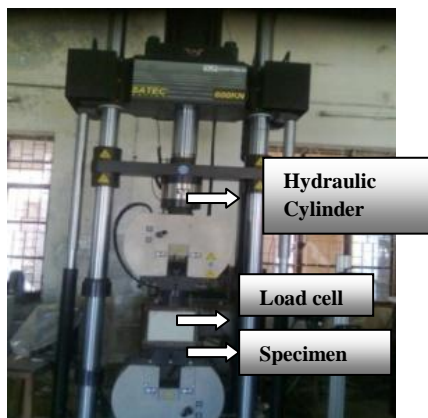


Figure 4.16 [a]

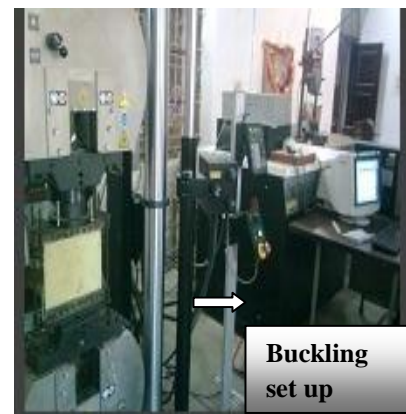


Figure 4.16 [b]

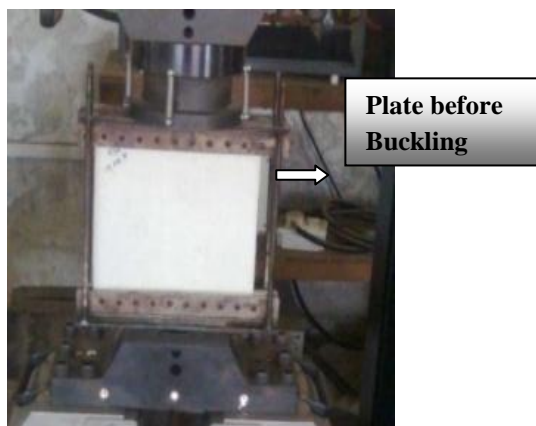


Figure 4.16 [c]

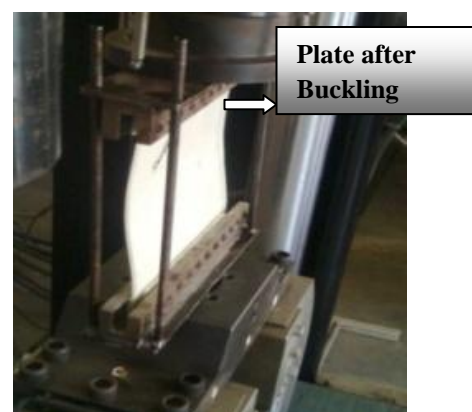


Figure 4.16 [d]

Figure 4.16 [a]: **INSTRON universal testing Machine (SATEC) of 600 kN capacities,**
Figure 4.16 [b]: **Buckling set up and test frame,** Figure 4.16 [c]: **specimen before buckling,** Figure 4.16 [d]: **Specimen after buckling**

4.7.2 Buckling Experiment (By Dynamic Approach)

Buckling Test is also conducted by dynamic approach. The test facility used to conduct stability test by dynamic approach is shown in Figure 4.17 [a] and Figure 4.17 [b].

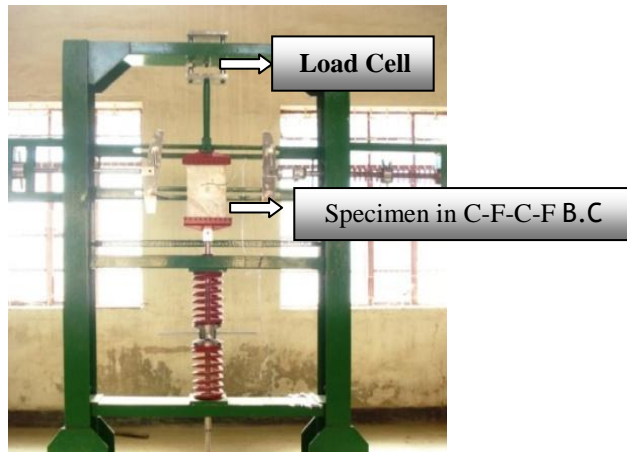


Figure 4.17 [a]

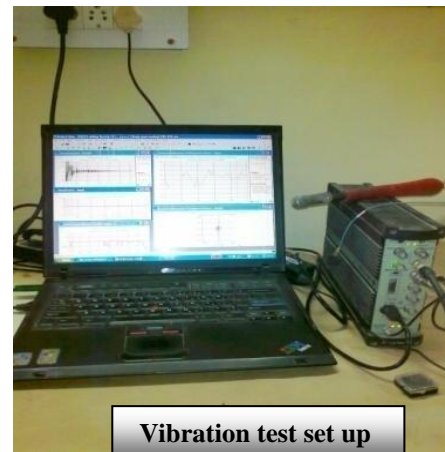


Figure 4.17 [b]

Figure 4.17[a]: **Experimental set up Fabricated for conducting Buckling Test by Dynamic approach**, Figure 4.17 [b]: **Vibration test set up**

4.7.2.2 Test Procedure

The specimens were loaded in the set up fabricated for buckling test in C-F-C-F boundary conditions. Load cell was put on the top of the test frame. In-plane static load was given manually with the help of the spring attached to the bottom of the specimen in the frame as shown in Figure 4.17 [a]. The accelerometer was put on the middle of the specimen and the specimen was excited with the help of modal hammer connecting to FFT Analyzer. A personal computer loaded with PULSE Labshop software was connected to the FFT analyzer to pick up the plate response data as shown in Figure 4.17[b]. After applying the desired static load and excited the plate, the response of the plate was constantly monitored on the FFT analyzer. All specimens were loaded slowly until buckling.

The load v/s frequency graph was plotted. The load is plotted on the x -axis and frequency was plotted on the y- axis. The first frequency in graph showed a tendency to approach to zero at a static load at critical buckling load, indicating the onset of buckling which is called critical buckling load.

4.8 Parametric Instability of Woven Fiber Composite Plates

Experiments are performed to investigate the parametric instability of rectangular composite plate are subjected to periodic in-plane loads under C-F-C-F boundary conditions. Special attention is paid to satisfy the boundary conditions considered in experimental models so as to draw conclusion with sufficient degree of confidence. In-order to verify the theoretical results and to highlight different parameters on the parametric instability of composite plates, different plates with different dimensions as given in Table 4.3, in chapter 4 is used in this investigation. In general, the experimental data exhibit good agreement with the theoretical predictions.

4.8.1 Parametric Instability Test Setup:

An overall view of the test facility used in the experimental study is shown in Figure 4.18 [a]-4.18 [d].The set-up has been designed to accommodate square and rectangular composite plate to study different parameter in C-F-C-F boundary condition.

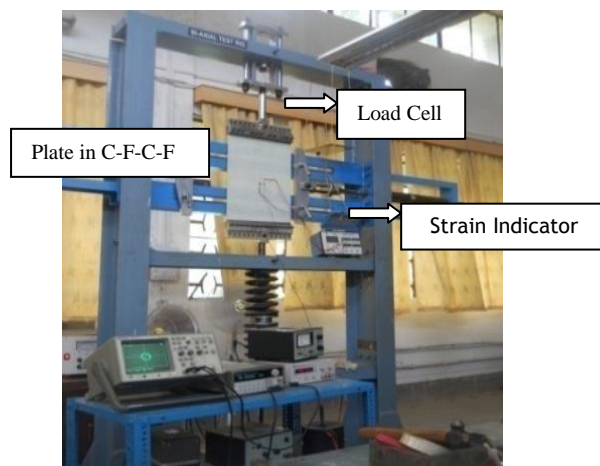


Figure 4.18[a]

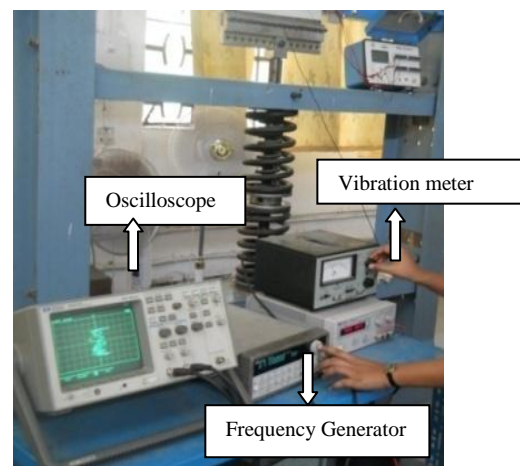


Figure 4.18[b]



Figure 4.18[c]

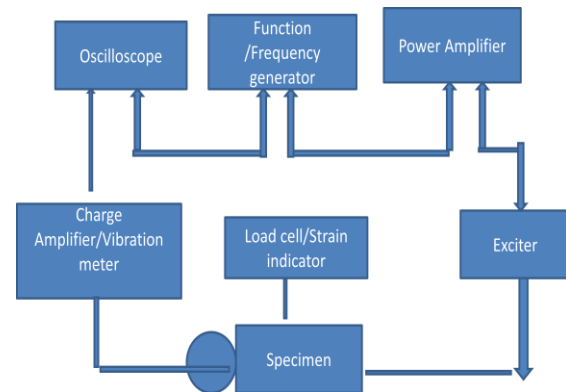


Figure 4.18[d]

Figure 4.18 [a]: **Parametric test set up with loading system**, Figure 4.18[b]: **measurement system**, Figure 4.18 [c]: **Oscilloscope indicating x-y plot**, Figure 4.18 [d]: **Schematic diagram for parametric instability experiments**

Basically, the experimental facility consists of (i) the loading system, (ii) the measurement system. The loading system consisted two vertical steel I-beam with a cross member at the top, which housed the loading assembly. The loading apparatus consists of a linear spring, an adjustable head, a lock nut, a threaded stud as shown in Figure 4.18 [a]. The specimen and the load cell were connected in series between the loading assembly and the threaded stud. This arrangement of loading, therefore, facilitates the application of a parametric load and permits direct measurement of the static in-plane load.

The measurement system consists of various measuring instrument i.e. vibration meter, frequency generator, and oscilloscope to measure the system parameters and the plate response as shown in Figure 4.18 [b]. The static load could be measured by reading of a calibrated load cell. An accelerometer could be stuck at various locations on the plate surface to pick up the plate response. The response received through accelerometer was connected with vibration meter show the plate response in graphical form in oscilloscope in x-y mode as shown in Figure 4.18 [c]. The laboratory apparatus has been designed to simulate C-F-C-F boundary condition. A schematic diagram for parametric instability experiments is also shown in Figure 4.18 [d].

4.8.2 Parametric Instability Experimental Procedure:

Prior to any experiment, precautions were necessary to make sure that each instrument is properly calibrated and the mechanical system is properly aligned. After clamped the plate specimen with the Frame properly as shown in figure under C-F-C-F boundary conditions, the digital strain indicator was adjusted to zero. The initial static load was then applied by combined movement of the screw jack mechanism and the adjusting screw, the applied load level was monitored by the load cell after due calibration. At the onset of instability, the amplitude and frequency of excitation was noted and frequency was changed till the plate again become stable. Thus boundary of instability region was established at various load combinations.

5.1 Introduction

The composite plates with arbitrary geometries, load and boundary conditions have important roles to play as the structural elements in aerospace, civil and other engineering structures. The composite plate, subjected to in-plane loading greatly affects the dynamic behavior of structure. In this chapter, the results of free vibration, buckling and parametric instability behavior of composite plates are presented. The effects of different geometrical parameters including number of layers, aspect ratio, fiber orientation and different boundary conditions of woven fiber composite plates are studied in details.

The studies in this section are grouped into three parts as follows:

- Vibration of woven fiber laminated composite plates.
- Buckling/ Stability effects of woven fiber laminated composite plates.
- Parametric instability of woven fiber laminated composite plates subjected to in plane periodic loading.

5.2. Free Vibration of Woven Fiber Laminated Composite Plates

This study deals with vibration behavior of woven fabric composite plate. The problem considered here is laminated composite plate ($a \times b$) subjected to free vibration in different boundary conditions.

5.2.1 Convergence Study

The convergence studies are carried out for non-dimensional free vibration of 4-layer simply supported antisymmetric angle ply square plates for different ply orientations and compared with Bert and Chen [1978] as shown in Table.5.1. A mesh of 10x10 mesh shows good convergence of the numerical solutions for free vibration of laminated composite plates.

Table 5.1: **Convergence study on free vibration of 4-layer simply supported laminated composite plates.**

$$a/b=1, a/h=10, E_{11}/E_{22}=40, G_{23}=0.5E_{22}, G_{12}=G_{13}=0.6E_{22}, \nu_{12} = 0.25.$$

$$\text{Non dimensional frequency, } \varpi = \omega a^2 \sqrt{[\rho / (E_{22} h^2)]}$$

Mesh Division	Non-dimensional frequencies for different ply orientations	
	30/-30/-30/30	45/-45/-45/45
4x4	17.65	18.47
8x8	17.63	18.46
10x10	17.63	18.46
Bert and Chen [1978]	17.63	18.46

5.2.2 Comparison with Previous Studies

Numerical computations are carried out to determine the capability of the present formulation to predict the natural frequency of woven fiber composite plates. To validate the program, the natural frequency of vibration obtained by this present formulation are compared with the numerical results published by previous investigators. The present formulation is validated for vibration analysis of composites panels in different boundary conditions as shown in Table 5.2. The four lowest frequency obtained by the present finite element are compared with numerical solution by Crawley [1979] using FEM for 8 layer ply Graphite/Epoxy plate, length=152mm, 76mm, Breadth=76mm and Thickness=1.04mm with laminate sequence, $[0_2/\pm 30]_s$, Chakraborty *et. al.* [2000] for woven roving $[0]_5$ for clamped boundary conditions and Ju *et. al.* [1995] for all boundary conditions using FEM. The comparison results show that there exists an excellent agreement between the present FEM and the previously studies in literature.

Table 5.2 Comparison of natural frequencies (Hz) of composite plate with previous study at different boundary conditions.

Boundary Conditions	Reference	Natural frequencies at different boundary conditions (All Frequencies in Hz)			
		1	2	3	4
C-F-F-F [0 ₂ /±30] _s	Crawley [1979] Exp	234.2	362	728.3	1449
	Crawley [1979] FEM	261.9	363.5	761.8	1662
	Present FEM	261.241	361.522	754.741	1592.13
C-C-C-C	Chakraborty <i>et. al.</i> [2000] Exp	116.0	232.0	320.0	412.0
	Chakraborty <i>et. al.</i> [2000] FEM	118.50	243.19	344.39	443.43
	Present FEM	118.58	243.644	346.46	441.39
S-S-S-S	Ju <i>et. al.</i> [1995]	164.37	404.38	492.29	658.40
	Present FEM	163.745	401.314	494.591	651.165
F-F-F-F	Ju <i>et. al.</i> [1995]	73.309	202.59	243.37	264.90
	Present FEM	72.534	201.398	243.549	263.260

5.2.3 Experimental and Numerical Results of Vibration

After validating the formulation with the existing literature, both the experimental [Exp] and Finite element results for vibration of laminated composite plates are presented. The geometrical dimensions which are taken for the woven roving composite plates are:

Length (a) =Width (b) =0.24m, Thickness (h) =0.0031m (For Eight-layer)

The material properties of the woven roving composite plates which are obtained from tensile test as per ASTM D 3039/D 3039 M [2008] and used for numerical studies are

$E_{11}=E_{22}=7.4\text{Gpa}$, $G_{12}=G_{23}=G_{31}=2.15\text{Gpa}$, $\nu=0.17$.

The effects of following parameters are choosen for vibration analysis of woven fiber composite plates.

- Effect of number of layers of a laminate
- Effect of fiber orientations.
- Effect of aspect ratio
- Effect of various boundary conditions

5.2.3.1 Effect of Number of Layers of Laminate

For the present study, to examine the effects of no. of layers of laminate, three different types of laminate are fabricated, which are made up of 8, 12 and 16 layers. The natural frequencies for free vibration of woven fiber composite plate are obtained both experimentally and numerically in cantilever boundary condition. The variation of natural frequencies with increasing layer of laminate for both experimental results and numerical results are shown in Figure 5.1.

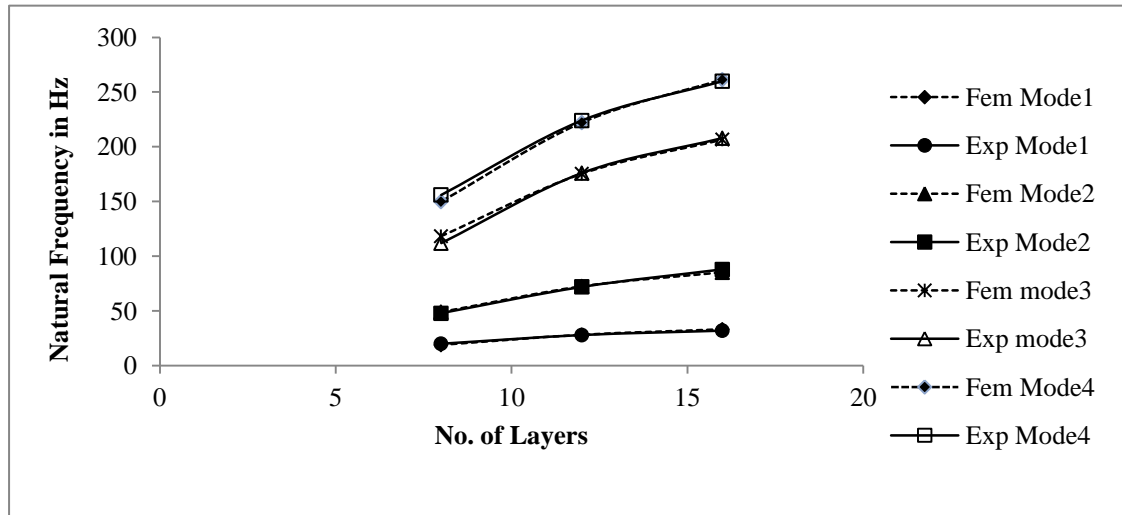


Figure 5.1: Variation of natural frequency with different no. of layers of woven fiber composite plates.

From Figure 5.1, it is observed that as the number of layers increases, the natural frequency also increases due to bending stretching coupling as expected. There is a considerable

variation in the different modes of natural frequency made up of 12 and 16 layers whereas for 8 layers of composite plates it is less. This variation is much more significant for higher modes of vibration of woven fiber laminated composite plates.

5.2.3.2 Effect of Fiber Orientation

In order to know the effect of fiber orientations on natural frequencies laminated plate (8-layers), three types of fiber orientations i.e. $[(0/0)_2]_s$, $[(30/-30)_2]_s$, $[(45/-45)_2]_s$ are considered. The variation of natural frequencies for both experiment and numerical solution is presented in Figure 5.2 for cantilever composite plates. The results obtained for free vibration of the plates by experimental and present FEM are in good agreement.

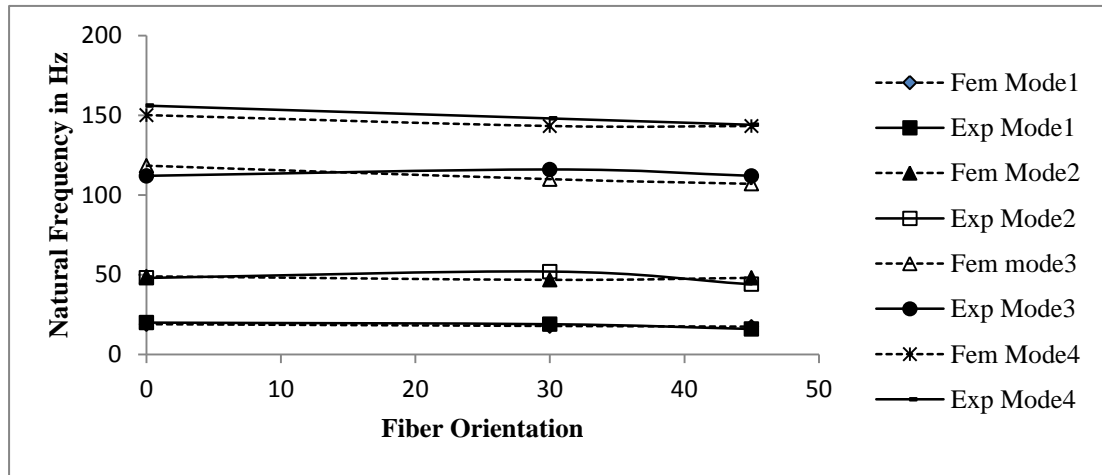


Figure 5.2: Variation of natural frequency with different fiber orientations of woven fiber composite plates.

As observed from Figure 5.2, the natural frequency of laminated composite plates decreases for 1st and 3rd frequency but for 2nd natural frequency it decreases and then increases. When angle of ply changes from 0^0 to 30^0 the natural frequency decreases and then increases up to 45^0 for this material and geometry.

5.2.3.3 Effect of Aspect Ratio

To study the effect of aspect ratio, four different types of aspect ratios for laminated composite plates are considered i.e. for a/b value (0.5, 1.0, 1.5 and 2.0). For aspect ratio 0.5, dimension of plate is considered as length(a)=120mm and breadth(b)=240mm. For aspect ratios 1.0, 1.5 and 2.0, length (a) remain constant i.e. 240mm, whereas the breadth(b) varies 240mm, 160mm and 120 mm respectively but thickness of the plate i.e. (h=0.0031m) remains

unchanged. The natural frequencies of cantilever laminated woven fiber composite plates are found out both experimentally and numerically. The variations of frequencies with different aspect ratios for both experimental and numerical results are presented in Figure 5.3.

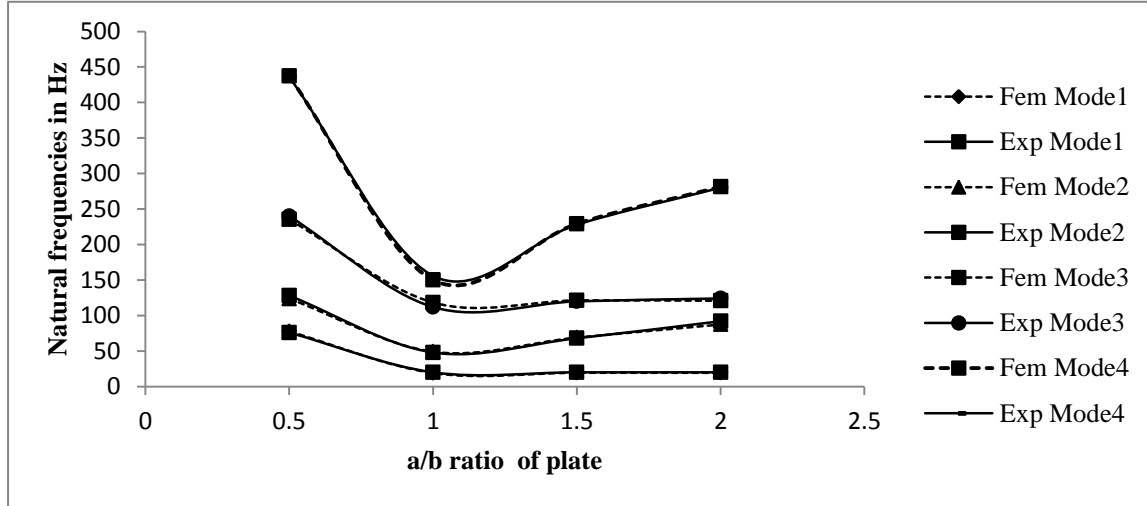


Figure 5.3: Variation of natural frequency with different aspect ratio of woven fiber composite plates.

As observed from Figure 5.3, there is decrease in fundamental natural frequency from 76 Hz to 20 Hz, with increasing value of a/b ratio from 0.5 to 2 experimentally. However, the frequencies of vibration of higher modes decrease significantly from aspect ratio a/b=0.5 to 1 and then the variation is not much significant except fourth lowest mode for both experimental and numerical result.

5.2.3.4 Effect of Various Boundary Conditions

Four types of boundary conditions i.e. simply supported (S-S-S-S), clamped(C-C-C-C), cantilever(C-F-F-F) and free-free (F-F-F-F), are considered for the analysis.

- Simply Supported boundary condition:
 $u=w=\theta_y=0$, at $x=0, a$ and $v=w=\theta_x=0$, at $x=0, a$
- Clamped boundary condition:
 $u= v=w= \theta_x= \theta_y=0$, at $x=0, a$ and $y=0, b$
- Cantilever boundary condition:
 $u= v=w= \theta_x= \theta_y=0$, at $x=0$

To investigate the effects of boundary conditions on the natural frequencies of a laminated composite plate, 12 layer plate is considered with 4 different types of boundary conditions i.e. C-C-C-C, S-S-S-S, C-F-F-F, F-F-F-F are considered. The variations of natural frequencies for the woven fiber composite plate with different boundary conditions are given graphically for both experimental and numerical results in Figure 5.4.

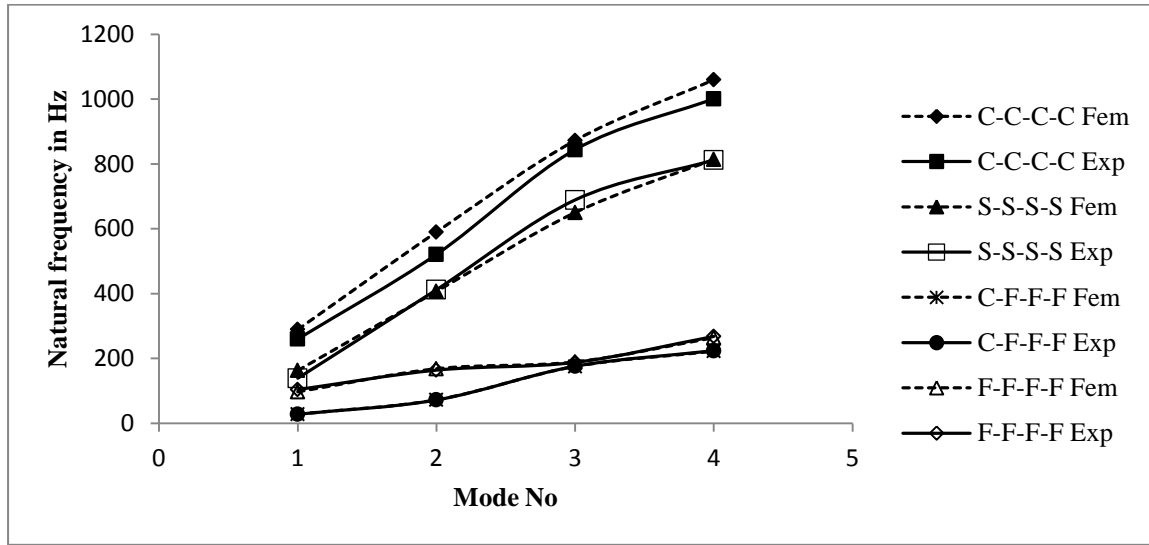


Figure 5.4: Variation of natural frequency with different boundary condition of woven fiber composite plates.

There is good agreement between the experimental and numerical results as shown in Figure 5.4. The natural frequencies are very less for cantilever condition as compared to the simply supported and clamped boundary conditions. There is better agreement between the experimental and theoretical results for the free-free and cantilever configurations. The agreement for the fixed-fixed results is just satisfactory. This indicates that the clamps for the fixed-fixed configuration are not ideal and that they introduce some assumptions in the boundary conditions. The cantilever boundary conditions results provide accurate experimental natural frequencies of several composite plates. The error obtained between the experimental result and numerical results in free-free boundary condition is maximum 7.2%. The error is probably due to thickness variation across the plates. One percent variation in thickness is observed to indicate large variation in frequency in numerical predictions.

5.3 Buckling Effects on Woven Fiber Laminated Composite Plates

This study deals with static stability or buckling behavior of woven fabric composite plates. The problem considered here consists of laminated composite plate (a x b) subjected to uniaxial loading in C-F-C-F boundary conditions.

5.3.1 Convergence Study:

The convergence studies are carried out for buckling analysis of 8-layer symmetric cross ply composite plates for cantilever [C-F-F-F] and two opposite sides clamped and other two sides free [C-F-C-F] boundary conditions and compared with Chattopadhyay and Radu [2000] using FEM as shown in Table.5.3. A mesh of 8x8 shows good convergence of the numerical solution.

Table.5.3: Convergence study of buckling load of the 8 layer symmetric cross ply composite plate for C-F-F-F and C-F-C-F boundary conditions.

$a=0.127, b=0.0127, \text{thickness}=0.001016, \rho=1500\text{kg/m}^3, E_{11}=134.4\text{GPa}, E_{22}=10.34\text{GPa},$
 $G_{12}=G_{13}=4.999\text{GPa}, G_{23}=1.999\text{GPa}, \nu_{12}=0.33$

Mesh Division	Critical Buckling Load for C-F-F-F and C-F-C-F boundary conditions.	
	C-F-F-F	C-F-C-F
4x4	16.329	263.521
8x8	16.331	259.833
10x10	16.329	259.6761
Chattopadhyay and Radu [2000]	(16.38)	(260.11)

5.3.2: Comparison with previous studies

The present formulation is further validated for buckling of composite plates with Baba [2007] for clamped-free-clamped-free boundary condition as shown in Table.5.4. The rectangular plate had eight layers of E-glass/epoxy composite (different fiber orientations). The comparison results show that there exists an excellent agreement between the present FEM and the previously published results of other authors.

RESULTS AND DISCUSSION

Table.5.4: Comparison of buckling load [in Newton] for laminated composite plates with C-F-C-F boundary conditions.

$E_1 = 39.0\text{GPa}$, $E_2=E_3=8.2\text{GPa}$, $G_{12}=G_{13}=G_{23}=2.9\text{GPa}$, $\nu_{12}= \nu_{23}= \nu_{31}=0.29$, Length=150mm, width=25mm, thickness=1.5mm.

Fiber Orientation	Baba Experimental [2007]	Baba FEM [2007]	Present FEM	% error
$[0]_8$	380	482.42	481.71	0.14%
$[90]_8$	101	106.33	101.39	4%
$[0/90]_{2s}$	319	366.52	364.66	0.47%
$[(0/90)_2]_{as}$	260	290.22	287.37	0.96%

The present formulation is then validated for buckling of angle ply laminated plates and compared with results of Narita and Leissa [1992] and Nair, Singh and Rao [1996] as shown in Table 5.5.The present FEM results match well with the angle-ply plate buckling solutions using Ritz method[1992] and the rectangular four node finite element results[1996].

Table 5.5: Comparison of non-dimensional buckling load for simply supported angle-ply($\theta^\circ / \theta^\circ / \theta^\circ$) plates.

$E_{11}=60.7$, $E_{22}=24.8$, $G_{12}=12.0$, $\nu_{12}=0.23$, $a/h=100$, $P_{cr}=N_x b^2/D_0$, $D_0=E_{11}h^3/12(1- \nu_{12} \nu_{21})$

Fiber Orientation	Non-dimensional Buckling Load		
	Present FEM	Narita and Leissa [1992]	Nair et.al[1996]
0	23.376	23.39	23.3778
30	25.331	25.42	25.2778
45	26.024	26.14	25.9514

5.3.3. Experimental and Numerical Results of Static Stability (Buckling) Study

After validating the formulation with the existing literature, both the experimental and numerical results for buckling analysis of laminated composite plates are presented in two opposite sides clamped and other two sides free [C-F-C-F] boundary conditions. Finite element analysis is used to analyze the linear critical buckling load of various laminated plates in order to see how changes in the laminated plates would affect the buckling load. Then experimental analysis is carried out. The dimension of the specimens was considered in Table.4.3 given in chapter 4. Here for buckling analysis, the investigation is aimed to study the effects of the following parameters

- Effect of number of layers of a laminate
- Effect of fiber orientations.
- Effect of aspect ratio
- Effect of various boundary conditions
- Effect of side to thickness ratio

5.3.3.1 Effect of Number of Layers of Laminate:

A composite laminate consists of different layers of lamina or plies. To examine the effects of no. of layers of laminate, three different types of laminate are fabricated, which are made up of 8, 12 and 16 layers. The size of plate is taken as 0.24m x 0.24 m having thickness varies from 0.0031mm for $[0]_8$, 0.0047 m for $[0]_{12}$ and 0.0056 m for $[0]_{16}$. The variation of buckling load with no. of layers of composite laminate for composite plate (both numerical and experimental) is graphically presented in Figure 5.5.

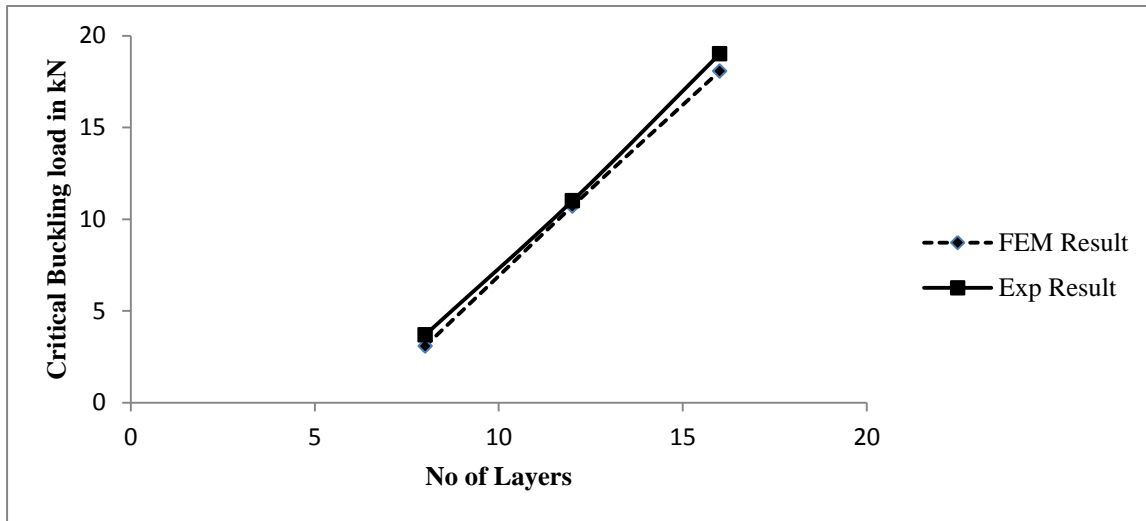


Figure 5.5: Variation of critical buckling load with number of layers of C-F-C-F woven fiber laminated composite plates.

The variation of critical buckling loads in kN are observed for C-F-C-F laminated square woven fiber composite plates for eight, twelve and sixteen layered. From Figure 5.5, it is found that with increase in the number of layers from eight, twelve and sixteen of the laminated composite plates, the critical buckling load is found to be of 3.7kN, 11kN and 19kN respectively. The variation of experimental results is about 19%, 12% and 5% higher than the FEM results for eight, twelve and sixteen layer respectively. This shows that with the increase of layers of laminated composite plate, the buckling load decreases.

5.3.2.2: Effect of Fiber Orientations

Fiber orientation angle is the main parameter for controlling buckling load capacity of composite plates. To investigate the effect of fiber orientations, three types of fiber orientations are considered. i.e. $[0]_8$, $[(30/-30)_2]_s$, $[(45/-45)_2]_s$. The fibers are rotated at the required orientations like 0° , 30° or 45° before matrix is applied to it. The size of plate is taken as $(0.240 \times 0.240 \times 0.0031) \text{ m}^3$. The graphical variation of critical buckling load with fiber orientation for both experiment and numerical solution is presented in Figure 5.6.

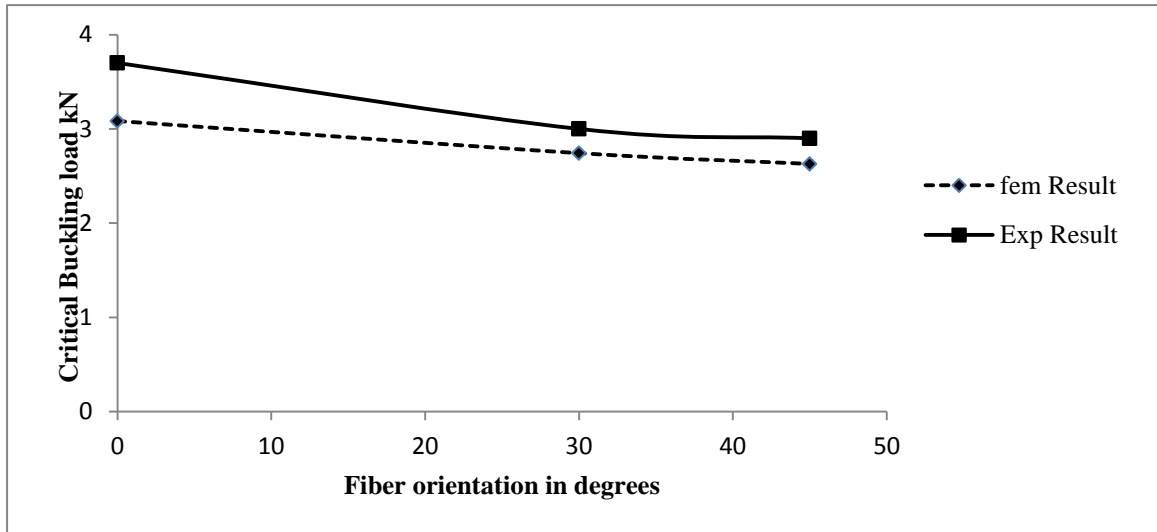


Figure 5.6: **Variation of critical buckling load with fiber orientation of C-F-C-F woven fiber laminated composite plates.**

As shown in Figure 5.6, the maximum critical buckling load for square laminated woven fiber composite plate was found for $[0]_8$ of fiber orientation angle and the minimum values of the buckling load occur at $[45/-45]_{2s}$. This behavior was experimentally obtained and checked numerically. From Figure 5.6, it is observed experimentally that the critical buckling load of composite plate is reduced 3.7 kN to 2.8 kN, when the fiber orientation angle increased from 0° to 45° . The percentage variation determined between numerical and experimental result is about 19%, 9%, and 10% as the ply orientation angle increases from 0° to 30° and 45° respectively. It may be concluded that, the plates yield highest stability resistance when fibers are aligned along the load direction. From the above results, it is understood that the fiber orientation of the lamina may be used as an index for quality control and can be used for tailoring or as safety factor for the laminated composites.

5.3.2.3 Effect of Aspect Ratio

Aspect ratio has a profound effect on buckling behavior. For large aspect ratio, the plate starts behaving like a column of finite width. With decreasing aspect ratio there is also a limit below which failure does not take place easily by elastic buckling. Aspect ratio is therefore an important parameter for designers in aerospace and other fields of engineering. To study the effect of aspect ratio, four different types of aspect ratios for laminated woven fiber

composite plates are considered. For different aspect ratios, the plate dimension varies, whereas the thickness of the plate i.e. ($h=0.0031\text{m}$) remains same. All plates are made up of eight layers with a stacking sequence of $[0]_8$. The graphical variation of critical buckling load with aspect ratio for both experiment and numerical solution is presented in Figure 5.7.

The dimensions of the plates are, for $a/b=0.5$ [120mm and $b=240\text{mm}$], $a/b=0.67$ [$a=160\text{mm}$ and $b=240\text{mm}$], $a/b=1$ [240mm and $b=240\text{mm}$] and $a/b=2$ [$a=240\text{mm}$ and $b=120\text{mm}$]

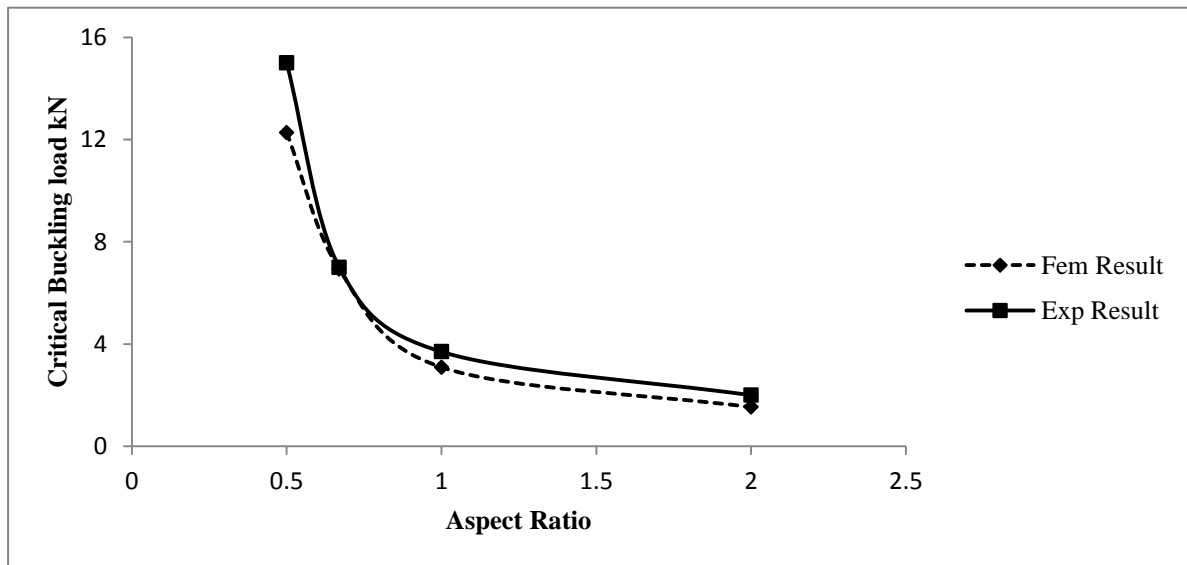


Figure 5.7: **Variation of critical buckling load with aspect ratio of C-F-C-F woven fiber laminated composite.**

The experimental results of critical buckling loads for different aspect ratios $a/b=0.5$, $a/b=1$ and $a/b=2$ for eight layered cross-ply symmetric C-F-C-F woven fiber laminated composite plates is shown in Figure 5.7. From the results, it is clear that the critical buckling loads are decrease from 15kN to 2kN , with increase in aspect ratio from 0.5 to 2.0 experimentally. As shown in Figure 5.7, although the difference between the values of the experimental and numerical buckling loads for lower aspect ratios is large, for higher aspect ratios this difference continues to decrease. Moreover, the experimental values coincide with the theoretical values when the aspect ratio is increases.

5.3.2.4: Effect of Side to Thickness Ratio (L/t)

To study the effect of length to thickness ratio different length of plates was taken as 120 mm, 160 mm and 240mm with constant thickness 3.1mm. The variation of critical buckling load of experimental results with present FEM results of C-F-C-F woven fiber composite plate.

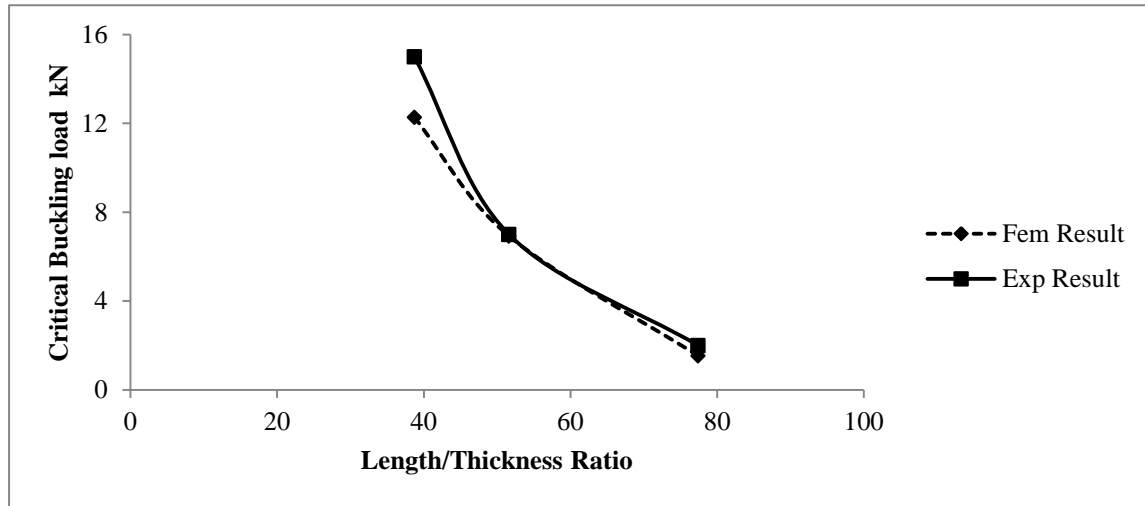


Figure 5.8: Variation of critical buckling load with L/t ratio of C-F-C-F woven fiber laminated composite plates.

The experimental results and FEM result of critical buckling loads for different length to thickness ratios for eight layered cross-ply symmetric woven fiber laminated composite plates for clamped-free-clamped-free boundary conditions are presented in Figure 5.8. As expected, the finite element results and corresponding experimental results shows a basic trend of reduction in buckling load with increasing L/t ratio. The Percentage of variation between experimental and numerical result for the Length/thickness ratio is 38.71, 51.61 and 77.41 is 22%, 15% and 17% respectively which shows that with the increase of L/t ratio the percentage of variation of buckling load is not uniform. The composite plates with higher L/t ratio have lower buckling load in clamped-free boundary conditions.

5.3.2.5: Effect of Boundary Conditions

In this study three types boundary conditions i.e. all sides simply supported (S-S-S-S), all sides clamped (C-C-C-C) and two sides clamped two sides free (C-F-C-F) are considered for

analysis. To investigate the effects of boundary conditions (B. C.) on the buckling load of a composite plate, the results are obtained numerically for composite plate (240x240x3.1) mm³ size and stacking sequence is [0]₈.

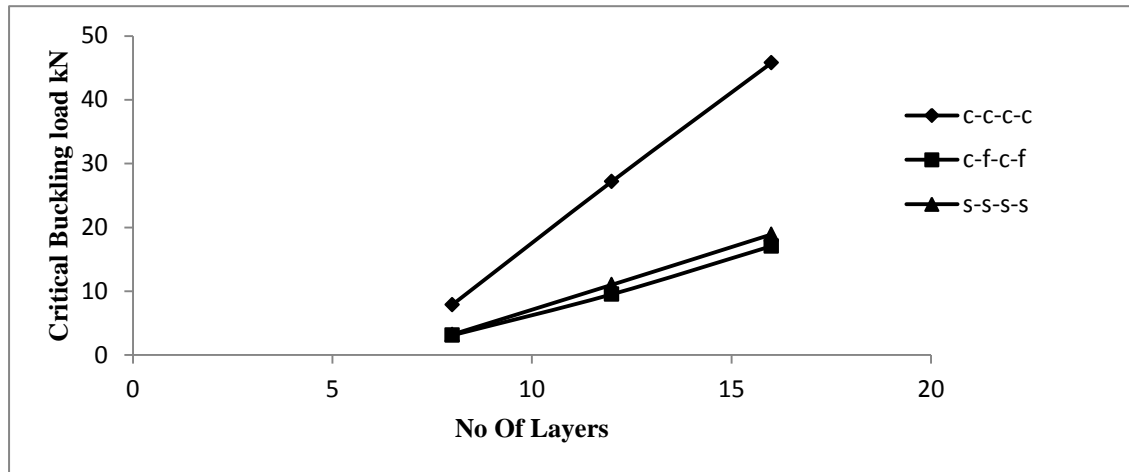


Figure 5.9: Variation of critical buckling load with no. of layers of woven fiber composite plates under different boundary conditions.

The effect of boundary condition on buckling load of composite plates is studied numerically. In this study, the critical buckling load is evaluated at three different boundary conditions that exhibit distinct behavioral characteristics. From Figure 5.9, it is noted that because of the rigidity of clamped boundary conditions the buckling loads laminated composite plates under clamped free clamped free and simply supported boundary conditions are much lower than those under fully clamped boundary condition for 8, 12 and 16 layer laminated composite plates respectively. The analysis and experiments indicate that the variation of the buckling loads is very sensitive in different boundary conditions.

5.3.2.6 Typical Experimental Determination of Buckling Load from Load v/s End shortening Displacement Graph

The critical buckling load from buckling analysis of laminated woven fiber composite plates is found experimentally by load v/s end shortening displacement graph. The load is plotted in y-axis and end shortening displacement in x-axis. For the critical buckling load, the point where left from the straight line has been determined on the graphics and the value of this

point on the y axis has been called as the critical buckling load. Graph of the experimental load/displacement graphs are shown in Figure 5.10 for 12- layers of laminated plate.

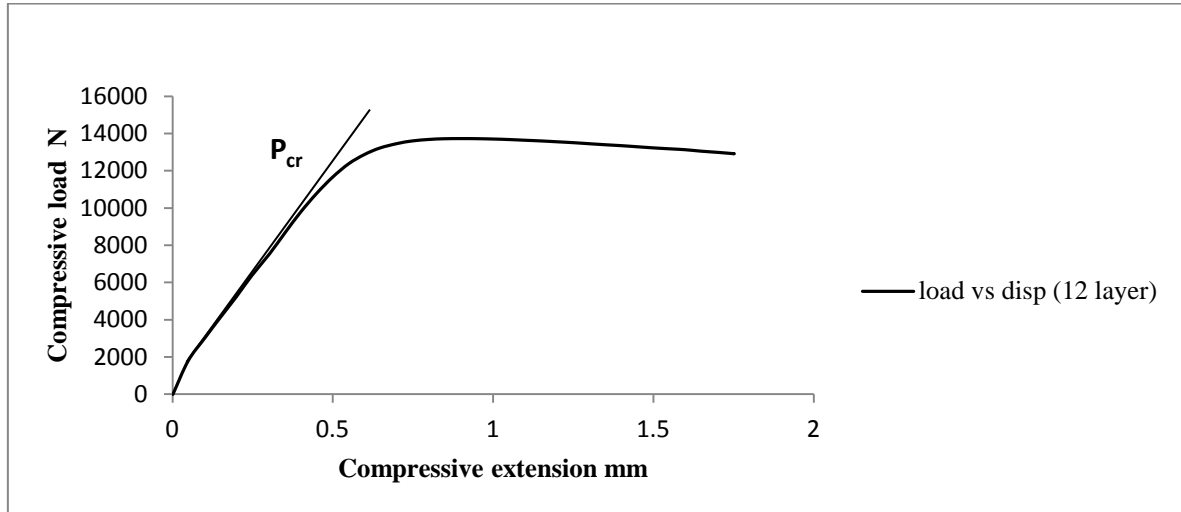


Figure 5.10: Typical variation of compressive load with end shortening displacement of 12-layer woven fiber laminated composite plates

5.3.4 Experimental Buckling Study by Dynamic approach

The variation of natural frequencies with harmonic in-plane load for a plate with dimension $[0.24 \times 0.24 \times 0.0031] \text{ m}^3$ for two side clamped and other two side free boundary condition for lowest mode only.

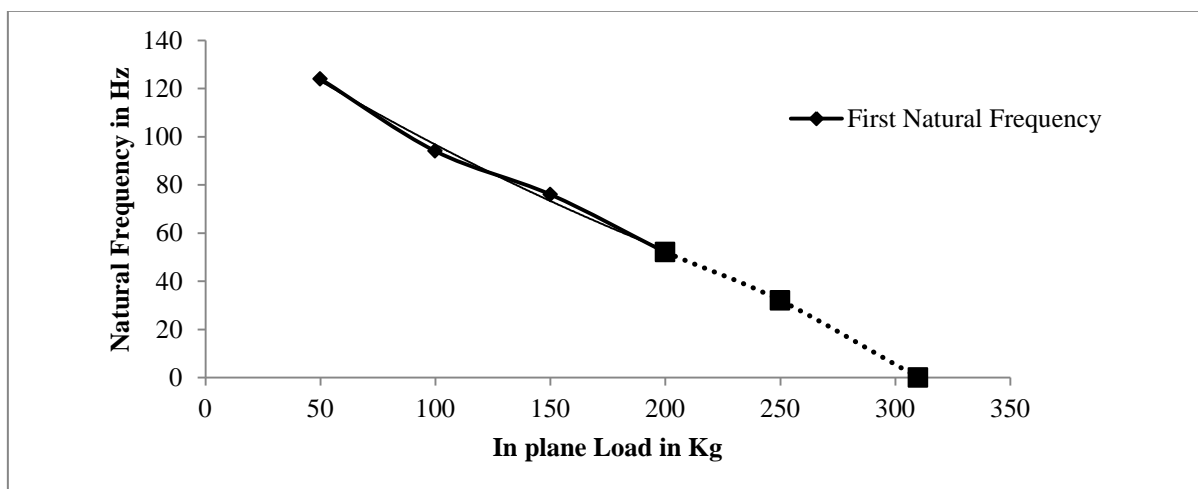


Figure 5.11: Variation of natural frequency of the plate with in plane load

It can be observed that the test results and finite element results compared favorably well. Natural frequencies decrease as the compressive load increases and the fundamental frequency extrapolated to zero at the respective value of the buckling load. Also, the first natural frequency as shown in Figure 5.11 show a tendency to approach zero at a static load of about 310 kg [3.04kN], indicating onset of buckling. This is good agreement with the finite element estimate the buckling load, which is about 3.084 kN for first mode.

5.4. Parametric Instability of Woven Fiber Laminated Composite Plates Subjected To In-Plane Harmonic Loading

The fundamental natural frequency of vibration and first critical buckling load are considered for the determination of parametric instability region. The principal instability regions of woven fiber laminated composite panel subjected to in-plane periodic loads is plotted with excitation frequency versus the dynamic in-plane load β . Here, a static load factor $\alpha=0.2$ is taken for parametric study of laminated composite plates unless otherwise stated. The structural instability may lead to large deflection or large amplitude vibrations of structural elements leading to local or global failures. So the analysis is focused on the determination of the primary instability region of laminated composite plates under harmonic in-plane loads. The width of primary instability region frequencies is the separation of the boundaries of the primary instability region for the given plate. This can be used as an instability measure to study the influence of the other parameters. This is the most dangerous zone and has the greatest practical importance. As can be seen, the primary instability region that occurs in the vicinity of 2ω ($\alpha=\beta=0$) and the upper and lower excitation frequencies of the plates decrease with the increase of the static load parameter. It is also observed that the primary instability region for each plate increase with increasing static and dynamic load parameter, and the width of the unstable zone is becoming more significant at the higher load parameter. The spectrum of the values of parameters causing unstable motion is called the dynamic instability region or DIR or parametric resonance. The variation of excitation frequency with dynamic load factor is showing a linear trend due to neglect of damping.

5.4.1: Convergence Study

The convergence study is done for square 8 layer symmetric cross-ply laminated woven fabric composite plates for C-F-C-F boundary conditions for different mesh divisions. Excitation frequencies of laminated composite plates are presented in Table 5.6. As observed, a mesh of 8x8 shows good convergence of the numerical solution of dynamic stability of woven fiber composite plates and this mesh are employed throughout the dynamic stability analysis of woven fiber composite plates in C-F-C-F boundary conditions

Table 5.6: Convergence study on excitation frequency of 8-layer symmetric cross ply C-F-C-F composite plate.

Length (a) =0.24m, Breadth (b) =0.24m, thickness=0.0031m, $E_{11}=E_{22}=7.4\text{Gpa}$, $G_{12}=G_{23}=G_{31}=2.15\text{Gpa}$, $\nu=0.17$.

Mess Division	Excitation frequency in Hz
	0/90/0/90/0/90/90/0
4x4	215.527
6x6	214.348
8x8	214.283
10x10	214.271

5.4.2: Comparison with previous studies

To validate the formulation, the frequencies of vibration, and the buckling load of laminated composite plates are computed and compared with previously published results from literature. The first natural frequency and buckling load obtained from the present finite element are compared with numerical solution published by Chattopadhyay and Radu [2000] in C-F-F-F and C-F-C-F boundary conditions in shown in Table 5.7. The formulation of parametric instability is also validated with Wang and Dawe [2002] Finite strip method (FSM) and Yang and Huang [1966] analytical solutions, obtained from Reddy's higher order shear deformation plate theory and Bolotin's method, is shown in Table 5.8.

RESULTS AND DISCUSSION

The present finite element results show good agreement with the previous numerical results published in the literature.

Table 5.7: Comparison of natural frequency and buckling load of the C-F-F-F and C-F-C-F symmetric cross ply (0/90/0/90) composite plates.

$a=0.127\text{m}$, $b=0.0127\text{m}$, thickness= 0.001016m , and 0.01016m , $\rho=1500\text{kg/m}^3$, $E_{11}=134.4\text{GPa}$, $E_{22}=10.34\text{GPa}$, $G_{12}=G_{13}=4.999\text{GPa}$, $G_{23}=1.999\text{GPa}$, $\nu_{12}=0.33$.

Boundary Conditions	L/h	Natural frequency & Buckling load	Chattopadhyay & Radu [2000] CLPT	Chattopadhyay & Radu [2000] FSDT	Present FEM
C-F-F-F	125	$\omega_1[\text{Hz}]$	82.15	82.12	81.467
		Pcr [N]	16.43	16.38	16.329
C-F-C-F	125	$\omega_1[\text{Hz}]$	522.85	521.15	516.572
		Pcr [N]	261.62	260.11	259.833
C-F-F-F	12.5	$\omega_1[\text{Hz}]$	820.52	795.09	782.551
		Pcr [N]	16344	15772	15637
C-F-C-F	12.5	$\omega_1[\text{Hz}]$	4664.4	4058.6	3778.9
		Pcr [N]	261623	165644	153190

Table 5.8: Comparison of excitation frequency in rad/sec for 4- layer symmetric cross-ply simply supported composite plates.

$a=b=0.254\text{m}$, $a/h=25$, $E_{22}=6.8948\text{Gpa}$ $E_{11}/E_{22}=40$, $G_{12}/E_{22}=G_{13}/E_{22}=0.6$, $G_{23}/E_{22}=0.5$, $\nu_{12}=0.25$.

$\alpha =$ static load factor	$\beta =$ dynamic load factor	Wang and Dawe [2002]		Yang and Huang [1966]		Present FEM	
		ω^U Upper bound frequency	ω^L Lower bound frequency	ω^U Upper bound frequency	ω^L Lower bound frequency	ω^U Upper bound frequency	ω^L Lower bound frequency
0	0	144.57	144.57	145.57	145.20	143.67	143.67
0	0.3	155.03	133.29			153.12	131.23
0	0.6	164.83	120.95	165.56	121.49	162.32	118.12
0	0.9	174.08	107.21			171.56	105.87
0	1.2	182.87	91.43	183.66	91.84	180.45	89.92
0	1.5	191.25	72.28			189.34	70.59
0	0	144.57	144.57			143.67	143.67
0.2	0.06	131.71	126.86			129.77	124.85
0.4	0.12	117.45	106.24	117.07	107.69	115.28	104.33
0.6	0.18	101.20	80.49			99.47	78.27
0.8	0.24	81.78	40.89	82.21	40.51	78.94	38.92

5.4.3 Experimental and Numerical Results for Parametric Instability

After validating the present formulation, the same is employed to study the effect of static load on the excitation frequency of woven fiber composite plates in C-F-C-F boundary conditions experimentally. For that a 12 layer woven fabric laminated composite rectangular plate of dimension (0.60mx0.35mx0.0047m) is considered. The effects of other parameters are studied numerically using the present formulation.

5.4.3.1 Effect of Static Load Factor

The effect of increase in static component of load from 0 to 0.2, 0.4, 0.6, and 0.8 on the excitation frequency of C-F-C-F 12 layer woven fiber laminated composite panel is shown in Figure 5.12 both numerically and experimentally.

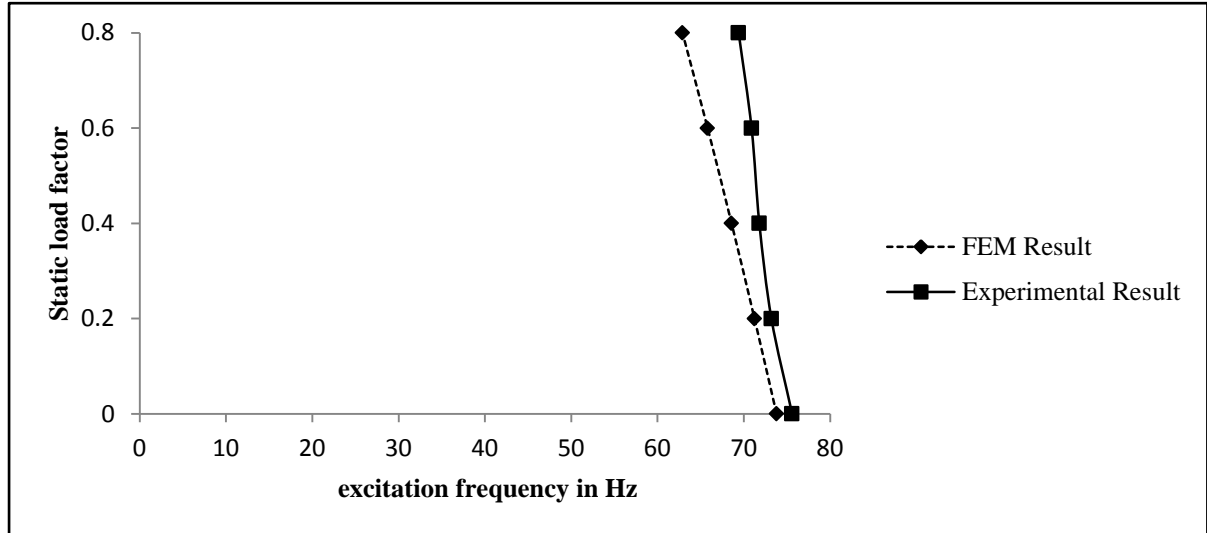


Figure 5.12: Variation of excitation frequencies with static load factor for 12-layer C-F-C-F woven fiber composite plates.

It is observed that with the increase of static load factor from 0 to 0.8, the excitation frequencies decreases from 75.6 Hz to 69.4 Hz experimentally. It is found that the variation between experimental and numerical results is about 2.44%, 2.75%, 4.69%, 7.74% and 10.34% for static load factor 0, 0.2, 0.4, 0.6 and 0.8 respectively. It is concluded that, as the static load factor increases, the percentage error is also increases.

5.4.4: Numerical Results for Parametric Instability

After validating the present formulation, the study is extended to the dynamic instability of woven fiber composite plates using finite element method for the following parameters.

- Effect of no. of layers
- Effect of static load factor
- Effect of aspect ratio
- Effect of boundary conditions

- Effect of fiber orientations
- Effect of length to thickness (l/t) ratio
- Degree of orthotropy

The principal instability regions of woven fiber laminated woven fabric composite panel subjected to in-plane periodic loads is plotted with dimensional excitation frequency (in Hz) versus the dynamic load factor β . Here, a static load factor $\alpha=0.2$ is taken for parametric study of laminated composite plates in C-F-C-F boundary conditions unless otherwise stated. So the analysis is focused on the determination of the primary instability region of laminated composite plate. The width of primary instability region frequencies is the separation of the boundaries of the primary instability region for the given plate. This can be used as an instability measure to study the influence of the other parameters. This is the most dangerous zone and has the greatest practical importance. As can be seen, the primary instability region that occurs in the vicinity of 2ω ($\alpha=\beta=0$) and the upper and lower excitation frequencies of the plates decrease with the increase of the static load parameter. The spectrum of the values of parameters causing unstable motion is called the dynamic instability region or DIR or parametric resonance. The industry driven woven fiber composite plates subjected to in-plane loading are considered here to study the effect of different parameters on the excitation frequency and width of instability regions of composite plates.

The geometrical dimensions which are taken for the woven roving composite plates are:

Length (a) = Width (b) = 0.24m. The material properties of the woven roving composite plates which are obtained from tensile test as per ASTM D 3039/D 3039 M and used for numerical studies are $E_{11}=E_{22}=7.4\text{Gpa}$, $G_{12}=G_{23}=G_{31}=2.15\text{Gpa}$, $\nu=0.17$. All the geometrical dimensions and material properties of the composite plates are same as described in table 4.3.

5.4.3.1. Effect of number of layers

For the present study to examine the effects of no. of layers of laminate, three different types of laminate are fabricated, which are made up of 8, 12 and 16 layers. The excitation frequencies are obtained numerically for C-F-C-F woven fiber laminated composite plates. The effect of increase of excitation frequency with number of layers of the laminated composite plates is illustrated in figure 5.13.

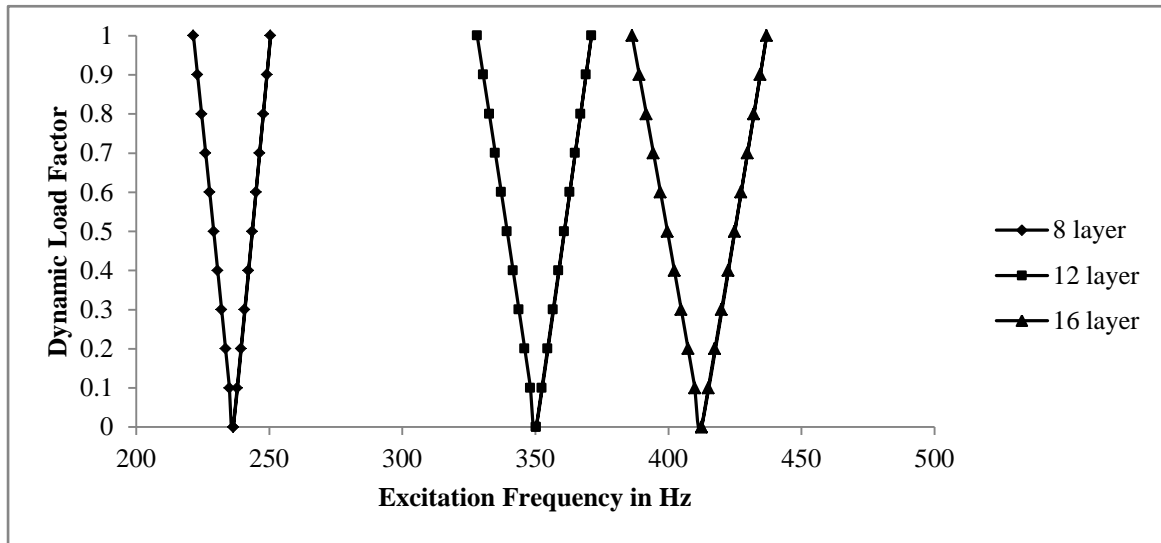


Figure 5.13: Variation of instability regions with no. of layers for C-F-C-F woven fiber laminated composite plates.

The variation of excitation frequency of composite plates with increase of dynamic load factor for three different numbers of layers is studied. As observed in Figure 5.13, the onset of instability occurs at 236.47Hz, 350.32Hz and 412.48Hz for 8, 12 and 16 layer respectively. However, the width of instability regions increases even with increase of number of layers. As expected, woven fiber laminated plates is more stable with increase in number of layers under periodic loads due to bending stretching coupling. The effects of number of layers shift the instability region to larger excitation frequencies, which reflect the fact that the instability of thicker plates occurs later with increase of stiffness.

5.4.3.2. Effect of static load factor

The effect of increase in static component of load for $\alpha = 0.2, 0.4, 0.6$, and 0.8 on the instability region of laminated composite panel subjected to C-F-C-F boundary conditions is shown for 16 layer woven fiber Laminated composite plates in Figure 5.14.

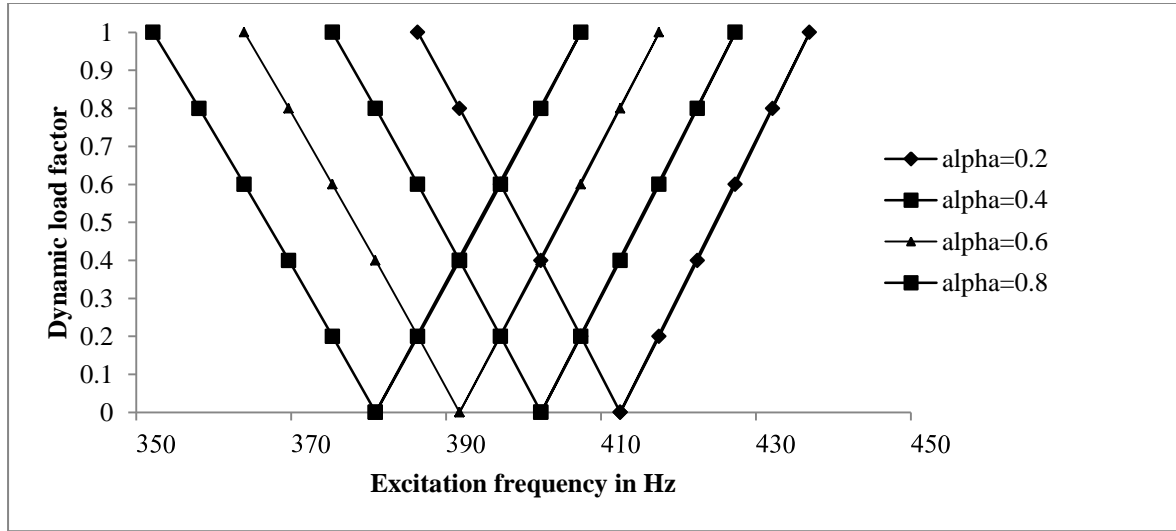


Figure 5.14: Variation of instability regions with static load factor for 16-layer C-F-C-F woven fiber composite plates.

It is observed that with the increase of static load factor from 0.2 to 0.8 , the onset of dynamic instability occurs earlier at 375.33Hz instead of 412.48Hz and the width of dynamic instability region also increases marginally. Also there is reduction of excitation frequencies with increase in static load factors from 0.2 to 0.8 . All further studies are made with a static load factor of 0.2 (unless otherwise mentioned).

5.4.3.3 Effect of aspect ratio:

The effect of increase in aspect ratio for $a/b=0.5, 1, 1.5$ and 2 on the excitation frequencies is analyzed for 8 layer woven fiber laminated composite plates. The Variation of excitation frequencies with dynamic load factor in different aspect ratio are shown for 8 layer woven fiber laminated composite plates in Figure 5.15.

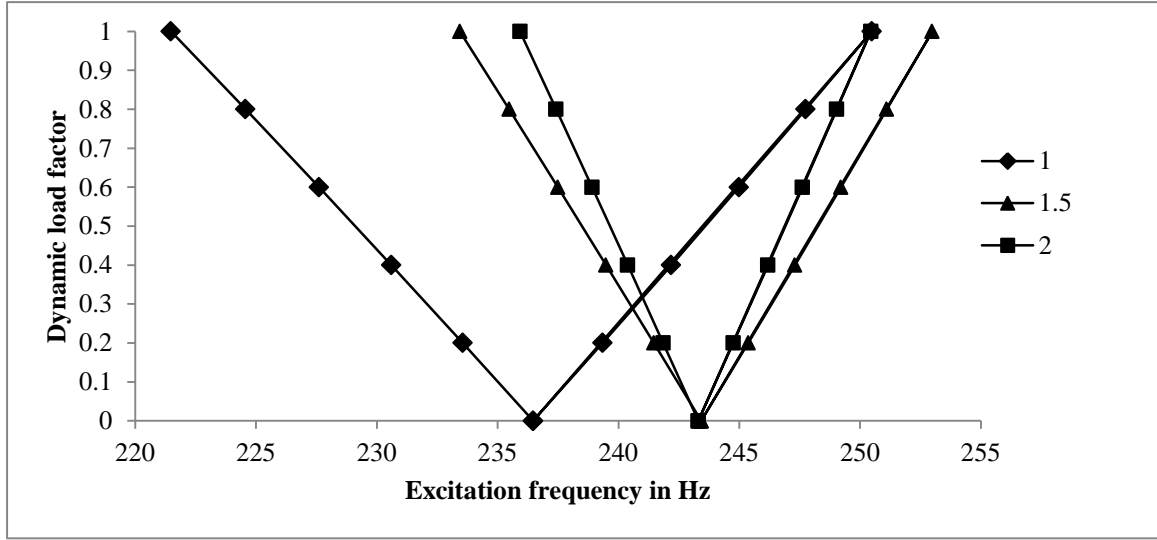


Figure 5.15: Variation of instability regions with aspect ratio for 8-layer C-F-C-F woven fiber laminated composite plates.

With increase in aspect ratios from 1 to 1.5, the excitation frequencies are increased whereas with further increase of aspect ratio from 1.5 to 2, the excitation frequencies decreased marginally due to reduction of effective stiffness of the plates. The study reveals that the onset of instability occurs earlier for laminated woven fiber composite square plates than rectangular plates subjected to C-F-C-F boundary conditions. However, the width of DIR is wider for square plates in comparison with rectangular plates. The width of instability regions increased marginally for rectangular plates than square plates. The increase in aspect ratio of laminated composite plates shifts the frequency of instability region to higher values and reduces the dynamic stability strength. As a result, the plates having higher values of aspect ratios are dynamically less stable.

5.4.3.4 Effect of boundary conditions

The effect of boundary conditions (CCCC, C-S-C-S, C-F-C-F, and SSSS) for $\alpha = 0.2$, on the instability region is analyzed for eight layer woven fabric laminated composite and the variation of excitation frequencies with static load factor are shown in Figure 5.16.

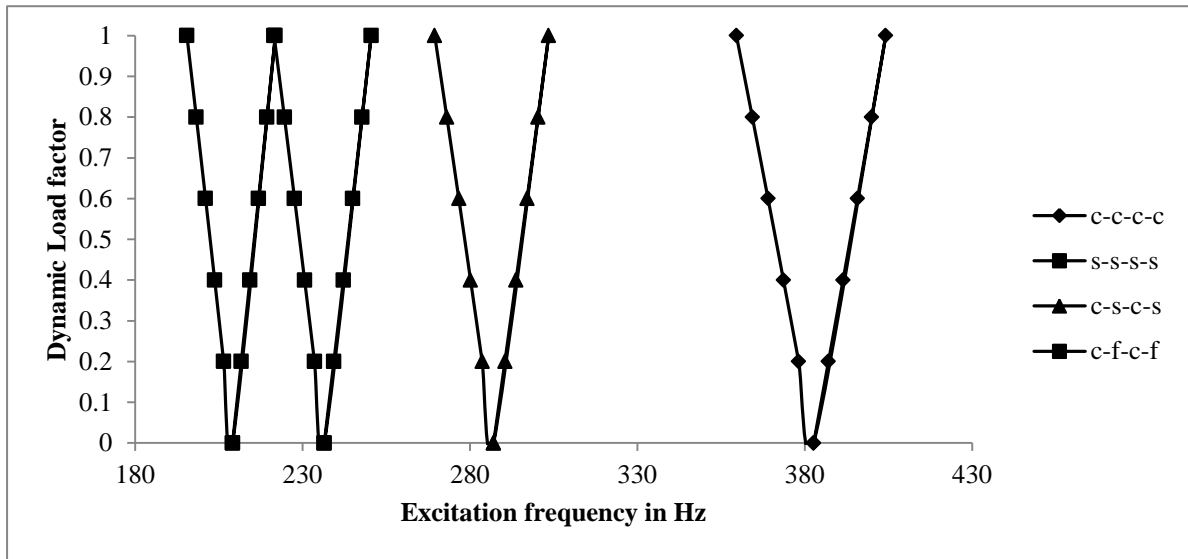


Figure 5.16: Variation of instability regions with boundary condition for 8 layer woven fiber laminated composite plates.

Figure 5.16 shows the influence of different boundaries (CCCC, C-S-C-S, C-F-C-F, and S-S-S-S) on the principal instability regions. The onset instability occurs at 209.07Hz for S-S-S-S, 236.47Hz for C-F-C-F, 287.06Hz for C-S-C-S and 382.67Hz for C-C-C-C boundary condition. The width of the instability regions are also decreased with the increase of restraint at the edges. The excitation frequencies are higher in C-C-C-C boundary condition than C-S-C-S and C-F-C-F. For S-S-S-S, boundary condition, the excitation frequency is minimum.

5.4.3.5 Effect of fiber orientations

To study the effect of ply-orientation of 0° , 30° and 45° on the excitation frequencies, the variation of instability region with dynamic load factor of eight layer C-F-C-F laminated woven fiber composite anti-symmetric angle-ply plates with excitation frequency with different ply orientation is shown in Figure 5.17.

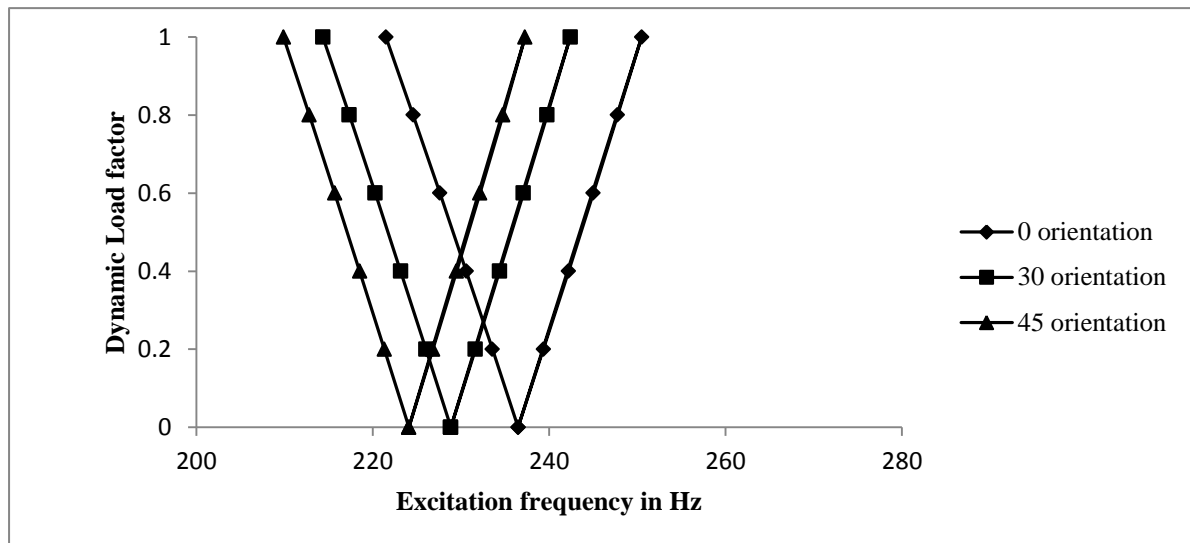


Figure 5.17: Variation of instability regions with fiber orientation for 8-layer C-F-C-F woven fiber laminated composite.

It is observed from the figure that greater the ply orientation the smaller the instability region. The excitation frequencies decreased marginally from 0° to 45° . The onset instability occurs at 224.07Hz, 228.84Hz and 236.47Hz for fiber orientation angle 45° , 30° and 0° respectively. The excitation frequencies are decreased with increase in lamination angle due to reduction of stiffness and strength of laminated plates. The onset of instability and the width of instability region is highly depends on lamination angle.

5.4.3.6 Effect of Thickness

The effect of thickness is studied for $h=2\text{mm}, 4\text{mm}, 6\text{mm}$ and 8mm keeping other geometries and material properties constant. The variation of excitation frequency (Hz) with dynamic load factor of C-F-C-F woven fiber laminated composite symmetric cross-ply plate is shown in Figures 5.18.

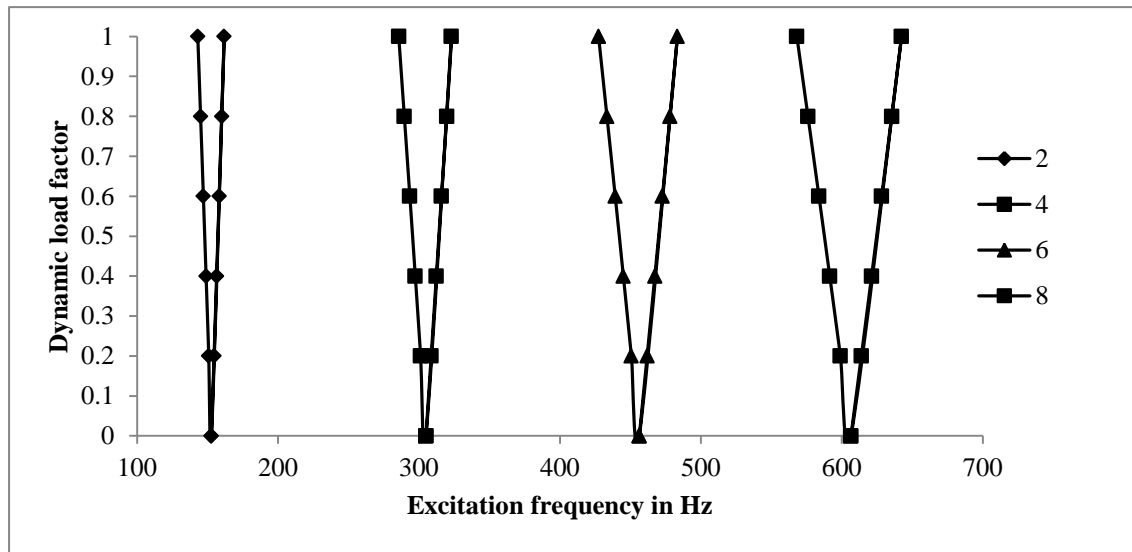


Figure 5.18: Variation of instability regions with thickness for C-F-C-F woven fiber laminated composite plates.

It is observed from the Figure 5.18 is that the onset of dynamic instability region occurs at 152.67Hz, 304.89Hz, 456.28Hz and 606.48Hz for thickness of 2,4,6 and 8 showing more stiffness with increase of thickness of laminates. The excitation frequencies are increases with increase in thickness of laminates. As seen, the width of the instability regions is increased with increase in thickness.

5.4.3.7: The effect of length to thickness ratio:

The effect of increase in side to thickness ratio for $l/t=25$ and 50 on the excitation frequencies is investigated for 8 layer woven fiber composite plates having constant thickness 4mm and varying dimension of length.

For $l/t=25$, $b=100\text{mm}$ and $t=4\text{mm}$, For $l/t=50$, $b=200\text{mm}$ and $t=4\text{mm}$

The variation of excitation frequency with dynamic load factor of woven fiber laminated composite symmetric cross-ply plate for increase in side to thickness ratio subjected to clamped free boundary condition is shown in Figures 5.19.

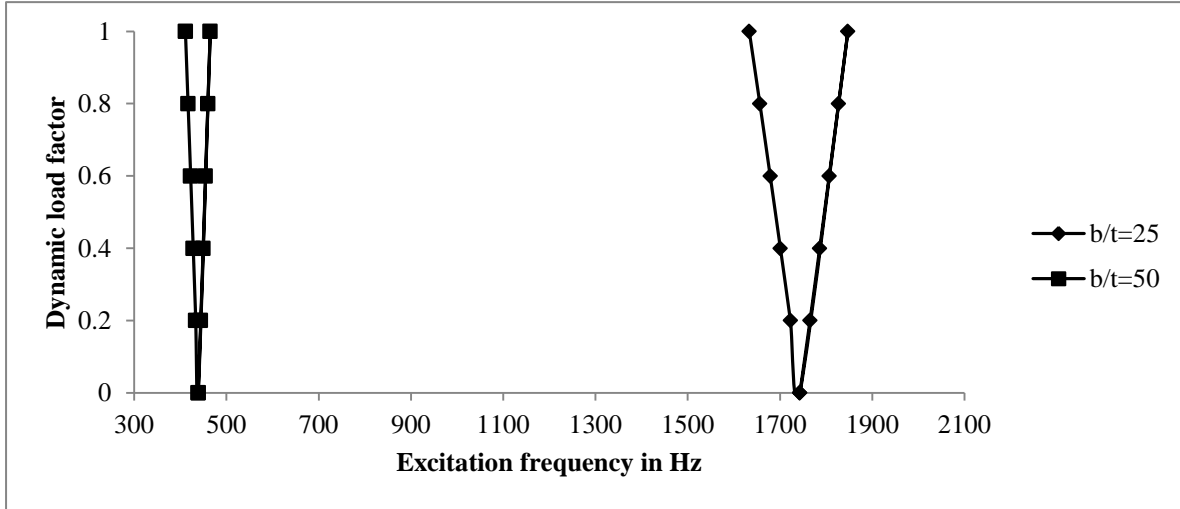


Figure 5.19: Variation of instability regions with side to thickness ratio for C-F-C-F woven fiber laminated composite plates.

It is observed from the Figure 5.19 that, the increase in side to thickness ratio the instability region is wider. The onset of instability occurs at 1722.5Hz and 433.66Hz for b/t ratio 25 and 50 respectively. The excitation frequencies are decreased significantly with increase in side to thickness ratio from 25 to 50 with increase in instability region. The thick plates are more dynamically stable than thin plates.

5.4.3.8: Effects of Degree of orthotropy

The effect of degree of orthotropy is studied for $E_1/E_2 = 40, 20, 10$, keeping other material properties constant. The variation of excitation frequency with dynamic load factor of eight layer C-F-C-F woven fiber composite square is shown in Figure 5.20. For $E_1/E_2 = 40$, $E_1=80\text{Gpa}$, $E_2=2\text{Gpa}$, For $E_1/E_2 = 20$, $E_1=40\text{Gpa}$, $E_2=2\text{Gpa}$, and For $E_1/E_2 = 10$, $E_1=20\text{Gpa}$, $E_2=2\text{Gpa}$

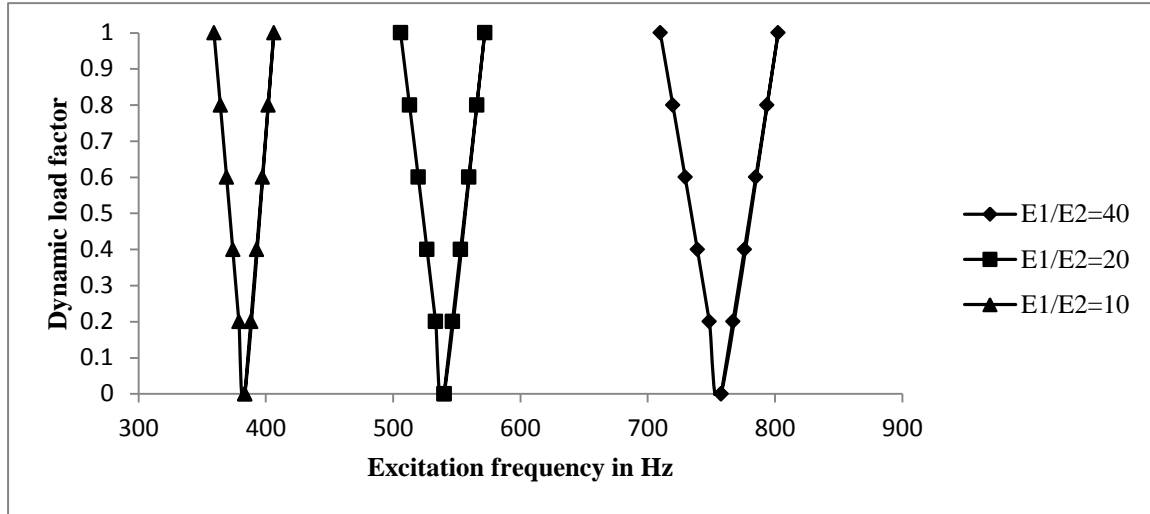


Figure 5.20: Variation of instability regions with degree of orthotropy for 8-layer C-F-C-F woven fiber laminated composite plates.

With the increase of degree orthotropy i.e. the increase in E_1/E_2 the onset instability occurs at 378.77Hz, 533.31Hz and 748.38Hz for E_1/E_2 ratio 10, 20 and 40 respectively. As seen, the width of the instability regions is increased with increase in orthotropy. The excitation frequency decrease with decrease in degree orthotropy. This shows that there is worst variation of stiffness and strength with increase in degree of orthotropy characteristics.

6.1 Introduction

The present work deals with a detailed investigation, including both experimental and numerical study using FEM based on first order shear deformation theory for the vibration, buckling and dynamic stability behavior of industry driven bidirectional woven fiber composite plates subjected to in-plane harmonic loading. At the same time, the numerical results of vibration, buckling and instability obtained from the above formulation are also experimentally checked in the laboratory by fabricating woven fiber glass /epoxy composite plate specimens. The natural frequency, buckling load and the instability regions are investigated for laminated woven fiber composite plate in this present study.

The experimental analysis allowed the mechanics of laminated composites to be investigated and understood more realistic manner. The influences of various parameters like effects of ply orientation, no. of layers, aspect ratio, side to thickness ratio and different boundary condition on the vibration, buckling and instability behavior of woven roving laminated plates are studied. The experimental result is in good agreement with results using FEM formulation. The property values such as density, geometrical parameters such as thickness etc are determined accurately. Also the material properties are determined experimentally by tensile test using INSTRON 1195. The broad conclusions that can be made from the above study are summarized separately for these three cases as given below.

6.2 Vibration of Composite Plates

The results of the experimental and numerical studies of vibration of laminated plates can be summarized as follows:

- ❖ The effect of different parameter like number of layers, aspect ratio , fiber orientation and boundary conditions including free-free, cantilever, simply supported, and fully clamped is presented in details. It is observed that comparisons performed between numerical predictions and experimental tests have a good correlation in cantilever and free-free conditions compared to other boundary conditions.

- ❖ The natural frequency of vibration of laminated composite plates is very less for cantilever than simply supported and fully clamped boundary conditions .
- ❖ There is decrease in fundamental natural frequency with increasing value of a/b ratio. However, the frequencies of vibration of higher modes decrease significantly from aspect ratio $a/b=0.5$ to 1.
- ❖ The strong dependence of the natural frequencies on fiber orientations is demonstrated .This shows that the designer has considerable control over the dynamic response of laminated composite structures. For cantilever boundary conditions, there is a decrease in natural frequency with increase in the orientation angle.

6.3. Buckling of Composite Plates

- ❖ A detailed experimental investigation is performed to study the static stability behavior of industry driven woven fiber composite plates which accounts for C-F-C-F boundary condition. There is a good agreement between the experimental and numerical results for buckling of laminated industry driven woven fiber composite plates.
- ❖ A compressive test frame is designed and built to accommodate the buckling experiments due to static and dynamic approach.
- ❖ The plates under clamped boundary conditions show the highest buckling load in the context of considered edge conditions due to restrain at the edges. As expected the buckling loads of laminated composite plates under clamped free and simply supported boundary conditions are much lower than those under fully clamped boundary condition.
- ❖ The different fiber orientation angle affects the critical buckling load. When ply orientation was increased from 0 to $[30/-30]$ and $[45/-45]$ fiber orientation angle, then the critical buckling load values was observed to decrease in both numerically and experimentally. So the composite plate with $[0]_8$ layup has highest buckling load and with $[45/-45]_{2s}$ layup has lowest buckling load.
- ❖ The buckling loads reduce significantly depending upon the side-to-thickness ratios and aspect ratios.
- ❖ The stability resistance increases with increase of number of layers due to effect of bending-stretching coupling.

6.4. Parametric Instability of Composite Plates

The parametric instability study of woven fiber laminated composite plates in subjected to periodic in- plane loads is examined. From the detailed experimental and numerical study, the following observation can be made:

- ❖ The excitation frequency of laminated fiber composite plates increases with increase of number of layers. So, woven fiber laminated plates increase with more number of layers have greater dynamic stability strength.
- ❖ The instability region is observed to be influenced by the lamination angle.
- ❖ The excitation frequencies of laminated fiber composite plates decrease with increase of static load factor.
- ❖ The boundary conditions play a crucial role in determining the instability region and response of square woven fiber laminated composite plates. A fully clamped plate exhibits highest excitation frequency when compares to other three types of boundary condition (C-S-C-S, C-F-C-F, and S-S-S-S). The width of the instability regions are also decreased with the increase of restraint at the edges.
- ❖ The onset of parametric instability occurs earlier with narrow instability region showing more stiffness with increase of thickness of laminates. The excitation frequencies increase with increase in thickness of laminates. The thick plates are more dynamically stable than thin plates.
- ❖ The increase in side to thickness ratio the instability region is wider. The excitation frequencies are decreased with increase in side to thickness ratio but not uniformly.
- ❖ With the increase of degree orthotropy i.e. the increase in E_1/E_2 the instability occurs at higher frequencies due to increase in stiffness. The excitation frequency decrease with decrease in degree of orthotropy.

From the above discussions, it is clear that the instability behavior of composite plates is influenced by the geometry, material, ply lay-up, ply orientation, boundary conditions. So the designer has to be careful while dealing with structures subjected to harmonic loading. This can be used to the advantage of tailoring during design of composite structures. The study can also be used for structural health monitoring of composite structures.

6.5. SCOPE FOR FURTHER WORK:

Though in this research topic, some studies have been attempted for dynamic stability behavior of composites but still many areas are left which require further investigation. The possible extensions to the present study are as presented below.

- The present study can be extended to dynamic stability of woven fiber composite plates subjected to hygrothermal conditions.
- The plates studied here are of laminated composite plates. The elements can be modified to delaminated composite plates subjected to hygrothermal conditions.
- The effects of damping on the instability regions of laminated woven fiber panels may also be studied.
- Material nonlinearity may be taken in to account in the formation for further extension of the dynamic stability of plates.
- Besides all these, there is a large scope of experimental investigations on dynamic stability of stiffened plates and shells.

BIBLIOGRAPHY

1. **Amirbayat, J.** and **Hearle, J. W. S.** The anatomy of buckling of textile fabrics: drape and conformability. *Journal of the textile institute*, **80**(1), 51-68, 1989.
2. **Ashton, J. E.** and **Anderson, J. D.** The Natural Modes of Vibration of Boron Epoxy Plates. *Shock and Vibration Bulletin*, **39** (4), 81-91, 1969.
3. **Ashton, J.E.** and **Love, T.S.** Experimental Study of the Stability of Composite Plates. *Journal of Composite Materials*, **3**, 230-242, 1969.
4. **ASTM Standard: D3039/D3039M-08.** Standard Test Method For Tensile Properties Of Polymer Matrix Composite Materials, 2008.
5. **Avila, A. F., Donadon, L. V.** and **Duarte, H. V.** Modal analysis on nanoclay epoxy-based fiber-glass laminates. *Composite Structures*, **83**(3), 324-333, 2008.
6. **Baba, B.O.** Buckling Behavior of Laminated Composite Plates. *Journal of Reinforced Plastics and Composites*, **26**, 1637-1655, 2007.
7. **Bathe, K.J.** Finite Element Procedures in Engineering Analysis. *Englewood Cliffs*, New Jersey: Prentice-Hall, 1982.
8. **Bert, C.W.** and **Mayberry, B. L.** Free vibrations of unsymmetrically laminated isotropic plates with clamped edges. *Journal of Composite Materials*, **3**, 282-293, 1969.
9. **Bert, C. W.** and **Chen, T. L. C.** Effect of shear deformation on vibration of antisymmetric, angle-ply laminated rectangular plates. *International journal of solids and structures*, **14**, 465-473, 1978.
10. **Bert, C.W.** and **Birman, V.** Dynamic instability of shear deformable anti-symmetric angle-ply plates, *International Journal of Solids and Structures*, **23**, 1053-1061, 1987.
11. **Bert, C.W.** and **Malik, M.** On the buckling characteristics of symmetrically laminated cross-ply plates. *Mechanics of Composite Materials and Structures*, **4**, 39-67, 1997.
12. **Bertholot, J. M.** and **Sefrani, Y.** Damping Analysis of Unidirectional Glass Fiber Composites with Interleaved Viscoelastic Layers: Experimental Investigation and Discussion, *Journal of Composite Materials*, **40** (21), 1911-1932, 2006.
13. **Bhimaraddi, A.** and **Stevens, L.K.** A higher order theory for free vibration of orthotropic, homogeneous, and laminated rectangular plates. *ASME Journal of Applied Mechanics*, **51** (1), 195–198, 1984.

14. **Birman, V.** Dynamic stability of un-symmetrically laminated rectangular plates, *Mechanics Research Communications*, **12**, 81-86, 1985.
15. **Bolotin, V.V.** The Dynamic stability of elastic systems. Holden-Day, San Francisco, 1964.
16. **Cawley, P. and Adams, R. D.** The predicted and experimental natural modes of free-free CFRP plates. *Journal of Composite Materials*, **12**, 336-347, 1978.
17. **Carlson, R.L.** An experimental study of the parametric excitation of a tensioned sheet with a crack like opening, *Experimental Mechanics*, **14**, 452-460, 1974.
18. **Cederbaum, G.** Dynamic stability of shear deformable laminated plates, *AIAA Journal*, **29**, 2000-2005, 1991.
19. **Chai, G.B.** Free vibration of generally laminated composite plates with various edge support conditions. *Composite Structures*, **29**, 249-258, 1994.
20. **Chai, G. B., Chin, S. S., Lim, T. M. and Hoon, K. H.** Vibration analysis of laminated composite plates: TV-holography and finite element method, *Composite Structures*, **23**, 273-283, 1993.
21. **Chai, G.B.** Buckling of Generally Laminated Composite Plates with Various Edge Support Conditions, *Composite Structures*, **29**, 299–310, 1994.
22. **Chai, G. B and Khong, P. W.** The Effect of Varying the Support Conditions on the Buckling of Laminated Composite Plates, *Composite Structures*. **24**, .99–106, 1993.
23. **Chakrabarti, A. and Sheikh, A. H.** Buckling of Laminated Composite Plates by a New Element Based on Higher Order Shear Deformation Theory. *Mechanics of Advanced Materials and Structures*, **10**, 303-317, 2003
24. **Chakrabarti, A. and Sheikh, A. H.** Dynamic instability of laminated sandwich plates subjected to in-plane partial edge loading, *Journal of Ocean Engineering*, Vol.**33**, pp. 2287-2309, 2006.
25. **Chakraverty, S., Bhat, R.B., and Stiharu, I.** Recent research on vibration of structures using boundary characteristics orthogonal polynomials in the rayleigh-ritz method. *Shock and vibration digest*, **31**(3), 187-194, 1999.

26. **Chakraborty, S., Mukhopadhyay, M. and Mohanty, A.R.** Free vibrational responses of FRP composite plates: experimental and numerical studies, *Journal of Reinforced Plastics and Composite*, **19**, 535-551, 2000.
27. **Chattopadhyay, A. and Radu, A.G.** Dynamic stability of composite laminates using a higher order theory, *Computers and Structures*, **77**, 453-460, 2000.
28. **Chen, T. L. C. and Bert, C.W.** Design of Composite-Material Plates for Maximum Uniaxial Compressive Buckling Load, *Proc. Okla. Acad. Sci.*, **56**, 104-107, 1976.
29. **Chen, B.X, and Chou, T.W,** Free vibration analysis of orthogonal woven fabric composites. *Composites: Part A (applied science and manufacturing)*, **30**, 285–297, 1999.
30. **Chen, C.C. and Yang, J.Y.** (1990). Dynamic stability of laminated composite plates by finite element method, *Computers and Structures*, **36**(5), 845-851.
31. **Chun-Sheng, Chen., Wei-Ren, Chen. and Rean-Der, Chien.** Stability parametric vibrations of hybrid Composite plates, *European Journal of Mechanics A/Solids*, **28**, 329-337, 2009.
32. **Clary, R. R.** Vibration characteristics of unidirectional filamentary composite material panels. *Composite Materials: Testing, Design (Second Conference)*, ASTM STP 497, 415-438, 1972,
33. **Clary, R.R. and Cooper, P. A.** Vibration characteristics of Aluminium plates reinforced with Boron-Epoxy composite material. *Journal of Composite Materials*, **7**, 348-365, 1973.
34. **Crawley, E. F.** The Natural Modes of Graphite/Epoxy Cantilever Plates and Shells. *Journal of Composite Materials*, **13**, 195-205, 1979.
35. **Datta, P.K. and Biswas, S.** Research Advances on Tension Buckling Behaviour of Aerospace Structures: A Review. *International Journal of Aeronautical & Space Science*, **12**(1), 1–15, 2011.
36. **Deolasi, P. J. and Datta, P. K.** Parametric instability characteristics of rectangular plates subjected to localized edge loading, *Computers and Structures*, **54**(1), 73-82, 1995.
37. **Deolasi, P.J. and Datta, P.K.** Experiments on the parametric vibration response of plates under tensile loading. *Experimental Mechanics*, **37**, 56-61, 1997.
38. **Dey, P. and Singha, M. K.** Dynamic stability analysis of composite skew plates subjected to periodic in-plane load, *Journal of Thin-Walled Structures*, **44**, 937-942, 2006.

39. **Dixon, P.** and **Wright, J.** Parametric instability of flat plates, Symposium on Nonlinear Dynamics, Loughborough University of Technology, 1972.
40. **Dong, F.Y.** The development of research on some problems in mechanics of fabric structures, *journal of textile basic science*, **4**(1), 64-70, 1991. (in Chinese)
41. **Dutt K. M.** and **Shivanand, H.K.** An experimental approach to free vibration response of carbon composite laminates, *journal of Advanced Engineering & Applications*, 66-68, 2011.
42. **Evan-Iwanowski, R.M.** On the parametric response of structures. *Applied Mechanics Review*, **18** (9), 699-702, 1965.
43. **Ewins, D. J.** Modal Testing: Theory and Practice, Wiley, New York, 1984.
44. **Faraday, M.,** On a peculiar class of acoustical figures, and on certain forms assumed by a group of particles upon vibrating elastic surfaces, *Philosophical Transactions of Royal Society, London*, **121**, 229-318. 1831.
45. **Fleck, N.A., Jelf, P.M.** and **Curtis, P.T.** Compressive failure of laminated and woven composite. *Journal of composites technology and research*, 212-222, 1995.
46. **Ganapathi, M., Boisse, P.** and **Solaut, D.** Nonlinear dynamic stability analysis of composite laminates under periodic in-plane compressive loads. *International Journal for Numerical methods in engineering*, **46**, 943-956, 1999.
47. **Gu, H.** and **Chattopadhyay, A.** An experimental investigation of delamination buckling and postbuckling of composite laminates, *Composites Science and Technology*, **59**, 903-910, 1999.
48. **Han, W.** and **Petyt, M.** Linear vibration analysis of laminated rectangular plates using the hierarchical finite element method-i. Free Vibration Analysis, *Computers and Structures*, **61**(4), 705-712. 1996.
49. **Hampson P.R.** and **Moatamedi M.,** A review of composite structures subjected to dynamic loading, *International Journal of Crashworthiness*, **12**(4), 411-428, 2007
50. **Hutt, JM** and **Salam AE** , Dynamic Stability of plates by finite element, *Journal of Engineering Mechanics, ASCE*, **3**, 879-899, 1971.

51. **Iannucci, L., Dechaene, R., Willows, M. and Degrieck, J.** A Failure Model for the Analysis of Thin Woven Glass Composite Structures under Impact Loadings, *Computers and Structures*, **79**(8): 785-799, 2001.
52. **Ibrahim, R.A.** Parametric vibration, Part-III, current problems (1), *Shock and Vibration Digest*, **10**(3), 41-57, 1978.
53. **Jones, R. M.** Mechanics of Composite Materials. McGraw Hill, New York, 1975.
54. **Jones, R. M.** Buckling of Bars, Plates, and Shells. McGraw-Hill, New York, 1975.
55. **Ju, F., Lee, H.P. and Lee, K.H.** Finite element analysis of free vibration of delaminated composite plate. *Composite Engineering*, **5**, 195-209, 1995.
56. **Kant, T. and Mallikarjuna,** A higher-order theory for free vibration of unsymmetrically laminated composite and sandwich plates. Finite element evaluations *Computer and Structures* **32**, 1125-1132. 1989.
57. **Kapania, R.K. and Raciti, S.,** Recent Advances in Analysis of Laminated Beams and Plates. Part ii: Vibrations and Wave Propagation. *AIAA Journal*. **27**, 935-946. 1989.
58. **Khdeir, A.A. and Reddy, J.N.** Free vibration of laminated composite plates using second order deformation theory. *Computers and structures*, **71**, 617-626, 1999.
59. **Kwon, Y.W.** Finite element analysis of dynamic stability of layered composite plates using a high order bending theory, *Computers and Structures*, **38**, 57-62, 1991.
60. **Lager, J. R. and June, R. R.** Compressive Strength of Boron-Epoxy Composites, *Journal of Composite Materials*, **3**, 48-56, 1969.
61. **Laila, D., Haji, A., Majid, A. and Shanor, B.** LOC Flutter of cantilevered woven Glass/epoxy laminate in subsonic flow. *ActaMech.sin*, **24**, 107-110, 2008.
62. **Lei, Xu, R., Wang, Shujie, Z. and Yong, L.** Vibration characteristics of glass fabric/epoxy composites with different woven structures, *Journal of Composite Materials*, **0**(0), 1-8, 2010.
63. **Leissa, A.W.,** A Review of Laminated Composite Plate Buckling. *Appl. Mech. Rev*, **40** (5), 575-591, 1987.
64. **Leissa, A. W.** Recent studies in plate vibrations: 1981-1985, part-i, classical theory. *Shock and vibration Digest*, **19**(2), 11-18, 1987.

65. **Leissa, A. W.** Recent studies in plate vibrations: 1981-1985, part-ii, classical theory. *Shock and vibration Digest*, **19**(3), 10-24, 1987.
66. **Leissa A. W.**, Buckling of Composite Plates, *Composite Structures*, **1**, 51-66, 1983.
67. **Liew, K.M., Xiang, Y., and Kitipornchai, S.** Research on thick plate vibration: A literature survey. *Journal of sound and vibration*, **180**(1), 163-176, 1995.
68. **Ma, C.C. and Lin, C.C.**, Experimental Investigation of Vibrating Laminated Composite Plates by Optical Interferometry Method, *AIAA Journal*, **30**(3), 491-497, 2001.
69. **Mahmood, A., Wang, X. and Zhou, C.**, Modelling strategies of 3D woven composites: A review, *Composite Structures*, **93**, 1947-1963, 2011.
70. **Moorthy, J., Reddy, J.N. and Plaut, R.H.** Parametric instability of laminated composite plates with transverse shear deformation, *International Journal of Solids and Structures*, **26**, 801-811, 1990.
71. **Nair, L. S., Singh, G. and Rao, G. V.**, Stability of Laminated Composite Plates Subjected to Various Types of In-Plane Loadings, *International. Journal of Mechanical. Sci.* **38** (2), 191-202, 1996.
72. **Narita, Y. and Leissa, A.W.** Frequencies and mode shapes of cantilever laminated composite plates. *Journal of sound and vibration*, **54**, 161-172, 1992.
73. **Nayfeh, A.H. and Mook, D.T.** Non-linear oscillations, John Wiley & Sons, New York, 1979.
74. **Nguyen, H., Ostiguy, G.L. and Samson, L.P.** Effect of Boundary conditions on the Dynamic Instability and Non-linear Response of Rectangular plates II: Experiments, *Journal of sound and vibration*, **133**(3), 401-422, 1989.
75. **Owen, D.R.J. and Li, Z.H.** A refined analysis of laminated plates by finite element displacement methods-II: vibration and stability, *Computers and Structures*, **26**, 915-923, 1987.
76. **Ozben, T.** Analysis of Critical Buckling Load of Laminated Composite Plates With Different Boundary Conditions Using FEM And Analytical Methods, *Computational Materials Science*, **45**, 1006-1015, 2009.

77. **Pannok, C. and Singhatanadgid, P.** Buckling analysis of composite laminate rectangular and skew plates with various edge support conditions, *The 20th Conference of Mechanical Engineering Network of Thailand*, Nakhon Ratchasima, Thailand, 18-20 October 2006,
78. **Pein, C.W. and Zahari, R.** Experimental Investigation of the Damage Behavior of Woven Fabric Glass/Epoxy Laminated Plates with Circular Cut-Outs Subjected to Compressive Force. *International Journal of Engineering and Technology*, **4**(2), 260-265, 2007.
79. **Pekbey, Y. and Sayman, O.** A Numerical and Experimental investigation of Critical Buckling Load of Rectangular Laminated Composite Plates with Strip Delamination, *Journal of Reinforced Plastics and Composites*, **25**, 685-697, 2006.
80. **Prabhakara, D.L. and Datta, P.K.**, Parametric instability characteristics of rectangular plates with localized damage subjected to in-plane periodic load, *Structural Engineering Review*, **5**(1), 71-79, 1993.
81. **Rayleigh, L.** On the crispations of fluid resting upon a vibrating support, *Philosophical Magazine*. **16**, 50-53, 1883.
82. **Reddy, J.N.**, Free vibration of antisymmetric, angle -ply laminated plates including transverse shear deformation by the finite element method, *Journal of Sound and Vibration*, **66**(4), 565-576, 1979.
83. **Reddy, J.N.** A review of refined theories of laminated composite plates, *Shock and Vibration Digest*, **22**, 3-17, 1990.
84. **Reddy, J. N. and Phan, N. D.**, Stability and vibration of isotropic and laminated plates according to a higher-order shear deformation theory, *Journal of Sound and Vibration*, **98**, 157-170, 1985.
85. **Roberts, J.C., Bao, G. and White, G.J.** Experimental, numerical and analytical results for bending and buckling of rectangular orthotropic plates, *Composite Structures*, **43**, 289-299, 1999.
86. **Sahu, S.K. and Datta, P.K.** Dynamic Instability Of Laminated Composite Plates Subjected To Non-Uniform Harmonic In-Plane Edge Loading, *Journal of Aerospace Engineering*. 214-295, 2000.

87. **Sahu, S. K. and Datta, P. K.**, Research Advances in the Dynamic Stability Behaviour of Plates and Shells: 1987-2005, *Applied Mechanics Reviews*, ASME, 2007, **60**, 65-75, 2006.
88. **Shrivastava, A. K. and Singh, R.K.** Effect of Aspect Ratio on Buckling of Composite Plates, *Journal of Composites Science and Technology*, **59**, 439-445, 1999.
89. **Shukla, K. K., Nath, Y., Kreuzer, E. and Sateesh, K.V.** Buckling of Laminated Composite Rectangular Plates, *Journal of Aerospace Engineering*, **18** (4), .215-223, 2005.
90. **Simites, G.J.** Instability of dynamically loaded structures, *Applied Mechanics Review*, **40**(10), 1403-1408, 1987.
91. **Somerset, J.H. and Evan-Iwanowski, R.M.** Influence of non-linear inertia on the parametric response of rectangular plates, *International journal of non-linear mechanics*, **2**(3), 217-232.
92. **Srinivasan, R.S. and Chellapandi, P.** Dynamic stability of rectangular laminated composite plates, *Computers and Structures*, **24**, 233-238, 1986.
93. **Stanbridge, A.B. and Ewins, D.J.**, Modal testing using a scanning laser Doppler vibrometer, *Mechanical Systems and Signal Processing*, **13** , 255–270, 1999.
94. **Supasak, C. and Singhatanadgid, P.** A comparison of experimental buckling load of rectangular plates determined from various measurement method, *Thai Society of Mechanical Engineers*. Retrieved from http://www.tsme.org/ME_NETT/ME_NETT18/fullpaper/amm/AMM. [Accessed February 2012].
95. **Timoshenko, S. P. and Gere, J. M.** Theory of Elastic Stability, 2nd ed, New York: McGraw-Hill; 1961.
96. **Tita, V., Carvalho, J. and Lirani, J.** A procedure to dynamic damped behavior of fiber reinforced composite beams submitted to flexural vibrations. *Materials research*, **4**(4) 315-321, 2001.
97. **Tuttle, M., Singhatanadgid, P. and Hinds, G.,** Buckling of Composite Panels Subjected to Biaxial Loading, *Experimental Mechanics*, **39**, 191-201, 1999.
98. **Wang, S. and Dawe, D.J.** Dynamic instability of composite laminated rectangular plates and prismatic plate structures, *Journal of Computer Methods in Applied Mechanics and Engineering*, **191**, 1791-1826, 2002.

99. **Whitney, J. M.** Buckling of Anisotropic Laminated Cylindrical Plates, *AIAA Journal*, **22**(11), 1641-1645, 1984.
100. **Whitney, J. M** and **Pagano N.J.** Shear deformation in heterogeneous anisotropic plates, *Journal of Applied mechanics*, **37**, 1031-1036, 1970.
101. **Wu, C. I.** and **Vinson, J. R.** The Natural of Vibrations of Plates Composed Composite Materials, *Journal of Fibre Science and Technology*, **2**, 97-109, 1969.
102. **Xu, L., Wang, R., Zhang, S.** and **Liu, Y.** Vibration characteristics of glass fabric/epoxy composites with different woven structures, *Journal of Composite Material*, **45**, 1069-1076, 2011.
103. **Xu, D., Hoa, S.V.** and **Ganesan, R.** Buckling analysis of tri-axial woven fabric composite structures. Part II: Parametric study-Unidirectional loading, *composite structures*, **72**, 236-253, 2006.
104. **Yang, J. and Huang, X.** Dynamic Stability Behavior of 3D Braided Composite Plates Integrated with Piezoelectric Layers, *Journal of Composite Materials*, **43**(20), 2223-2238, 2009.
105. **Yang, P. C., Norris, C. H.** and **Stavsky, Y.** Elastic Wave Propagation In Heterogeneous Plates, *International Journal Of Solids And Structures*, **2**, 665-684, 1966.
106. **Zhao, Q.** and **Hoa, S.V.** Triaxial Woven Fabric Composites with Open Holes (Part I): Finite Element Models for Analysis, *Journal of Composite Materials*, **37**(9): 763-789, 2003.
107. **Zhang, Y. T.** and **Fu, Y.B.A.** Micromechanical model of woven fabric and its application to the analysis of buckling under uniaxial tension (part1): the micromechanical model, *International journal engineer science*, **38**(17), 1895-1906, 2000.
108. **Zhang, Y. T.** and **Fu, Y.B.A.** Micromechanical model of woven fabric and its application to the analysis of buckling under uniaxial tension (part 2): Buckling analysis, *International journal engineer science*, **39**(1), 1-13, 2001.
109. **Zhang, Y.X.** and **Yang, C.H.** Recent developments in finite element analysis for laminated composite plates, *Composite Structures*, **88**, 147-157, 2009

APPENDIX

Flow chart of program for instability of laminated woven fiber composite plates subjected to in plane harmonic load.

